

POSITRONIUM COMPLEX FORMATION: MECHANISMS, SOLVENT EFFECTS
AND ITS APPLICATION TO THE STUDY OF MOLECULAR PHENOMENA

by

Eugene Stephen Hall

Dissertation submitted to the Graduate Faculty of the
Virginia Polytechnic Institute and State University
in partial fulfillment of the requirements for the degree of
DOCTOR OF PHILOSOPHY

in

Chemistry

APPROVED:

Hans J. Ache~~ff~~, Chairman

Jetty R. Bartschmid

Philip L. Hall

Luther K. Erice

George Sanzone

July, 1978

Blacksburg, Virginia

DEDICATION

The author wishes to dedicate this work to his parents, Mr. and Mrs. Eugene Hall and to his sisters, Christine, Georgia, Gretchen and Jill Hall.

ACKNOWLEDGMENTS

The author wishes to express his gratitude and appreciation to Dr. Hans J. Ache, his research advisor, whose guidance, encouragement and critical evaluations have been invaluable throughout this work.

Special thanks are extended to Dr. Hampton Smith, for his moral support, encouragement to go on, and for his general concern; to Dr. George Sanzone and Dr. Philip L. Hall for their helpful discussions and to Dr. John C. Schug, for his general and helpful advice on quantum chemistry. He wishes to acknowledge the present and past members of the positronium research group, Belkacem Djermouni, Dr. Ted Handel and Dr. Jerry Jean for their helpful discussions. He wishes to thank the present and past members of Dr. Hans Ache's Radiochemistry research group for their kindness and support.

He would also like to thank the Chemistry Department's Glassblowing and Electronic Shops for their fine work and assistance, and the Division of Chemical Sciences, Fundamental Interactions Branch, for providing financial aid.

Special thanks are also extended to Ms. Donna Tyree and Mrs. Doris Smith for typing this manuscript, and to the "All World Chemistry" basketball team for providing excellent physical exercise.

TABLE OF CONTENTS

	Page
ACKNOWLEDGMENTS	iii
LIST OF FIGURES	vii
LIST OF TABLES	x
INTRODUCTION	1
CHAPTER 1. Basic Principles of Positronium Chemistry	4
A. The Positron	4
B. Positron Decay	6
C. Positron Annihilation	9
D. Basic Physical and Chemical Properties of Positronium	13
E. Models of Positronium Formation	18
F. Positronium Reactions	27
CHAPTER 2. Experimental Techniques	37
A. Introduction	37
B. Positron Sources	38
C. Fast-Slow Delayed Coincidence Counting	41
D. Instrument Calibration	46
E. Positron Lifetime Spectra	48
F. Sample Preparation	53
G. Solutes and Solvents	61
CHAPTER 3. Reactions of Thermalized o-Ps	64
A. Introduction	64
B. Reactions of Positronium with Diamagnetic Organic Molecules	64
C. Positronium Complex Formation	66

	Page
D. Analysis of Positronium Lifetime Spectrum	72
CHAPTER 4. Solvent Effects on the Stability of Positronium Complexes in Solution	78
A. Introduction	78
B. Evaluation of Solvent Effect	80
CHAPTER 5. Positronium Reactions: Diffusion or Kinetic Controlled?	88
A. Introduction	88
B. Studies of Positronium Reactions in Various Solutions of CuCl_2	91
C. Bubble Model and Diffusion Controlled Mechanism	95
CHAPTER 6. Study of Inclusion Complex Formation	109
A. Introduction	109
B. Kinetic Equations	114
C. Calculation of K_c (Molecular Complex Formation Constant) .	117
D. Steric and Geometric Factors	121
CONCLUSIONS	129
A. Summary	129
B. Future Possibilities	130
REFERENCES	132
APPENDIX. Data Tables	136
A. Rate Constants for the Reaction of Thermal Ortho- Positronium with Nitrobenzene or o-Nitrotoluene in Various Molefractions of n-Hexane/Benzene Solutions at 21°C	137
B. Temperature Dependence of the Annihilation Rate, λ_2 , for the Reaction of Thermal Ortho-Positronium with Different Solvents	139

	Page
C. Temperature Dependence of the Observed Rate Constants for the Reaction of Ortho-Positronium with CuCl_2 or Substituted Nitroaromatics in Different Solvents	141
D. Reactions of Thermal Ortho-Positronium with Nitro- aromatics, Cyclohexaamylose (CH) or Inclusion Complex (Nitroaromatics + CH) in H_2O at 21°C , pH 3.5 and Ionic Intensity 0.5	144
VITA	147
ABSTRACT	

LIST OF FIGURES

Figure	Page
1. Energy Spectrum of Positrons Emitted from Sodium-22 . . .	8
2. Positronium Annihilation	11
3. Characteristics of Hydrogen and Positronium	15
4. Some Physical Properties of Para- and Ortho-Positronium in the Ground State	17
5. Ore Model of Ps Formation	20
6. (a) Energy Diagram of the Ore Gap and (b) Hypothetical Positronium Formation Probability in Gaseous Argon . . .	21
7. Formation of the Spur During the Last Path of the Positron (a) No Positronium Formed. (b) Positronium Formation	24
8. Reactions of Ortho-Positronium	28
9. Lattice Potential as Represented by the Free Volume Model	30
10. Angular Distribution in Two-Quantum Annihilation	33
11. Computed and Experimental Momentum Distributions for N-Hexane	35
12. Decay Scheme of Sodium-22	39
13. Simple Fast-Slow Timing System	43
14. "Prompt" Cobalt-60 Calibration Spectrum	47
15. Typical Positron Lifetime Spectrum	50
16. Calcomp Plot of Benzene Standard	52
17. Sample Vial Used for Data Taken at Room Temperature . . .	54
18. Sample Vial in the Counting Position	56
19. Two-Tier Sample Vial and Source Used for High Temperature Measurements: (a) Disassembled Vial and Source and (b) Assembled Vial and Source	57

Figure	Page
20. Sample Vial Attached to Degassing Bulb	59
21. Experimental Arrangement Used for High Temperature Lifetime Measurements	60
22. Experimental Setup for Low Temperature Lifetime Measurements	62
23. Electronic Polarizabilities, P_E , of Simple Hydrocarbons Plotted Against Rate Constants k_{obs} for Reactions with Ps.	69
24. Gas-Kinetic Model of o-Ps Interactions with Matter	71
25. Experimental Determination of k_{obs} for Ps Reactions with Nitrobenzene in 0.3 MF Benzene/Hexane	75
26. Arrhenius and Non-Arrhenius Behavior of Ps Reactions in Different Systems	77
27. k_{obs} for Ps Reactions with o-Nitrotoluene and Nitro- benzene in Different Solvents vs $1000/T$	79
28. Typical Arrhenius Behavior for Ps Reacting with Nitro- aromatics Showing the Thermodynamic Parameters	82
29. Potential Energy Surface for Ortho-Positronium Reacting With a Molecule VIA Complex Formation	83
30. $1/k_{obs}$ vs Mole Fraction of N-Hexane in N-Hexane-Benzene Solutions of Nitrobenzene and o-Nitrotoluene	85
31. Arrhenius Plots for Ps Reacting with $CuCl_2$ in Different Solvents	92
32. Arrhenius Plots for Ps Reacting with $CuCl_2$ in H_2O and Ethyleneglycol	93
33. Arrhenius Plots for Ps Reacting with Various Nitro- aromatics in Different Solvents	95
34. Determination of E_η (Activation Energy of Viscosity) for N-Hexane	96
35. $(k_{obs}\eta)/T$ vs T for Ps Reactions with $CuCl_2$ in Different Solvents	99
36. $(k_{obs}\eta)/T$ vs T for Ps Reactions with Various Nitro- aromatics in Different Solvents	100

Figure	Page
37. k_{obs} Calculated vs k_{obs} Experimental for Ps Reactions in Different Systems	105
38. k_{obs} as a Function of Viscosity for Ps Reactions with $CuCl_2$ in Various Mixtures of Ethyleneglycol/Ethanol Solutions	107
39. Cyclohexaamylose	111
40. $(\tilde{\lambda}_2^0 - \tilde{\lambda}_2)^{-1}$ vs $1/[Cyclohexaamylose]$ for the Determination of K_c (Molecular Formation Constant)	119
41. Steric Factors Involved in Lowering of K_c	125

LIST OF TABLES

Table	Page
I. Examples of Chemical Compounds Showing Strong/Weak Interactions With Thermal Ps Atoms	67
II. Thermodynamic Data for the Reactions of o-Ps in Toluene, n-Heptane and n-Pentanol Solutions	81
III. Observed Rate Constants, k_{obs} , Entropies of Activation, Energies of Activation and Viscosity for Ps-CuCl ₂ Reactions in Various Solutions	89
IV. Observed Rate Constants, k_{obs} , Energies of Activation and Viscosity for Ps-Nitrobenzene in Various Solutions	90
V. Experimental and Calculated Observed Rate Constants, k_{obs} , and Calculated and Experimental Energies of Activation for Ps-Nitrobenzene and Ps-CuCl ₂ Reactions in Various Solvents	103
VI. Molecular Dimensions of Cycloamyloses	110
VII. Inclusion Complex Formation Constants, K_C , for Various Guest Molecules Binding in the Cavity of Cyclohexaamylose.	113
VIII. Inclusion Complex Formation Constants, K_C , and Rate Constants, $k_{QD(OBS)}$, for the Interaction of the Inclusion Complexes of Various Nitroaromatics With Cyclohexaamylose (CD) at pH 3.5, Ionic Intensity 0.5, in Aqueous Solution at 22°C.	120
IX. Comparison of Different Rate Constants (k_{obs}) for Ps Reacting with Various Guest Molecules in Aqueous Solution at pH 3.5 Ionic Intensity 0.5 and Inclusion Complex Formation Constants, K_C , for the Interaction of Various Guest Molecules in the Cyclohexaamylose Cavity	122
X. Influence of the Steric Effect in Lowering the Inclusion Formation Constants, k_C , for Various Guest Molecules in the Cavity of Cyclohexaamylose	124

INTRODUCTION

In the beginning when man came into existence he was both intrigued and fascinated with his environment. He was very curious about simple phenomena and what caused them. He immediately set out to gather all the knowledge he could about his environment to increase his ability to solve problems. Today, this curiosity has brought us to the development of highly sophisticated electronic gadgetry to help one explore the fascinating branches of science such as chemistry and physics. In these two sciences there are many phenomena which have direct effects on the environment in which these processes take place. One such process is the nuclear transformation which changes or alters the surroundings when it takes place.

In some scientific communities the positron is known as an exotic particle. It is a stable particle but since it exists in this world of antimatter, its lifetime is very short. It is annihilated together with an electron on the order of a fraction of a nanosecond in the condensed phase. One way of increasing its lifetime is by forming a bound state between itself and an electron whose spin is parallel relative to that of the positron spin, i.e., ortho-positronium.

In this bound state, the lifetime of the positron is considerably longer. After positronium is formed, its stability with regard to annihilation will be determined by its surroundings. Recently it has been shown that positronium reacts very rapidly with a certain class of compounds, mainly the diamagnetic nitroaromatics and inorganic ions in solution whose redox potential are greater than -0.9 eV. These

reactions occur with very high bimolecular rate constants and result in an apparent shortening of the lifetime of the positron.

Nuclear chemistry connects the mutual influence of transformations of atomic nuclei and elementary particles along with the properties of their molecular environment. It has been demonstrated throughout the literature that the Mössbauer effect and positron annihilation are directly influenced by both the chemical and physical makeup of their environment. For example, positron annihilation techniques can be used to accurately determine the T_g (glass transition temperature) of polymers which is an important parameter in the plastics industry. Also this technique has been useful in studies in solid state chemistry such as properties of semi-conductors.

The scope of this thesis involves the relations which the solvent plays in stabilizing the complexes formed between Ps and nitroaromatics in solution and the various thermodynamic variables associated with these processes. It also includes the evaluation on the effects displayed by a host of different solvents on complexes formed between Ps and CuCl_2 and the role which these solvents play in stabilizing these complexes. It will also be shown that these reactions are not solely diffusion controlled as was interpreted in the past by different researchers.

The fact that Ps loses some of its reactivity towards nitroaromatics when they are already complexed with another molecule can be utilized to determine the molecular formation constant, K_c , for inclusion compounds. Using Ps as a probe, it can provide valuable information about the

influence of steric factors on the ability of guest molecules to bind in the cavity of cyclodextrin.

BASIC PRINCIPLES OF POSITRONIUM CHEMISTRY

A. The Positron

In some scientific communities, the positron is classified as an "exotic" particle and it was the first anti-particle to be observed. The positron is an elementary particle belonging collectively with electrons, positively and negatively charged μ -mesons (muons) and with the neutrino to the class of particles known as leptons. These particles have "lepton numbers," or "lepton charge," L , equal to -1 or +1. The positron ($L_e^+ = -1$) is the antiparticle of the electron ($L_e^- = +1$). These two particles can be annihilated as a pair with the emission of one, two, or three gamma rays. Since the positron is the antiparticle of the electron it has the same rest mass $m_e = 9.1 \times 10^{-28}$ g or in energy units 0.51 MeV. It also carries a charge like the electron but opposite in sign; i.e., a positive electric charge of $e = 4.8 \times 10^{-10}$ (CGS), e.s.u. = 1.6×10^{-19} C. The spin of the positron like that of the electron is $S = \frac{1}{2}$ (in units of $\hbar = 1.05 \times 10^{-27}$ erg sec). Particles with half integer spins (protons, neutrons, muons) all obey Fermi-Dirac statistics. The magnetic moment of the positron is $\mu = +1$, because the magnetic moment and spin are parallel whereas for the electron $\mu = -1$ because the magnetic moment and spin are antiparallel.

Dirac¹ showed in 1930 by theoretical arguments that the positron could exist in nature. He showed that the solutions to his relativistic electron wave equations ($E = \pm (m_e^2 c^4 + p^2 c^2)^{1/2}$) must have two solutions, both positive and

negative. These solutions show that there are both positive and negative energy states. These energy states have a minimum value of $m_e c^2$, where m_e is the mass of an electron and c is the speed of light. Instead of throwing away the negative solution as having no physical meaning, Dirac postulated that the negative energy states were partially filled and could not be observed. After this, he further postulated that these negative energy states corresponded to a particle with a mass equal to the mass of an electron but having an opposite charge. This interpretation can be understood in terms of the "hole theory." It says that since electrons are only observed in positive energy states, then the negative energy states must be completely filled with electrons. When a photon has energy greater than the rest mass of two electrons ($2m_e c^2$) an electron can be raised from its negative energy state to a positive one. The "hole" left by this transition in the continuum or "sea" of negative energy states should have the properties of a positive electron, i.e., the positron.

Two years after Dirac's "hole" theory, the existence of the positron was confirmed by Anderson² when he observed this particle in a cloud chamber while performing experiments on cosmic rays. Today, positrons have been observed in radioactive decays and Dirac's postulate has been confirmed.

Another interpretation of the solutions to Dirac's relativistic equations was proposed by Feynman.³ Feynman's interpretation is that electrons and positrons are considered as particles traveling in time in a potential. Electrons would travel forward in time while positrons would travel backwards in time. If this is true, then positrons would

scatter forward in time and pair production will result when electrons scatter backward in time. This would result in the annihilation of a positron with an electron. Even though Feynman's interpretation has no physical meaning, it has found success in applying his interpretation to several problems in the theory of elementary particles.

B. Positron Decay

Positron decay was first discovered in 1934 by Joliot and Curie⁴ while bombarding heavy nuclides with alpha particles. Positron decay takes place in nuclei that are proton rich in relation to their most stable isobars, i.e., neutron deficient nuclei. This leads to a decrease in the neutron - proton ratio approaching the value of one, whereby nuclides obtain a higher stability.

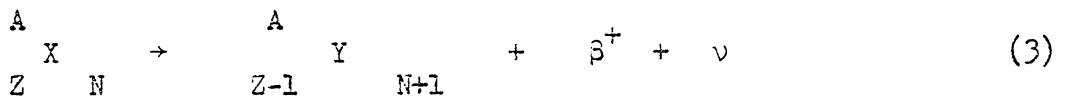
There are three types of beta decay: (1) Negatron emission (β^-), (2) Positron emission (β^+), and (3) Electron capture (EC). For positron decay, a proton within the nucleus of a neutron deficient nuclide is transformed into a neutron, positron and neutrino. The equation for this transformation can be written as



Energetically, this can only happen when the mass of the parent nucleus, M_p , is greater than the sum of the mass of the daughter nucleus, M_d , and the rest mass of two electrons, m_e .

$$M_p > M_d + 2m_e \quad (2)$$

The consequences of this decay are that the mass number of the nuclide (A) stays the same while the atomic number (Z) decreases by one. This can be represented by the following equation:



If the energetics of positron decay are not met, another process, EC, will compete with positron emission. It can occur when $M_p > M_d$. It must be noted that the positron cannot exist in the nucleus due to difficulties in conserving angular momentum and it is therefore emitted simultaneously with a neutrino so that angular momentum is conserved.

The binding energy released in positron decay is divided up between the positron, and the recoil energy of the neutrino and the daughter nuclide. This energy may range from a few hundred keV up to several MeV. Even though positron emission corresponds to transitions between discrete energy states, its energy spectrum is continuous due to the simultaneous emission of a neutrino which shares part of the binding energy from positron emission. The maximum number of positrons emitted in an energy distribution will have energy at one third the end point energy. The positron energy spectrum⁵ for sodium-22 is shown in Figure 1 and the maximum energy or end point energy is 0.544 MeV. As mentioned earlier, the most probable energy of positrons emitted in this decay is about 0.18 MeV.

Fermi⁶ was the first to develop an elementary theory of beta decay. This theory helped to explain many phenomena in beta decay such as half-lives and the energy spectra of beta particles. Following Fermi's

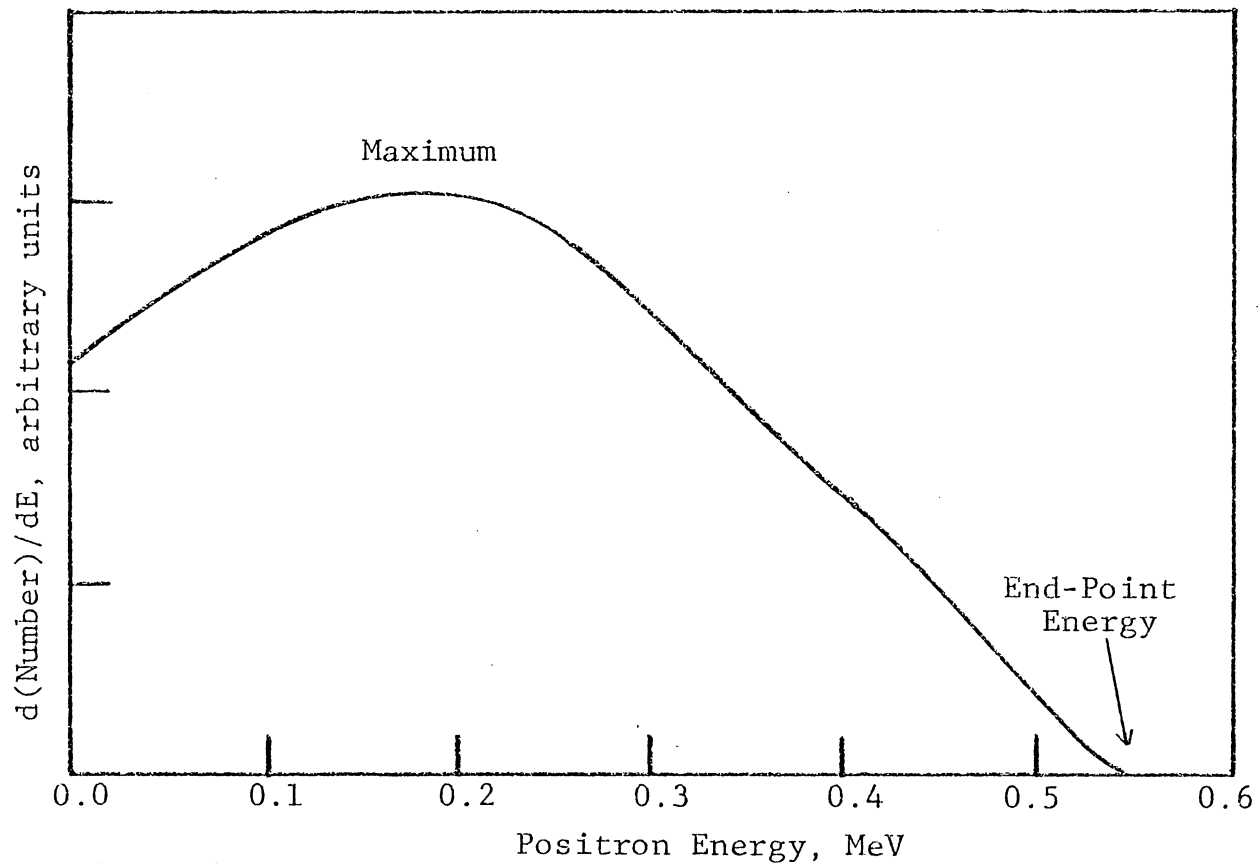


Figure 1. Energy Spectrum of Positrons Emitted from Sodium-22.
(From Ref. 5)

theory, several years later new particles (mesons, neutrinos) were discovered in nuclear physics. Lee and Yang⁷ used these new particles to their advantage in developing a new quantitative theory of beta decay which helps explain the observed polarization of positrons emitted in radioactive decays. The degree of polarization is given by v/c which is the ratio of the velocity of the positron to the velocity of light.

C. Positron Annihilation

The kinetic energy of a positron is reduced primarily through inelastic collisions with the medium. While passing through the medium, they can induce ionization as well as excitation in the medium. In water, Tao and Green⁸ have estimated that it takes about 7 psec for the positron to reach the first ionization potential of water. They also estimated the total time it takes for the positron to be thermalized to be 100 psec. Positrons and electrons, just like any matter-anti-matter-pairs, have a high probability of annihilating on collision. This probability is inversely proportional to the kinetic energy of the positron. The total energy of annihilation can be represented as,

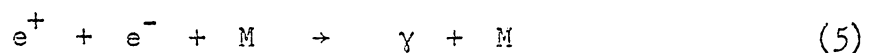
$$E = 2m_e c^2 + KE_{e+} + KE_{e-} \quad (4)$$

where m_e is the rest mass of an electron, c is the speed of light and KE_{e+} and KE_{e-} are the kinetic energies of the positron and electron, respectively. From this equation, it can be shown that the minimum energy released is 1.02 MeV. This energy is seen as two 0.51 MeV gamma rays which are used in positron lifetime measurements.

To be specific, since the positron is the anti-particle of the electron, it will therefore experience a very short life in an environment so rich in negative electrons and it will be annihilated together with an electron. According to Goldanskii,⁹ less than five percent of the positrons emitted in condensed media will be annihilated during the slowing down process.

The theory of positron annihilation¹⁰ predicts that either one, two, or three photons will be produced when a positron and electron annihilate. If the electron and positron meet with their spins antiparallel, i.e., singlet (1S_0) interactions, then the selection rules require that an even number of photons be produced, i.e., two. These two photons will travel in opposite directions, i.e., 180° if the positron-electron pair annihilate at rest. If the electron and positron meet with their spins parallel, i.e., triplet (3S_1) interaction, then the selection rules require that an odd number of photons be produced, i.e., three. These three photons must always lie in a plane so that their momenta can add up to zero if the electron-positron pair annihilate at rest. The 3 photons produced will have an energy equal to the sum of the e^+ and e^- rest mass, i.e., 1.02 MeV. Positron annihilation from these two states are shown schematically in Figure 2.

It is also possible that either no photons are produced or one photon is produced. For one photon emission, the annihilating electron has to be strongly bound in an atom in a third body, M, so that the nucleus can absorb part of the photon recoil energy.



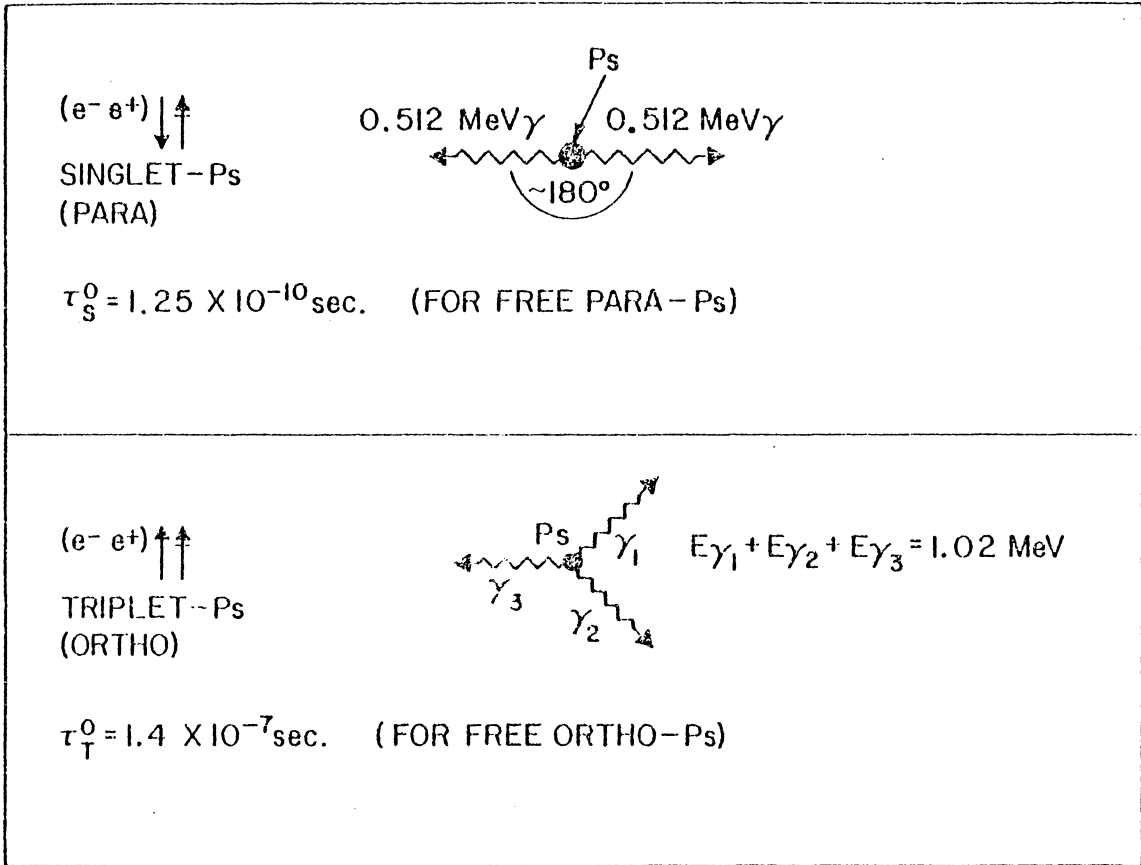


Figure 2. Positronium Annihilation

If no photons are to be emitted, it is required that two third bodies be present to absorb all the photon recoil energy.



For these last two processes to occur, the positron must have very high kinetic energy and these processes are usually not observed. Up to today, nonradiative positron annihilation has never been observed experimentally.

According to Goldanskii, there are three mechanisms by which positrons are annihilated.⁹ They are the following: (1) immediate annihilation as "free" positrons in collisions with electrons in the environment, (2) capture by an atom or molecule followed by annihilation, (3) interaction with an electron to form a long lived bound state (positronium) followed by annihilation. Mechanism (3) will be discussed in detail in the next section.

In 1934 Dirac¹ calculated the cross section for two photon annihilation, $\sigma_{2\gamma}$, for non-polarized positrons and electrons annihilating at non-relativistic velocities with the electron at rest. This cross section can be represented as,

$$\sigma_{2\gamma} = \pi r_0^2 c/v \quad (7)$$

where $r_0 = 2.8 \times 10^{-13}$ cm, the classical radius of an electron, c , the speed of light, and v , the velocity of the annihilating positron. It is easy to see that the probability of annihilation increases as the velocity of the positron decreases. Then the rate for two photon

annihilation depends on the number of electrons per cm^3 , n , and can be represented as,

$$\lambda_{2\gamma} = \sigma_{2\gamma} n v \quad (8)$$

For a multi-electron system, Equation (8) becomes

$$\lambda_{2\gamma} = \pi r_0^2 c \rho N Z_{\text{EFF}} / M \quad (9)$$

where, M is the molecular weight of the substrate, ρ is the density, r_0 , is the classical radius of the electron, N is Avogadro's number, c is the speed of light, and Z_{EFF} is the effective number of electrons seen by the positrons. Z_{EFF} is usually taken as the valence electrons in the substrate M . Using Equation (9) and assigning $Z_{\text{EFF}} = 8$ for water, one can calculate the theoretical two photon annihilation rate in water to be 2.2 nsec^{-1} which is in good agreement with the experimental value.

In 1949 Powell and Ore¹¹ were the first to calculate the ratio of the two photon to three photon annihilation rates. This value came out to be $\lambda_{2\gamma}/\lambda_{3\gamma} = 1115$. The probability of singlet to triplet ratio can be calculated from the following reasoning: since the singlet state has $J = 0$, $m = 0$, (only one way to be formed) and the triplet state has $J = 1$, $m = 0, \pm 1$ (three ways to be formed) then the ratio is 1:3, with this, one can calculate that $\sigma_{2\gamma}/\sigma_{3\gamma} = \lambda_{3\gamma}/\lambda_{2\gamma} = 1115/3 = 372$.

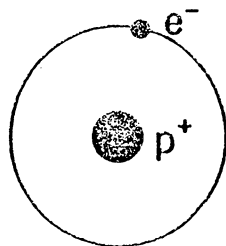
D. Basic Physical and Chemical Properties of Positronium

In some scientific communities, positronium is termed an "exotic" atom. This atom has been the subject of numerous research projects.

It results from the interactions of positrons with matter to form a stable positron-electron bound state. In 1934 Mohorovicic¹² proposed the existence of such an atom to account for the unusual emission spectra of some nebulae. It was not until 1951 that this atom was discovered in the United States by Deutsch.¹³ Today many scientists consider it to be the lightest atom in the universe (919 times lighter than hydrogen), being the only atom without a heavy nucleus. The ionization potential for the $e^+ e^-$ bound state was calculated to be 6.77 eV by Ruark.¹⁴ He also coined the name "positronium" for this bound state. The symbol for positronium, Ps, was first introduced in a paper by McGervey and de Benedetti.¹⁵

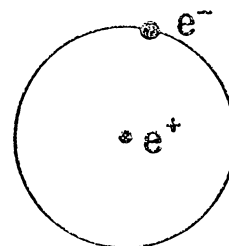
The comparison between positronium and hydrogen is shown in Figure 3. The reduced mass of the hydrogen atom is $\mu_H \approx m_e$, and the reduced mass of positronium atom $\mu_{Ps} \approx m_e/2$. From the simple Bohr theory, the binding energy (ionization potential) of the positronium atom can be calculated by $IP_{Ps} = e^4 MZ^2 / 2\hbar^2 n^2$ for a given principal quantum number n , and this value is one-half that of the ionization potential of hydrogen or 6.8 eV. The Bohr radius for Ps is $r = \hbar^2 n^2 / e^2 MZ^2$ and for $n = 1$ is twice the value of the hydrogen atom or 1.06 Å. The orbital velocity for the electron (and the positron) is $v = e^2 Z / \hbar n$. This is the same as in the hydrogen atom ($v = \lambda c \approx 2.2 \times 10^8$ cm/s for $n = 1$). The electron and positron revolve around each other thus constituting a two center system which should not react the same way as hydrogen does, which is a typical one-center system.

HYDROGEN-ATOM



REDUCED MASS: $\approx m_e$
BOHR RADIUS: 0.53 \AA
IONIZATION POT.: 13.6 eV

POSITRONIUM



$\frac{m_e}{2}$
 1.06 \AA
 6.8 eV

Figure 3. Characteristics of Hydrogen and Positronium.

Positronium, the bound state of an electron and positron, is formed in two ground states. A diagram showing these two ground states are shown in Figure 4. Singlet positronium (1S_0) or para-positronium (P-Ps) is formed when the positron and electron meet with their spins antiparallel. The wave function for para-positronium ($J=0, m=0$) contains both electron and positron parts and is

$$\psi_{0,0} = 1/\sqrt{2} \left[e^-(\alpha)e^+(\beta) - e^-(\beta)e^+(\alpha) \right] \quad (10)$$

Triplet positronium (3S_1) or ortho-positronium (o-Ps) is formed when the positron and electron meet with their spins parallel as shown in Figure 4b. There are three wave functions for o-Ps corresponding to $J=1, m=0, \pm 1$. They are the following:

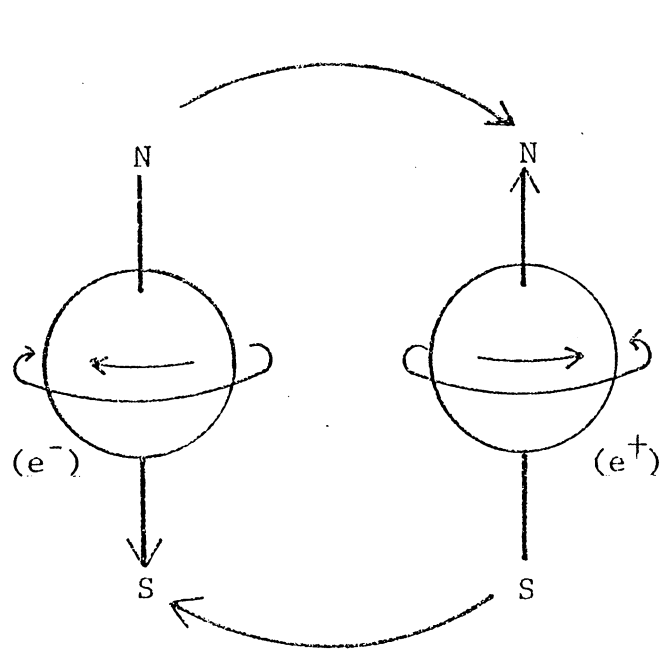
$$\psi_{1,1} = e^-(\alpha)e^+(\alpha) \quad (11a)$$

$$\psi_{1,0} = 1/\sqrt{2} \left[e^-(\alpha)e^+(\beta) + e^-(\beta)e^+(\alpha) \right] \quad (11b)$$

$$\psi_{1,-1} = e^-(\beta)e^+(\beta) \quad (11c)$$

where α and β are spin up ($\hbar/2$), and spin down ($-\hbar/2$), functions, respectively. Statistically then, 75% of the positronium formed is o-Ps and the remaining 25% should be para-positronium.

The intrinsic lifetime of p-Ps can be calculated from Equation (9). To correctly account for the density of the electron at the position of the positron, the term $\rho N_0 Z_{\text{EFF}}/M$ in Equation (9) must be replaced by the density of the electron wavefunction, $|\psi(0)|^2$, whose spins are antiparallel to that of the positrons. Since para-positronium is



Para-Positronium

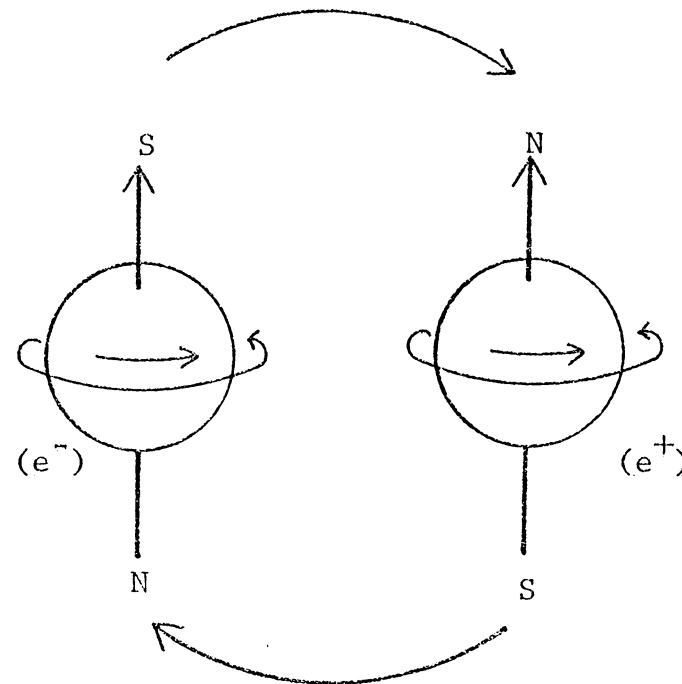
Singlet state 1S

Spins are antiparallel

Magnetic poles are parallel

Disintegrates into 2 photons

Intrinsic lifetime = 0.125 nsec



Ortho-Positronium

Triplet state 3S

Spins are parallel

Magnetic poles are antiparallel

Disintegrates into 3 photons

Intrinsic lifetime = 140 nsec

Figure 4. Some Physical Properties of Para- and Ortho-Positronium in the Ground State.

produced 25% of the time, a factor 1/4 must be inserted into the equation. Therefore, the annihilation rate for para-positronium can be calculated to be

$$\lambda_{2\gamma}^0 = 4\pi r_0^2 c |\psi(0)|^2 \quad (12)$$

For free positronium in the ground state,

$$|\psi(0)|^2 = 1/(\pi)(\mu_{Ps} e^2/\hbar^2)^3 \quad (13)$$

Substitution of values gives $\lambda_{2\gamma}^0 = 8 \times 10^9 \text{ sec}^{-1}$ for the annihilation rate. The intrinsic lifetime is $1/\lambda_{2\gamma}^0 = \tau_2^0 = 0.125 \text{ nsec}$. It can be seen that the intrinsic lifetime of ortho-positronium is 1115 times longer than para-positronium.

E. Models of Positronium Formation

Ore¹⁶ was the first to develop a model to accurately account for positronium formation in the gas phase but today it is also applied to Ps formation in the liquid phase. According to the Ore model, certain energy requirements must be met before positronium can be formed. In a collision between a positron and a substrate, M,



the positron abstracts an electron from the substrate. This reaction will depend on the ionization potential, IP_M , of the substrate. If the kinetic energy of the positron is greater than the ionization potential of the substrate, M, then the probability for ionization will predominate over positronium formation.

From this, the ionization potential of the substrate can be taken as the upper limit for positronium formation and the process will be endothermic when its ionization potential is greater than that of Ps. Therefore, only those positrons whose kinetic energies are greater than $IP_M - 6.8$ eV can form positronium. This is taken as the lower limit for positronium formation. As a general rule, the energy condition that must be met for positrons forming positronium is $IP_M > KE_{e^+} > (IP_M - 6.8)$ eV and the kinetic energy of the positronium formed will be between 0.0 eV and 6.8 eV. This positronium formation energy region is known as the "Ore gap." Competition between Ps formation and excitation of the substrate may occur if the kinetic energy of the positron is greater than the first excitation potential, E^* , of the substrate



The Ore model is based on the following simplified assumptions:

- (1) All positrons reach the top of the Ore gap, IP_M , without being annihilated.
- (2) There is a statistical distribution of positron energies in the Ore gap.
- (3) All positrons in the Ore gap will form positronium.

From these assumptions, it follows that the maximum positronium formation probability is $P_{MAX} = 6.8 \text{ eV} / IP_M$.

A general diagram to help explain the Ore gap model can be found in Figure 5. A typical Ore gap energy diagram and hypothetical positronium formation probability for argon gas is shown in Figure 6.

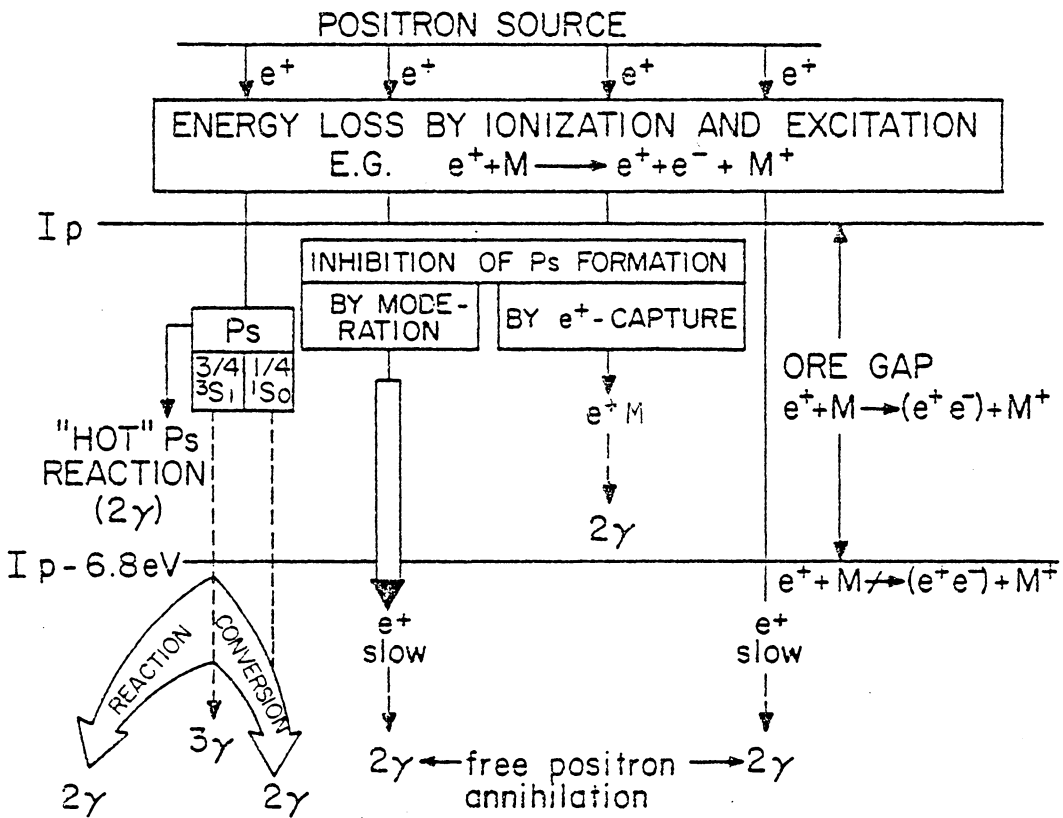
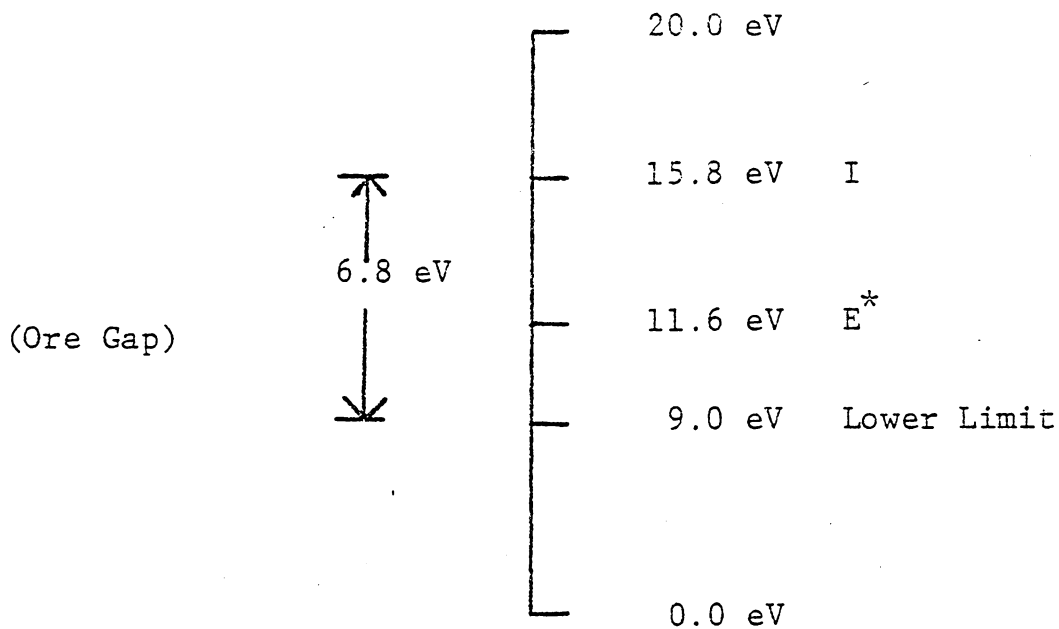
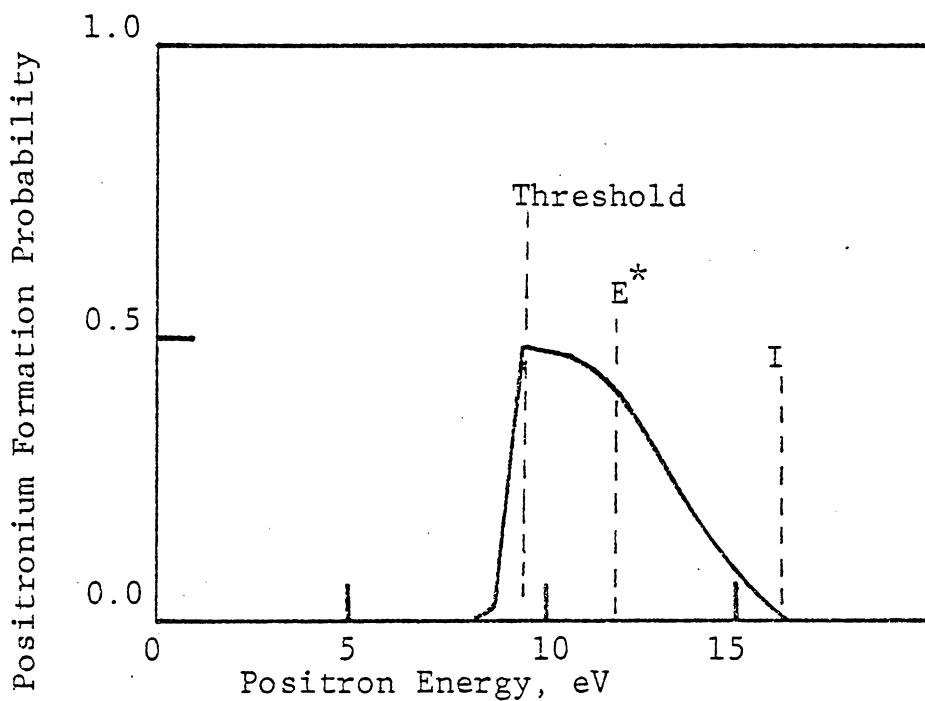


Figure 5. Ore Model of Ps Formation.



(a)



(b)

Figure 6. (a) Energy Diagram of the Ore Gap and
 (b) Hypothetical Positronium Formation
 Probability in Gaseous Argon.
 (From Ref. 16)

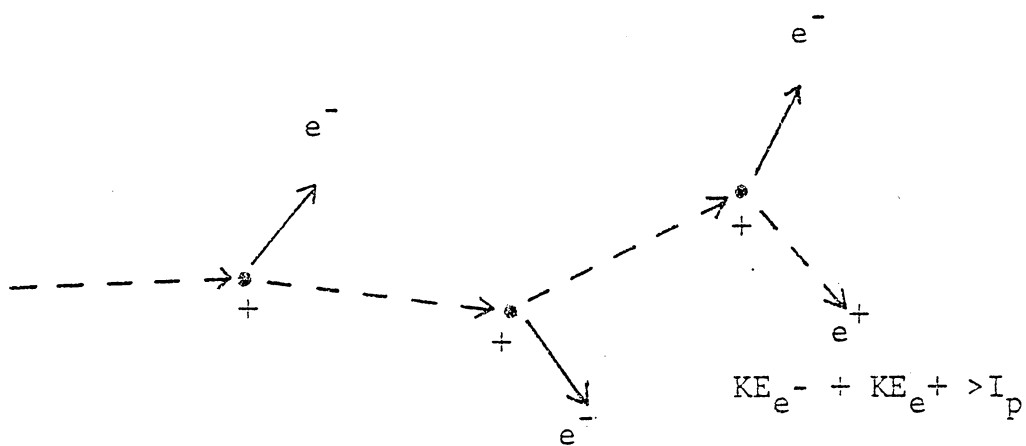
Gittleman¹⁷ performed several experiments on positronium formation in gases and he experimentally determined the positronium formation probabilities for a variety of gases to average about 30%.

In many cases, the ionization potential of positronium is less than the lower energy level of the Ore gap. In this region, positrons may undergo positron complex formation with the substrate. Positron complex formation is also possible in the Ore gap which will lead to inhibition of positronium formation. Besides positron complex formation, there is another process which can compete with positronium formation: moderation of the positron's energy below the lower limit of the Ore gap. The process of inelastic and elastic collisions could lead to agitation of molecular rotations and vibrations. Positron capture by addition of positrons to a substrate molecule XY can either be dissociative (16) or non-dissociative (complex formation) (17).

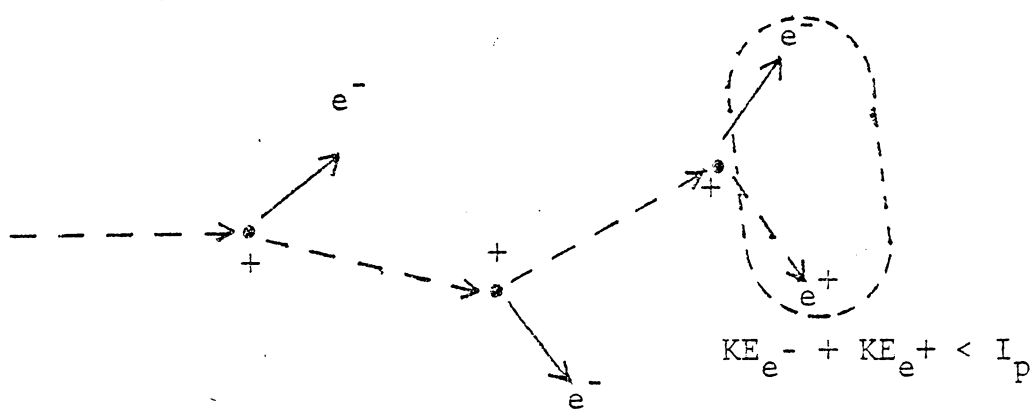


Experiments dealing with inhibition of positronium formation have been studied in many laboratories which confirm that not all positrons which reach the Ore gap actually form positronium. Thus the Ore model is capable of explaining simple reactions of positrons in the gas phase, but this model is of limited use in condensed phases where the width of the Ore gap must be considered to be a function of intermolecular forces like dipole-dipole interactions and a function of dissociation energies.

Mogensen¹⁸ recently proposed a new model for positronium formation in condensed phases which is known as the "spur reaction model." When an energetic particle is emitted in a medium, it is slowed down by causing ionization and electronic excitation of the medium (see Figure 7). The electrons, ions, free radicals, neutral molecules and excited molecules formed along the path of the energetic positron and those formed along the path of secondary electrons make up what is known as the "spur." Many of these metastable products in the spur have fairly long lifetimes on the order of microseconds or less, which is long compared to the intrinsic lifetime of positronium. Therefore, there is a high probability that a slow positron can pick up an electron in the spur and form positronium. The size of the spur has been estimated to range in size from 10\AA to 1300\AA . The size of the spur is a function of the molecules' structure, their ionization potentials and their dipole moments. According to Figure 7b, positronium is formed when a thermalized positron comes under the coulombic attraction of an electron in the spur so that the positron and electron move together. Energy conditions that must be met for this to happen are that $(KE_e^+ + KE_e^-) < IP_{Ps}$ (coulombic attractive force). According to this requirement, the positronium formation probability, P, should be a function of the separation distance, r_t , between a thermalized positron and a thermalized electron in a medium of dielectric constant ϵ . Then according to the Onsager equation, the probability for them to escape combination is $1-P = \exp(-r_c/r_t)$ where $r_c = e^2/kT$ where k is the Boltzmann constant, T is the absolute temperature and e is the



(a)



(b)

Figure 7. Formation of the Spur During the Last Path of the Positron. (a) No Positronium Formed. (b) Positronium Formation. (From Ref. 18)

electron charge. Then r_c should obtain a critical value when the potential energy of the positron and electron equals the thermal energy kT . It must be pointed out that other processes compete with positronium formation in the spur. They are electron capture, electron ion recombination, positron capture, and diffusion of both the electron and positron out of the spur. A change in solvent from a less viscous solvent to a more viscous solvent should confirm the diffusion of the positron and electron out of the spur. Any process leading to a longer lifetime of electrons in the spur should also increase the formation probability. One such process is the solvation of the electron. Any solvent whose molecules are unreactive toward the solvated electron should also lead to a higher formation probability. On the other hand, addition of electron scavengers, i.e., species with high electron attachment cross sections (high electron affinities) should cause the availability of the electrons in the spur to be reduced and hence the positron formation probability is reduced. This was indeed the case in several compounds studied by Wild, *et. al.*¹⁹ in this laboratory. Another process which can affect the number of available electrons is the presence of an electric field. According to Mogensen, the presence of an external electric field will decrease the Ps yield simply because some of the positrons and some of the excess electrons which probably would have contributed to the Ps formation are removed from the spurs by this field. Mogensen's spur model explains some of the experimental results but not all of them.

To account for the inability of the spur model to explain certain experimental results, Tao²⁰ proposed a new model known as the "modified

spur model." This model combines both the Ore gap and the spur reaction model and is made up of two reactions. According to Tao, the first reaction takes place when the total kinetic energy of the positron and electron pair is greater than the IP_{Ps} (6.8 eV). (See Figure 7a.)



The electron and positron in the spur are free to move with respect to each other thus being quickly moderated by the presence of densely packed molecules in the medium. According to the Ore model, the kinetic energy of these positrons and electrons will lie in the "Ore gap" thus forming positronium. The second reaction which could take place happens when the total kinetic energy of the positron-electron pair is less than IP_{Ps} . (See Figure 7b).



According to the spur reaction model, the positron will undergo a close encounter with an electron and the positron - electron pair will be drawn together by coulombic attraction thus causing the particles to move towards each other thus forming positronium. Because of the controversies still existing about the detailed mechanism of Ps formation, the results presented in this thesis are primarily discussed in terms of the Ore model.

F. Positronium Reactions

Positronium reactions can shorten the lifetime of Ps as compared with its intrinsic lifetime in free space as mentioned in Section D. This process occurs in all systems but it is less noticeable in para-positronium because its lifetime is so short that it doesn't have time to interact with the medium, but a shortening of the intrinsic lifetime of ortho-positronium from 140 nsec down to a few tenths of a nanosecond occurs in condensed phases. In the early literature, there are three main types of Ps reactions, classified as pickoff, conversion and chemical reaction. These reactions are shown schematically in Figure 8.

The so-called pickoff annihilation occurs shortly after the formation of Ps. The positron is removed from o-Ps when it undergoes a close encounter with the electron cloud of a substrate molecule and then is annihilated as a free positron together with an electron of an opposite spin from the substrate molecule. This encounter increases the overlap between the positron part of the wave function of o-Ps and the electrons of the substrate molecule thus increasing the electron density at the position of the positron in o-Ps. Hence the positron literally "picksoff" an electron from a substrate molecule. This process leads to a decrease in the o-Ps lifetime and an increase in the 2γ yield.

Several authors have been able to correlate the pickoff annihilation rate to various molecular parameters. Cook, Grey and Sturm²¹ experimentally determined the annihilation rate of 193 organic liquids. They observed a direct correlation between the average annihilation

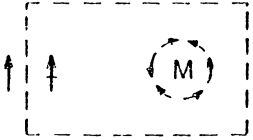

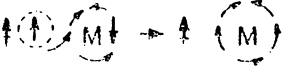
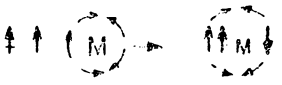
REACTION	MECHANISM	AVERAGE LIFETIME OF PRODUCT (sec)	PHOTONS EMITTED	AVERAGE LIFETIME OF o- Ps APPEARS TO BE
PICKOFF		—	$2\gamma/3\gamma = 372/1$	SHORTER
CONVERSION		1.25×10^{-10} (P-Ps)	2γ	SHORTER
OXIDATION		$\sim 0.5 \times 10^{-10}$ (IN COND. PHASE) (FREE POSITRON)	$2\gamma/3\gamma = 372/1$	SHORTER
COMPOUND FORMATION		est. $\sim 0.5 \times 10^{-10}$ (COMPLEX)	$2\gamma/3\gamma = 372/1$	SHORTER

Figure 8. Reactions of Ortho-Positronium (Intrinsic Lifetime $\tau_T^0 = 140$ nsec).

cross sections $\langle\sigma v\rangle$ and the electron polarizability of normal alkanes using their refractive indices. Using these values they were able to calculate partial quenching cross sections for 27 functional groups which can be used to predict molecular quenching cross sections since they are additive. The average error for the 151 calculated cross sections was 1.79%. The cross sections for the remaining 42 compounds could not be calculated due to unusual structures such as keto-enol forms. Difficulties were also encountered due to a low value of the o-Ps intensity, I_2 .

Berko, Brandt, and Walker²² were the first to relate the pickoff process in the condensed phase to a "free volume model." In this model, the positronium atom is assumed to be located in a position between the molecules. They made the following assumptions: (1) Mutual polarization of the lattice and the positronium can be neglected. (2) The positronium is assumed to be thermalized. (3) The lattice potential has the shape of a rectangle. The height of the potential well is U_0 , with radius, r_0 , corresponding to an excluded volume, V_0 , and electron density, ρ_0 . The unit cell has a radius, $r_1 > r_0$ and a cell volume V_1 . Then the free volume V^* , is $V_1 - V_0$. (See Figure 9 for a qualitative description.)

Molecular properties of the liquid, temperature changes, pressure changes, hydrogen bonding, steric hinderance, and viscosity, just to name a few, will affect the free volume of a liquid.

Then according to the "free volume model" an increase or decrease in the lifetime of positronium should be observed as the free volume changes. The lifetime of positronium will be decreased as the free volume is decreased. This decrease in free volume causes an increase

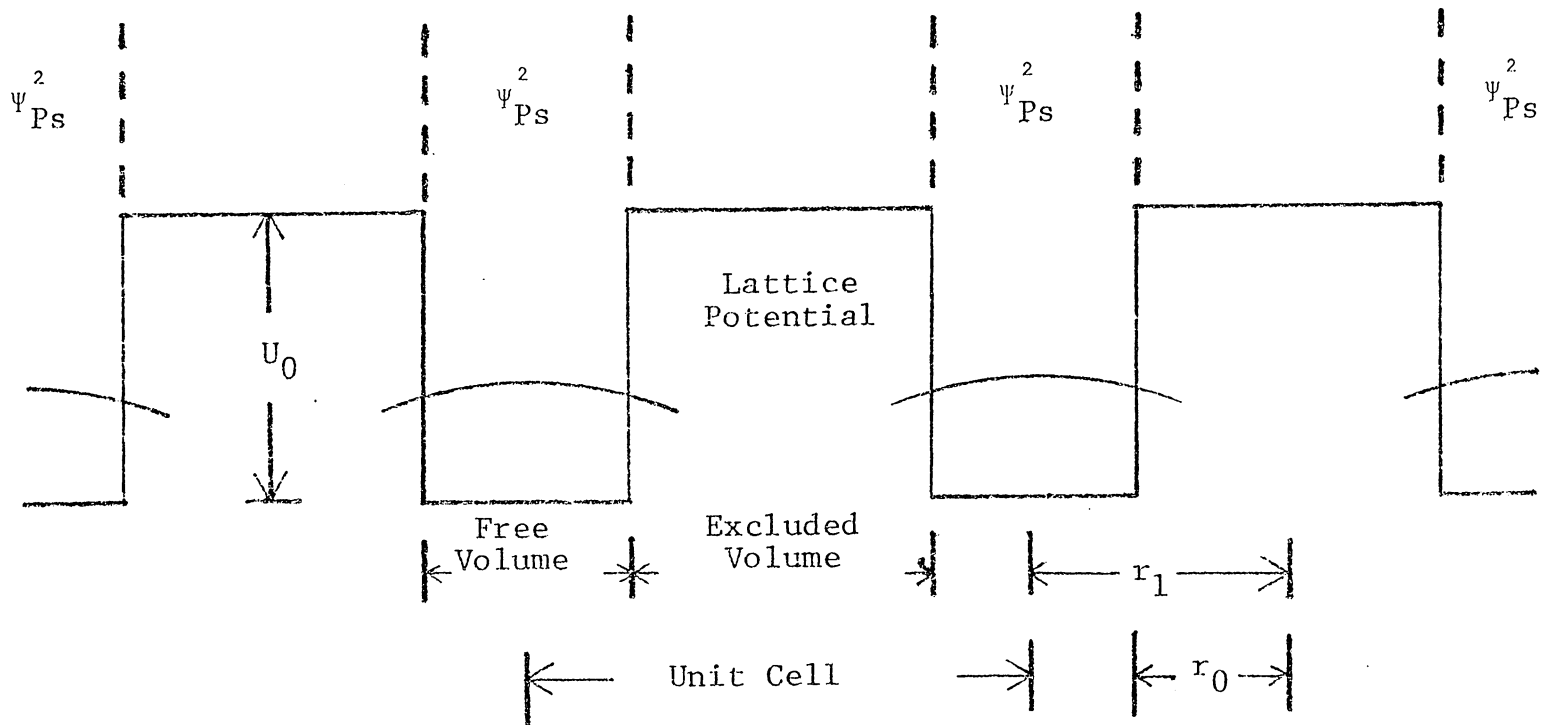


Figure 9. Lattice Potential as Represented by the Free Volume Model.
 (From Ref. 22)

in the electron density at the position of the positron in positronium. Experiments performed by Henderson and Millett²³ revealed that changes in pressure alters the lifetime of o-Ps. They showed that the lifetimes of o-Ps, τ_2 , in 22 organic liquids increases linearly with an increase in the specific volume ratio, v/v_0 , where v_0 is the volume at STP. Johnson, Stump, and Wilson²⁴ confirmed this behavior and they showed the relation between the lifetime of o-Ps and the pressure to be $\tau_2 = \tau_2^0 \exp(-\mu\Delta v/v_0)$ where μ is a constant for each liquid, Δv is the change in the volume as a function of pressure, τ_2^0 is the lifetime at 1 atm and 30°C. Therefore, the lifetime of Ps in a given substance will be inversely proportional to the density of the substance.

Using the "free volume model" positron lifetime studies on polymers can be used to characterize some of their physical properties. One such property of an amorphous polymer is its glass transition temperature, T_g . Since T_g is a function of the free volume which is in turn a function of the temperature, the lifetime of o-Ps will increase as one approaches T_g from a lower temperature. Stevens and Mao²⁵ used the changes in the lifetime of o-Ps to calculate the glass transition temperatures of atactic polystyrene. One can see that the mean lifetime of o-Ps depends sensitively on the temperature and physical state of the polymer. This again confirms the free volume model but it must be pointed out that this model is only valid when no other mechanisms compete with the pickoff process.

The de Broglie wave length of a thermalized (.025 eV) Ps atom at room temperature is calculated to be 55Å. This value is several times

larger than dimensions of the free volume. The Ps atoms in the condensed phase will have high mobilities with ranges close to intermolecular spacings.

When o-Ps is converted to p-Ps and when p-Ps annihilates it emits two photons in opposite directions ($\theta=\pi$) depending on whether the center of mass of the positron-electron pair is at rest. Generally, the center of mass of the pair is not at rest as evidenced by angular correlation studies. The electron-positron pair does possess some kinetic energy when they annihilate and a plot of the number of counts versus the angle (θ) appears as a bell shaped curve centered around $\theta=\pi$. The deviation from 180° is given by $\Delta\theta \approx 2v/c$ where v is the velocity of the electron-positron pair and c is the speed of light. These deviations are only a few milliradians in all practical cases. These plots should reveal some information about the momentum distribution in the free volume and also about electron momentum distribution. Using this technique, the momentum distribution,²⁶ $G(p)$ versus p , (the momentum) can be calculated. According to Ferrell,²⁷ this momentum distribution should consist of two components, as shown in Figure 10. The first component is attributed to self-annihilation of the positron-electron pair where the electron comes from a free electron and should give rise to a low momentum component, I_N . The higher component is due to pickoff annihilation of the positron in o-positronium with a "tight" or bonding electrons in the substrate. The intensity of p-Ps, I_N , in the momentum distribution should be equal to $I_2/3$, one-third of the o-Ps intensity in the lifetime spectra. Chuang, Hogg, and Kerr²⁸

ANGULAR DISTRIBUTION CURVE

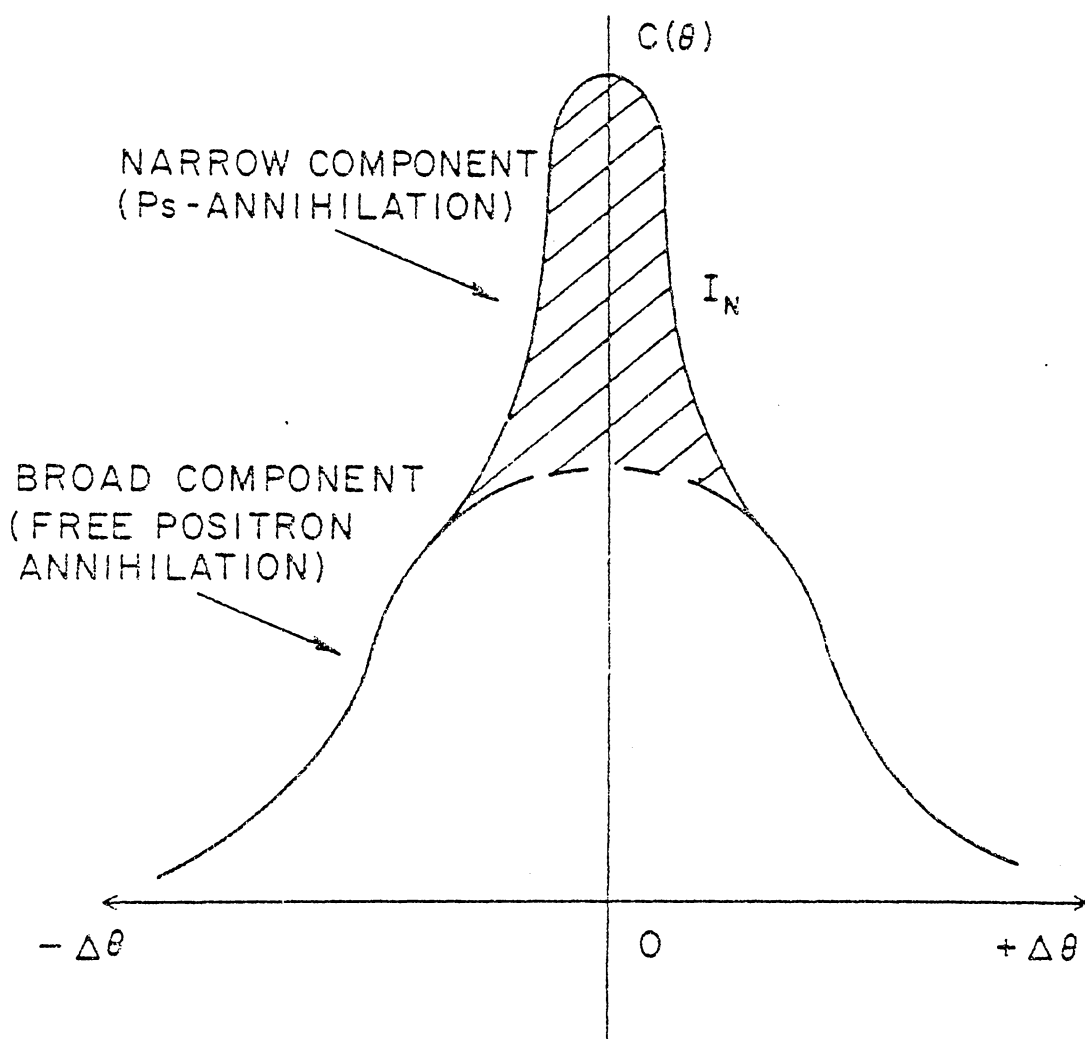
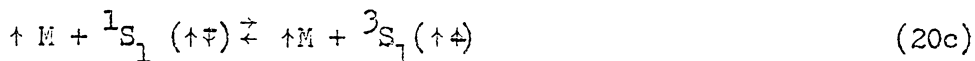
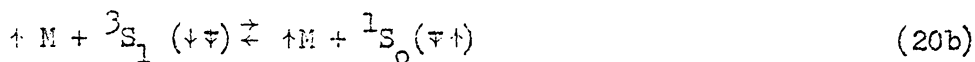
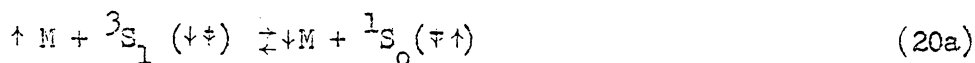


Figure 10. Angular Distribution in Two-Photon Annihilation.

used this relationship to calculate the momentum distribution in benzene and hexane along with the halogenated derivatives of these compounds. These authors concluded that pickoff annihilation in these compounds occurred almost exclusively with the electrons in the carbon-halogen, C-C, C-H, bonds. These correlations also confirm the "free volume model." Using angular correlation studies, they showed that the areas under the curves A and B in Figure 11 are related to the number of electrons in the C-C, C-H hybrid orbitals.

The second type Ps-reaction is the spin conversion which occurs when positronium comes under the influence of a magnetic species such as O_2 , NO_2 , NO , and certain transition metal cations and their complexes. In this process, the electron in positronium can undergo a spin flip as shown in Equation (20), resulting from an exchange of electrons in the collisions of o-Ps or p-Ps with paramagnetic species. Either o-Ps to p-Ps or p-Ps to o-Ps but the latter possibility (20c) is highly unlikely due to the short lifetime of p-Ps.



By using quantum mechanical arguments, Ferrell²⁹ was able to show that the only condition for a spin flip to occur is that o-Ps or p-Ps undergo a close encounter with an atom or molecule having unpaired electrons. It is not necessary for the unpaired electron of the

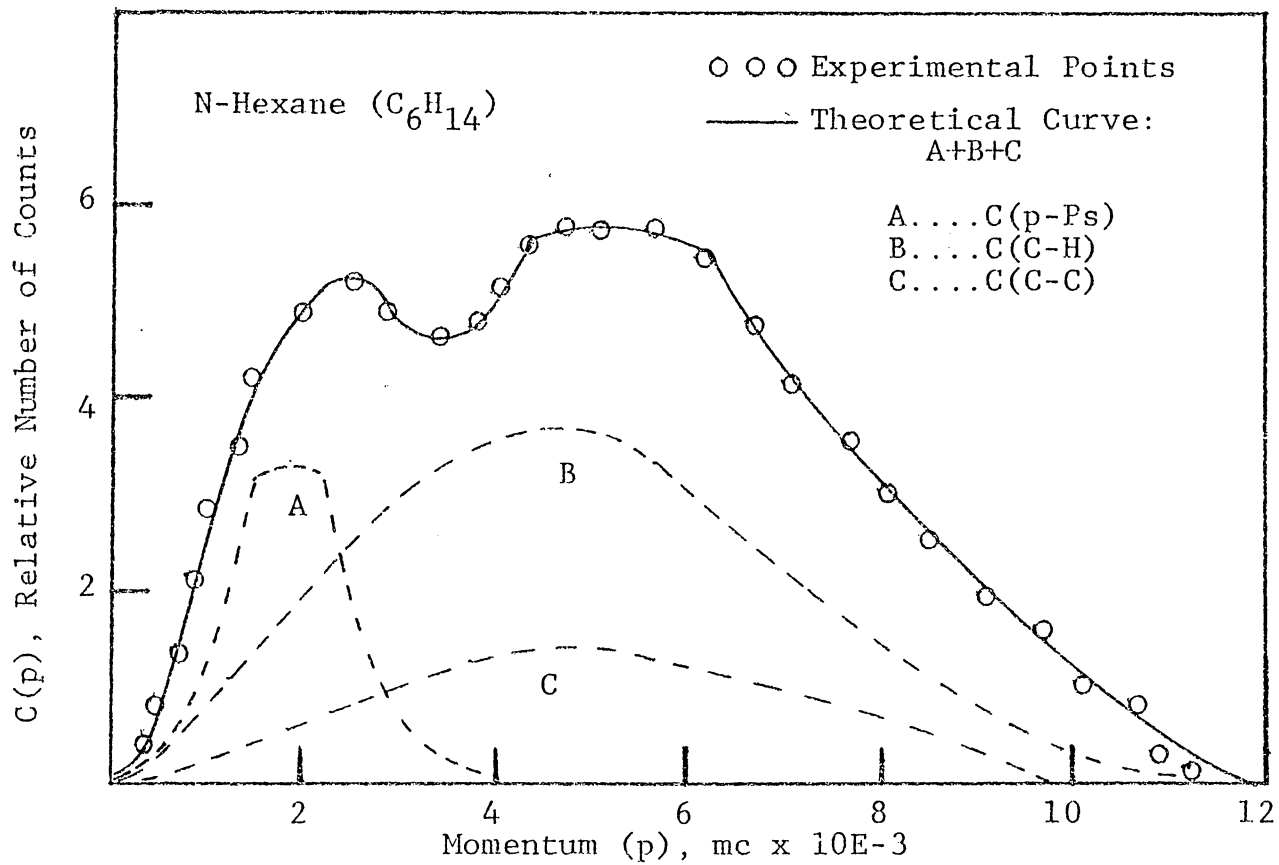
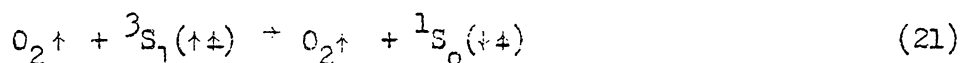


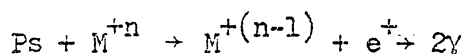
Figure 11. Computed and Experimental Momentum Distributions for N-Hexane. (From Ref. 28)

substrate, M, to undergo a spin flip as evidenced from Equation (20b). For example, oxygen molecules in the triplet state can cause a spin flip of the electrons in o-Ps while its own electron will not undergo a spin flip.

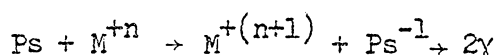


The third type of Ps reactions are different types of chemical reactions. This category can be broken down into four subcategories according to Tao and Green:⁸

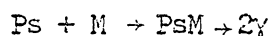
1) oxidation by electron transfer



2) reduction



3) compound formation



4) double decomposition



Double decomposition is a rare event and it seldom happens, but it can be important for positronium atoms above thermal energies. This thesis is concerned with the first and third type of the chemical reactions which will be discussed in Chapters 3 and 5, respectively.

EXPERIMENTAL TECHNIQUES

A. Introduction

There are several exotic particles associated with nuclear decays and nuclear reactions. These particles have very short lifetimes on the order of less than 10^{-4} seconds. The lifetimes of these particles can be determined by delayed coincidence techniques. One of the most widely studied exotic particles is the positron. The lifetime of this particle is mainly measured by using delayed coincidence techniques.³⁰

This technique requires that a start pulse be used from a nuclear event to signify the beginning of this event and a stop pulse to signify the end of this event. From the elapsed time between these pulses, the lifetime of the positron can be determined. Problems in physics and chemistry research often require the analysis of distributions of time intervals in very short times. Bell³¹ and his co-workers introduced a sophisticated electronic device called the time-to-pulse-height-converter (TPHC) to drastically improve the lifetime measurements of the positron. They also introduced the fast-slow principle to obtain better resolution of the lifetime measurements. Basically, this instrument measures the time interval between separate start and stop logic pulses and converts them to an output pulse whose amplitude is precisely proportional to this interval.

Specially designed dewars and sample vials were developed to make measurements on various systems in this work. By varying the experimental conditions such as temperature and solvent, different thermodynamic quantities were determined from the lifetime spectra of the

positron and from the lifetime of o-positronium. From these different quantities, kinetic and thermodynamic information can be obtained and hence the mechanism by which the positron and positronium react can be determined. More specifically, the mechanism of o-positronium-complex formation was determined. This thesis was devoted to the study of o-Ps complex formation and how this complex can be used to investigate the effects of the environment on this complex.

B. Positron Sources

Today, in positronium chemistry, two sources of positrons are commonly used, copper-64 and sodium-22. Copper-64 is mainly used in angular correlation studies where high specific activities are required. All the data taken in this work originated from the use of sodium-22.

Sodium-22 has a half life of 2.58 years. It can be bought from any number of radionuclide manufacturers as carrier free $^{22}\text{NaHCO}_3$ or $^{22}\text{NaCl}$ solutions. Carrier free sodium-22 used in this work was diluted to a specific activity from 3 to 5 μCi . The decay scheme of ^{22}Na is shown in Figure 12. From the diagram one can see that 90% of the decays of ^{22}Na produce positrons. Electron capture (EC) decay accounts for the other 10% of the decays. From the diagram, one can also see that the ground state of ^{22}Na is 2.840 MeV above the ground state of ^{22}Ne and 1.564 MeV above the first excited state of ^{22}Ne . The positron will have a maximum kinetic energy of only 0.544 MeV because of the energy requirements based upon positron decay as explained in Chapter 1. The transition from the first excited state of ^{22}Ne to the ground state of ^{22}Ne takes only 3 psec. The energy difference between these two levels is

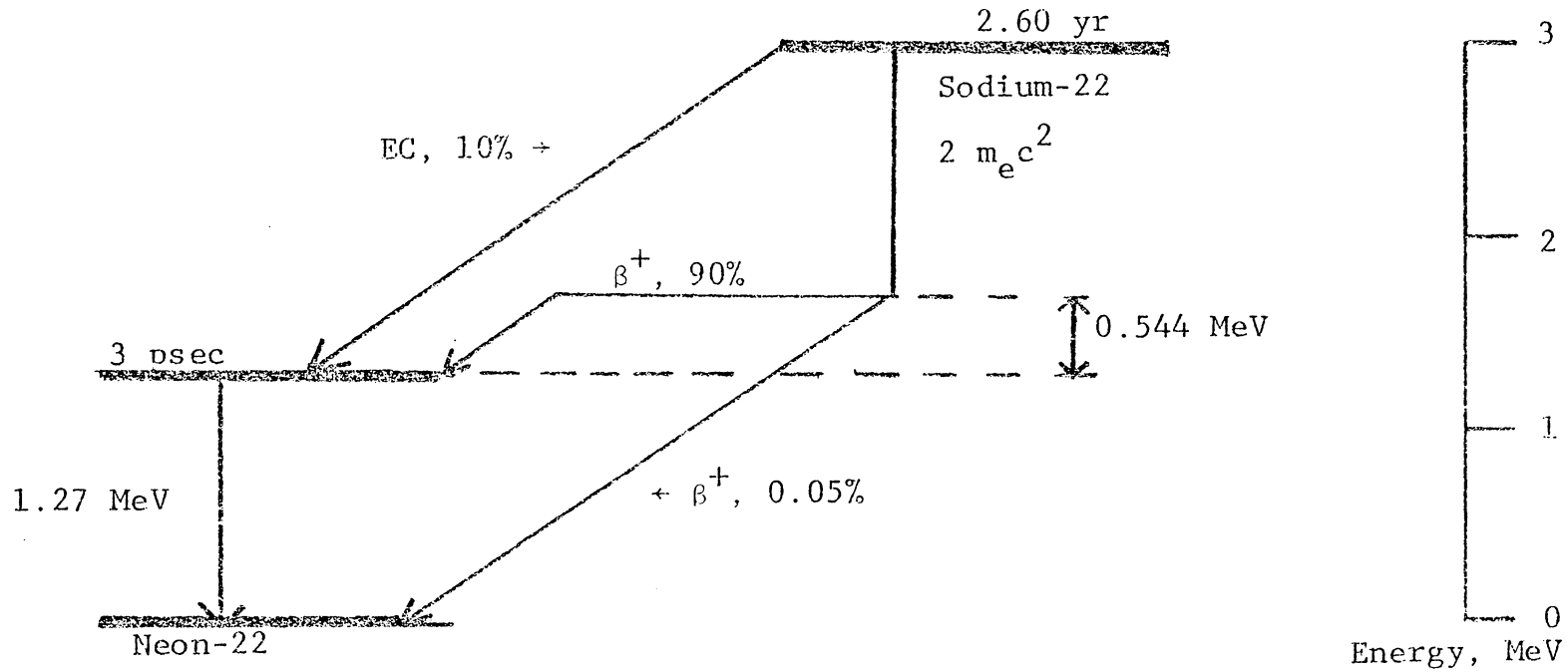


Figure 12. Decay Scheme of Sodium-22. (From Ref. 32)

(2.840 - 1.564 MeV) 1.276 MeV which is energy liberated as a gamma-ray. So, for all practical purposes, one can assume that the birth of the positron and the emission of the 1.276 MeV gamma ray occur simultaneously and this gamma ray can be used to start the zero-time start pulse needed in the fast-slow coincidence timing circuit.

Aluminum foils were used for the studies of o-Ps complex formation. These foils were about 5 mm by 10 mm with a thickness of about 0.021 mm. These sources were prepared by adding the sodium-22 solution drop by drop from a 1 ml syringe with a number 25 tip on the Al foil. The drops on the aluminum foil were then dried under an incandescent lamp at atmospheric pressure. This was repeated several times until the desired activity was reached. Since some of sodium-22 will dissolve in the solvents used, the foil must be resupplied with sodium-22 after about 4 uses. The sodium-22 lost in the solution can be recovered and reused by evaporating the solution to dryness and dissolving the residue in distilled water.

A new source has been devised by Dezsi, Kajcsos and Molnar³³ and all data collected during the CuCl_2 and inclusion compound studies were carried out with this new source. It consisted of a thin foil of soda lime glass into which ^{22}Na has been diffused. Furthermore these glass foils have an almost infinite lifetime depending on how carefully the researcher handles them. The introduction of this new source proved to be very economical since less than 1% of the initial ^{22}Na is lost after the first use and subsequent uses showed no further losses of Na. The repeated use of these foils prevents the generation of

large amounts of liquid radioactive waste as is the case if ^{22}Na is directly added to the solution.

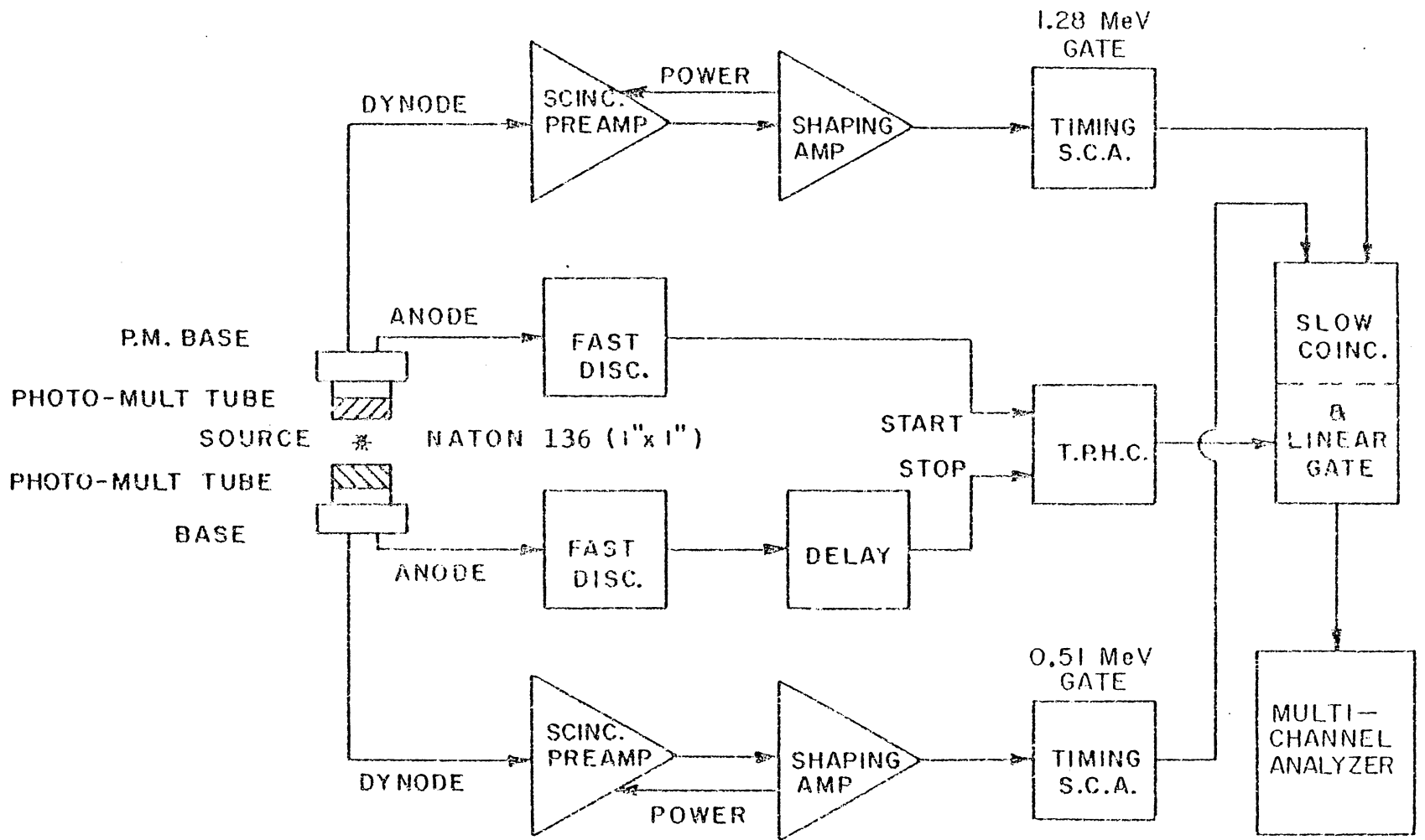
These glass sources were prepared by dropping 3-5 μCi of ^{22}Na from a 1 ml syringe with a #25 needle tip onto a 7 mm by 15 mm soda lime glass foil with a thickness of 0.03 mm. After each drop was deposited on the glass, it was dried by the use of an incandescent lamp at atmospheric pressure. After the desired amount of ^{22}Na had been deposited on the glass foil, the glass source was annealed in an oven for 24 hours at 1000°F . At this temperature, 99% of the ^{22}Na had been diffused into the soda lime glass. The source was then checked in nitrobenzene, a solvent which quenches thermal o-Ps, and was found to have an I_2 , which is the intensity of the long lived component in the positron lifetime spectra, (see below) of less than 2%. In addition to the use of these new glass sources during this thesis research, two new types of sample vials were developed. One vial was designed for concentration studies at room temperature and the other was for temperature studies. These vials will be discussed under the section on sample preparation.

C. Fast-Slow Delayed Coincidence Counting

There are three different types of experiments which can give information about the environment in which positrons annihilate. They are: (1) the distribution in time of the two photon annihilation events, (2) the three photon or two photon annihilation rates, the sum of which must remain constant from substance to substance, and (3) the

angular correlation between the two photons in 2γ annihilation. All experiments in this thesis were carried out via the first method and the data were collected by use of the fast-slow coincidence timing system in Figure 13. As seen from the diagram, each unit is made up of a phosphor optically coupled to a photo-multiplier (PHOTO-MULT) tube. The phosphors used in this work were Naton 136 plastic scintillators whose dimensions are 1" by 1". The decay time of these plastic scintillators are short as compared to lifetime of the positrons and they have a higher light output than other scintillators (NaI(Tl)). The photomultiplier tubes used were 12 stage (diodes) RCA 8575 mounted onto an Ortec 265 photomultiplier base (PM BASE). These bases were used because they produced the highest gain, fastest rise time, and they have low thermal noise. The output signals from these detectors are then simultaneously fed into two coupled electronic circuits. From the diagram, one can see that one circuit consists of a fast inner loop and the other a slow outer loop. Each circuit has two sides, a start and a stop side.

The inner circuit was used to accurately determine the time interval between the birth of the positron and its subsequent annihilation into two 0.51 MeV gamma-rays. The output from the anode of the detector (PM BASE) is fed directly to an Ortec 417 constant timing unit (FAST DISC). Operating at a biased voltage, the units can be set so as to minimize the noise levels in the circuit by controlling the lower threshold limit for accepting pulses from the photomultiplier tube. Each of the two fast discriminators produces fast timing pulses which are sent directly to an Ortec 437 time-to-pulse-height-converter (TPHC).



47

Figure 13. Simple Fast-Slow Timing System

When the zero-time pulse arrives, a clock in the TPHC is started and a pulse whose height is proportional to the time difference between the birth of positron and its annihilation, the latter indicated by the arrival of a stop pulse generated by the 0.51 MeV photon, is produced. If no stop pulse is seen within a preset time (0.05 μ s), the unit is reset back to zero and awaits another start pulse. The pulse from the TPHC must meet certain energy and coincidence conditions before it is allowed to pass into the multichannel analyzer (MCA). This is accomplished by the so-called slow circuit which assures that one is timing an event from the same nuclear event, i.e., birth of the same positron to its annihilation. An Ortec 425 variable delay unit is put into the fast circuit to calibrate the channel width, time increment per channel, of the multichannel analyzer. Pulses from the dynodes of the photomultiplier tubes are used in this circuit. Since these pulses are rather weak, they must be amplified by using an Ortec 113 scintillation preamp (SCINT PREAMP), and then shaped and amplified by using an Ortec 440 shaping amplifier (AMP). Both the start and stop sides of the slow circuit use an Ortec 420 timing single channel analyzer (TIMING SCA). One single channel analyzer (start side) was biased by setting an energy window at about 1.28 MeV. This is the energy resulting from the de-excitation of the first excited state of ^{22}Ne to the ground state of ^{22}Ne when a positron has been emitted. If a pulse is larger or smaller than this energy, the single channel analyzer will reject the pulse, therefore, letting pass only the pulses with the correct energy. The stop side of the slow circuit has a timing single channel analyzer which is set at about 0.511 MeV and works as described above

for the start side. The 0.511 MeV signifies the annihilation of the positron. If both start and stop pulses reach the Ortec 409 slow coincidence (COINC) and linear gate unit within a preset time interval, the slow coincidence unit will open the linear gate and the signal from the time-to-pulse-height converter (TPHC) will be allowed to pass into the multichannel analyzer. This preset time was set at 1 μ s. This time is called the resolving time of the instrument. A Packard 400 channel multichannel analyzer was used to sort the pulses from the time-to-pulse-height converter. Each channel corresponded to a certain time (0.07 nsec). Once 20,000 counts were stored in the zero channel of the M.C.A., the data of these pulses were then retrieved and punched out on paper tape so that the information can be transferred to computer cards and then to the computing center for lifetime analysis of the positrons.

In summary, the positron lifetime measurement starts when the start detector receives the zero-time pulse, which corresponds to the emission of a positron, and continues until the stop pulse from the annihilation of that positron is received from the stop detector. After this, the lifetime of the positron is stored in the MCA and the coincidence circuits are erased in order to measure the lifetime of another positron, thus repeating this on and on, until 20,000 coincidences are stored in the zero channel of the MCA. This procedure is the same as if there were a large number of positrons at time $t=0$ and observing their lifetime distribution.

D. Instrument Calibration

The lifetime measurements had to be calibrated before any values could be reported. For this, the channel number corresponding to a zero time event had to be known as well as the time interval per channel (Δ) for the multichannel analyzer. This was accomplished by counting an aqueous ^{60}Co source sealed in a pyrex tube with the energy windows set at 1.27 MeV and 0.51 MeV which are the start and stop signals, respectively. ^{60}Co emits two photons simultaneously which has energies at 1.173 MeV and 1.333 MeV. The 1.333 MeV photon triggered the start circuit while Compton scattering from the 1.113 MeV photon triggered the stop pulse. Ideally, the time interval between the detection of the start and stop signals should be zero and one should observe a sharp spike where all the counts (coincidences) are stored in the one channel of the MCA. Instead, a broadening of the peaks was observed which was due to "jitter" in the circuits which is caused by time uncertainties from noise in the signal or the discriminating circuit. The counting system was also calibrated using a standard consisting of a glass source in benzene sealed in a pyrex tube.

In order to determine the time interval per channel (Δ), a delay of a known number of nanoseconds was used in the stop side of the fast circuit by using an Ortec 425 variable delay unit. This shifted the zero channel to the right about 100 channels as shown in Figure 14. Thus the time interval between the channels (Δ) can be calculated by dividing the difference between the two channels by the delay in nanoseconds used to shift the zero channel to the right.

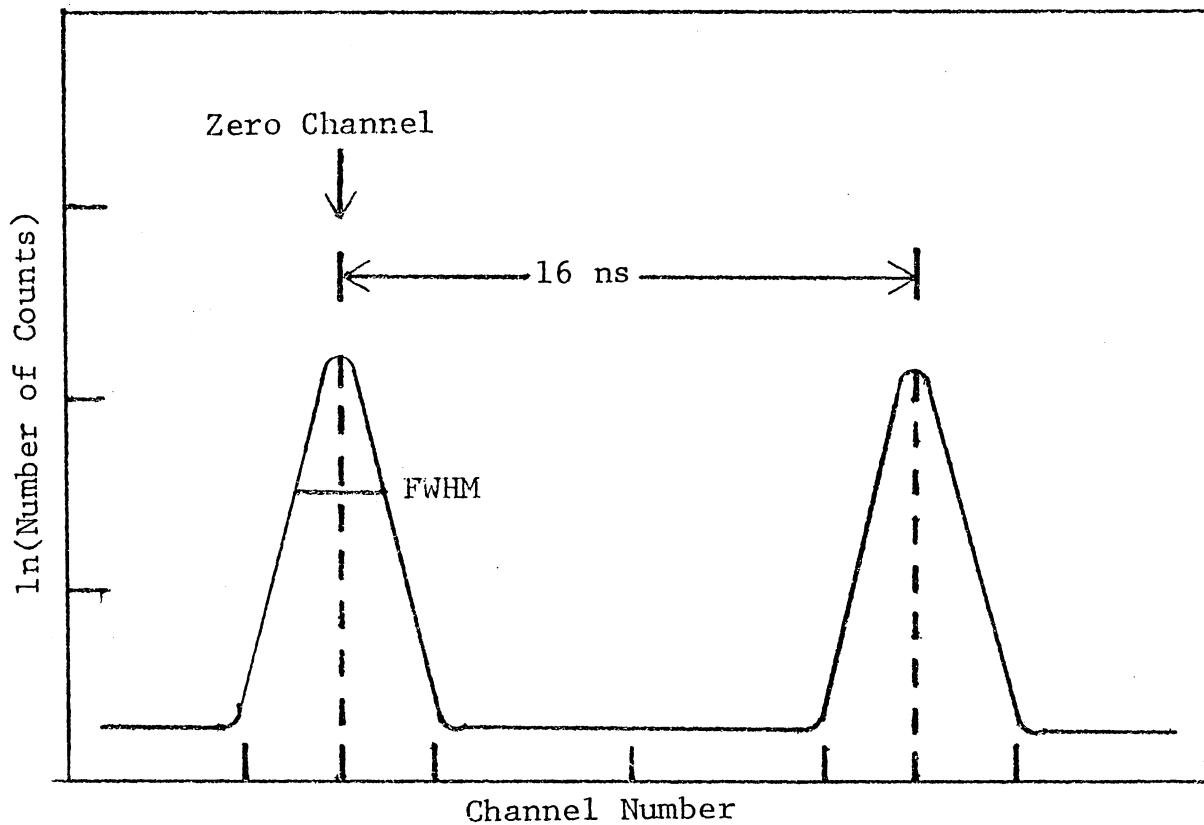


Figure 14. "Prompt" Cobalt-60 Calibration Spectrum.

The value for delta used in the collection of all the data in this thesis was 0.07 nsec/channel. The resolution of the instrument can then be calculated by the product of delta times the full width at half maximum for a prompt ^{60}Co peak. The resolution for the data taken in this work was less than 400 psec. The resolution could be improved by narrowing the window around 0.51 MeV at the expense of a decrease in count rate.

E. Positron Lifetime Spectra

The counting system just described was used to measure accurately the two photon time dependent annihilation rate, $R_{2\gamma}(t)$, of positrons. Shown in Figure 15 is a plot of the natural log of the number of counts (coincidences) on the ordinate axis versus time on the abscissa. The maximum number of counts appears in the zero channel ("prompt").

All of the reactions with positrons in this study were run in the condensed phase. Therefore, the lifetime spectrum of the positrons will appear as two components. The first or short lived component, λ_1 , (steepest slope) will be due to the decay of free positrons which have not formed a bound state, to the decay of p- P_s and possibly to the hot Ps reaction products. These three lifetimes cannot be resolved by the instrument used in this work. The second or long lived component, λ_2 , is due to the decay of ortho-positronium. It is important to note that even though ortho-positronium is the triplet state with 3 photon decay, its positron annihilates as a consequence of the various reactions which the ortho-positronium undergoes with a singlet electron by two photon emission. As one can see, this can drastically reduce the

lifetime of ortho-positronium thus giving one valuable information about the mechanisms responsible for its reduction.

A multicomponent exponential spectrum can be represented as the following:

$$N(t) = \sum_i A_i e^{-\lambda_i t} + \text{Background} \quad (1)$$

where A_i 's are the pre-exponential factors which weight each individual component, and the λ_i 's are the rates for the different modes of positron decay. Since the number of counts as a function of time is just the rate for the two photon process, and since we are dealing with a two component exponential spectrum, Equation (1) can be rewritten as

$$R_2\gamma(t) = D \exp(-\lambda_1 t) + C \exp(-\lambda_2 t) + \text{background}$$

where D and C are related to the number of positrons annihilating with rates λ_1 and λ_2 , respectively. For a two component positron lifetime spectrum, the relative areas under each component is referred to as the intensities (I). (See Figure 15). The intensity of the long lived component, I_2 , can be related to the amount of o-Ps formed, and the intensity of the short lived component, I_1 , can be related to the number of p-Ps formed, amount of free positrons annihilating and possibly to the number of Ps undergoing hot reactions, but these three components cannot be resolved by the instrument used in this research. I_1 and I_2 are calculated by integrating the positron lifetime spectrum from $t=0$ to $+\infty$ and compared with the total area of the lifetime spectrum. These intensities along with their respective λ 's can be calculated by a computer program originally written by Gunning³⁴ and

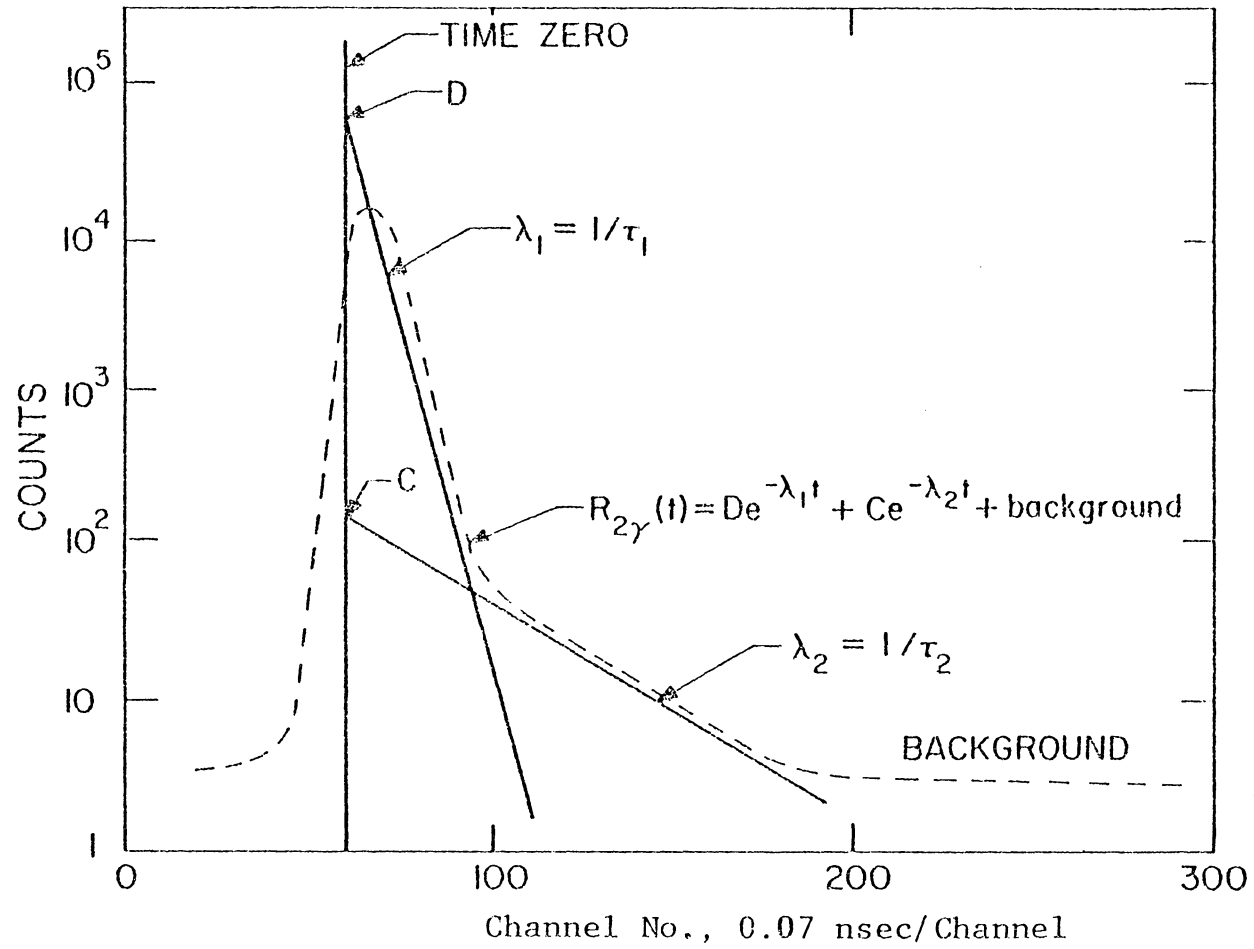


Figure 15. Typical Positron Lifetime Spectrum.

Tao³⁵ and then modified in this laboratory. The programs were run on an IBM 370/155 computer system at the Virginia Tech Computing Center. Basically, the program performs a linear least squares analysis on each component in the spectrum beginning with the longest lived component and then constructs a calculated spectrum. If the fit (complicated function of the standard deviation) of the calculated spectrum to the actual spectrum is less than two, which is a good fit, the values of the I's, λ 's and the fit will be printed out. These values were calculated using the PAL program, which is just the modified version of Tao's and Gunning's program. Using the PAL program, these values along with a Calcomp Plot of the experimental spectrum together with the calculated spectrum are obtained as a permanent print out for rate constant determinations. A typical Calcomp Plot of a benzene standard is shown in Figure 16.

This figure is a plot of the base ten logarithm of the coincidence rate versus time which is the same as a first order reaction with slope, λ_i , equal to the rate of decay. The lifetime and the intensity of the two components as calculated by the PAL program are $\tau_1 = 0.353$ nsec, $\tau_2 = 3.00$ nsec, $I_1 = 63.5\%$, and $I_2 = 36.5\%$. It must be noted that $\lambda_i = 1/\tau_i$. Due to the finite time resolution of the positron-lifetime measurement fast-slow coincidence circuit, the PAL program starts the calculations of the parameters I_i , λ_i a few channels to the right of the zero channel lifetime spectrum. The total area under the two components is normalized to 100%. In this work, λ_1 remained fairly constant at 2.8 ns^{-1} in the liquid phase.

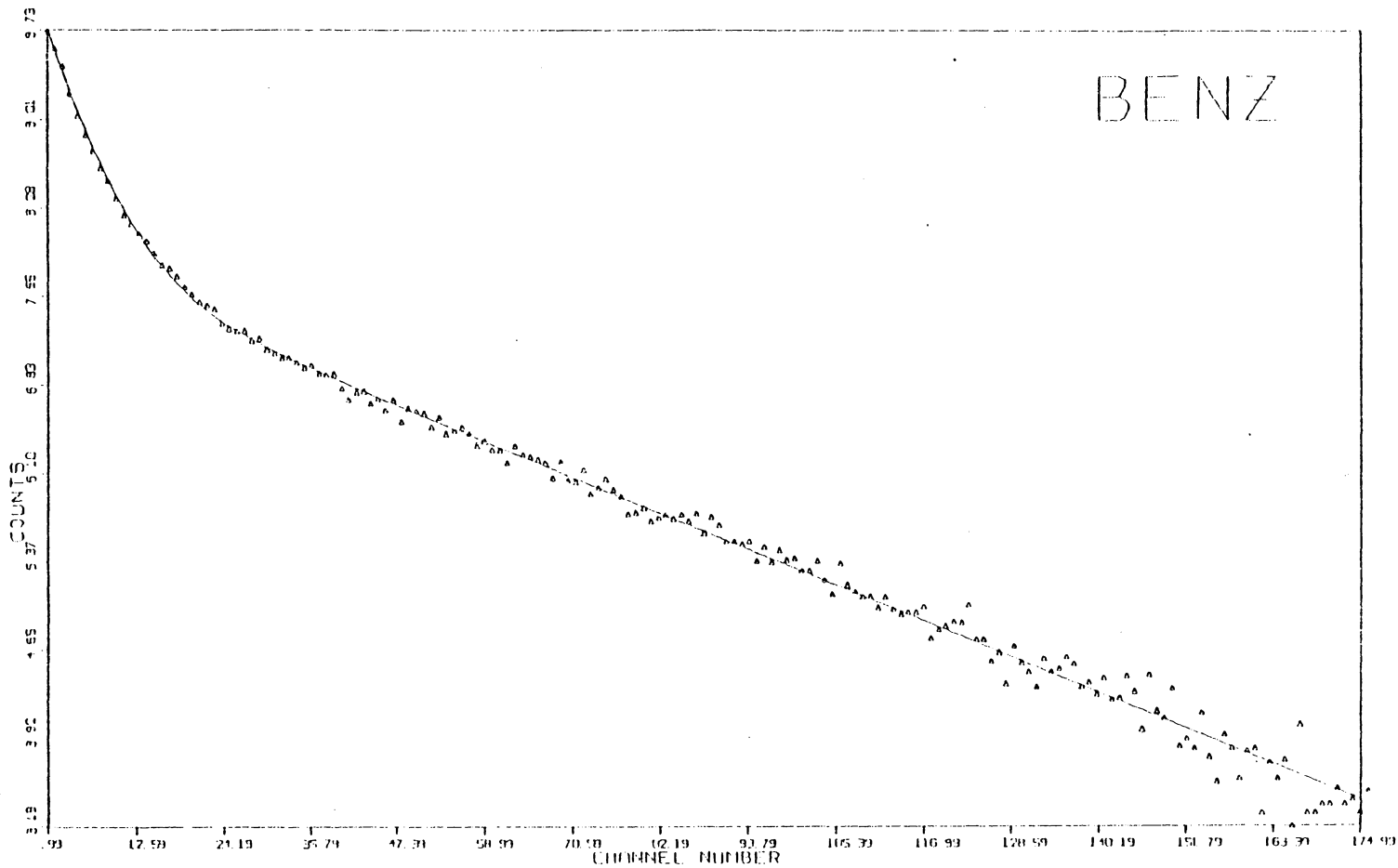


Figure 16. Calcomp Plot of Benzene Standard.

Of chemical interest are the annihilation rates of ortho-positronium, λ_2 , and its intensity, I_2 (amount of o-Ps formed). However, several researchers have used the program POSITRON-FIT³⁶ to analyze for three components in the position lifetime spectrum. This program can also be used for source corrections when calculating λ_2 and I_2 but was not needed here because the number of positrons annihilating in the glass source is small (less than 2%) and therefore the PAL program proved sufficient.

F. Sample Preparation

Two different specially designed cylindrical pyrex glass sample vials were used in the collection of data. The sample vial used for the data taken at room temperature is shown in Figure 17. This special vial is about 250 mm long and has a 20 mm i.d. at the top and 10 mm i.d. at the bottom. A side arm at an angle of 60° was attached to isolate the glass source from the solution while degassing. This side arm was used because while freezing the solution, the glass foil would be broken if it were in the solution. The base of the sample vial was V shaped for two reasons: (1) it prevented the vials from cracking during degassing of solvents which expanded on freezing, (2) and it prevented the sample from climbing up the sides of the vial while thawing out which would cause some of the sample to adhere to the sides thus changing the concentration of the sample. 2 ml of the sample were introduced into the sample vial by means of a glass capillary syringe. The top was then put on the vial and was held by means of a #35 clamp. The stopcock was closed and the vial was

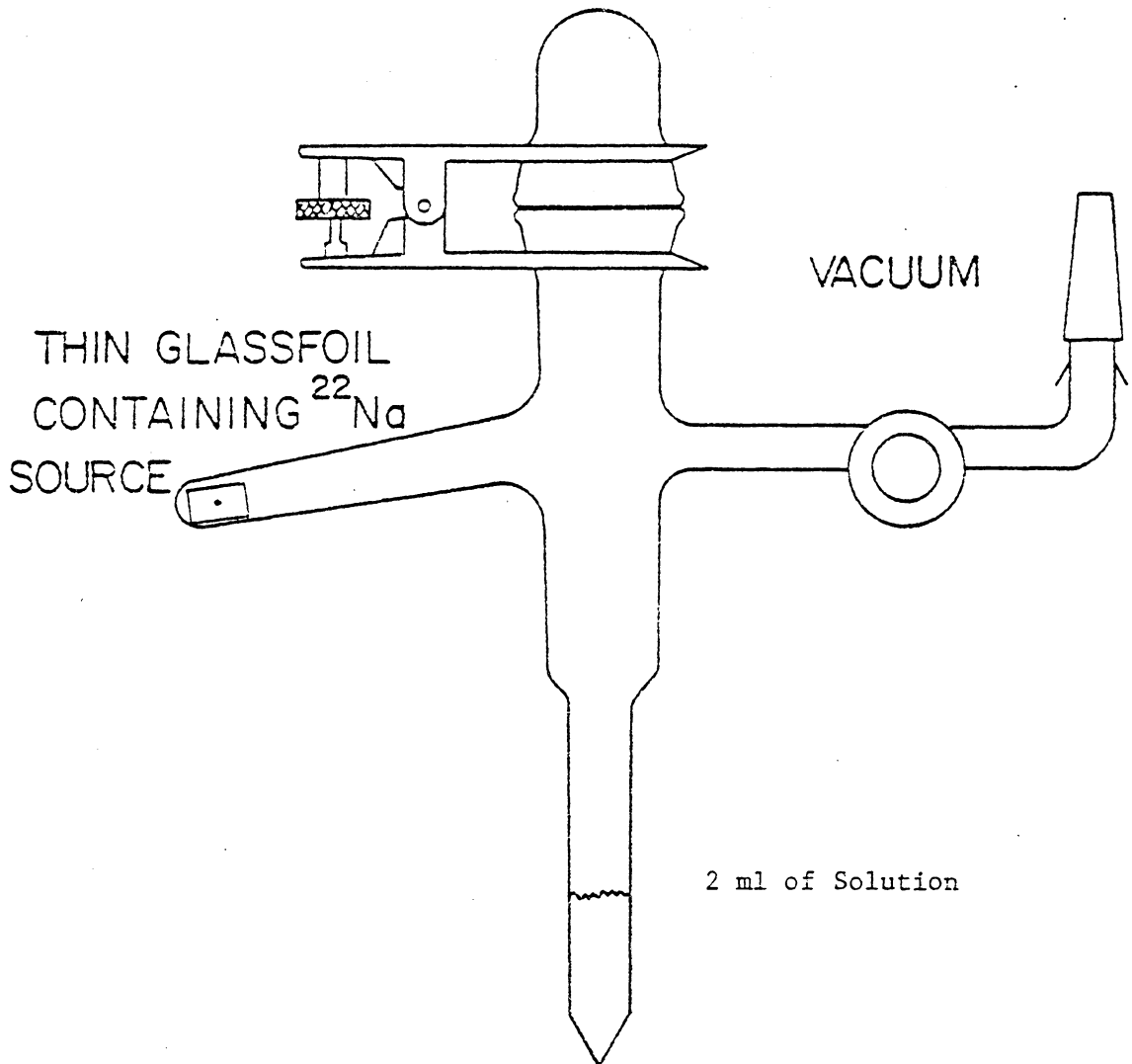
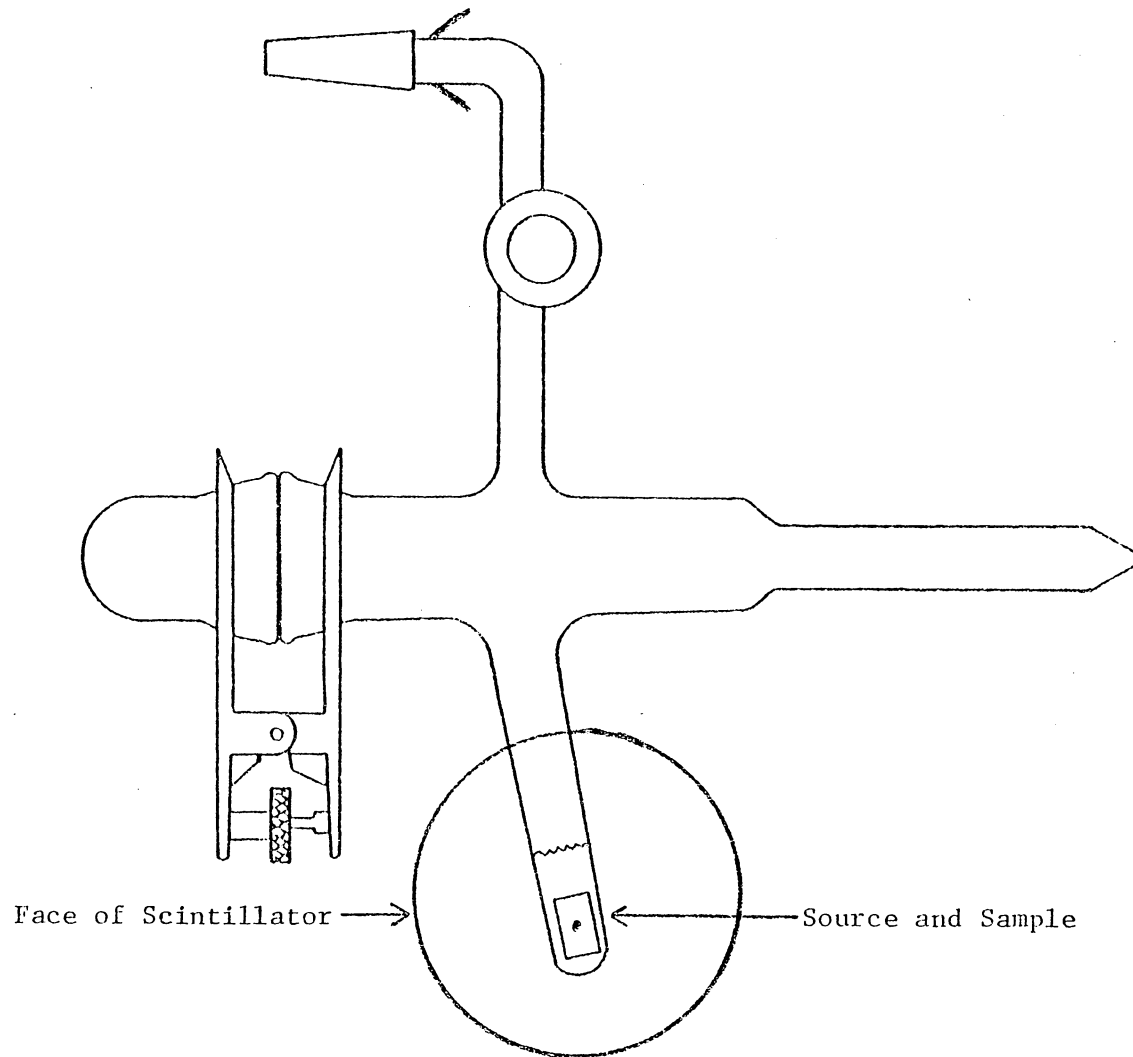


Figure 17. Sample Vial Used for Data Taken at Room Temperature.

attached to the manifold of the vacuum line for degassing. The sample was frozen in liquid nitrogen, and while the sample was still in liquid nitrogen the stopcock was opened thus subjecting the contents of the vial to a vacuum at 10^{-5} torr. This removed the air initially present in the vial. The stopcock was then closed and the liquid nitrogen removed, and the contents of the vial was left to thaw out at room temperature. This process was repeated until all the dissolved air was removed. Usually this takes about six degassing cycles and is accomplished when no air bubbles can be seen during the thawing process. This degassing was performed because Celitans³⁷ and Cooper³⁸ showed that dissolved oxygen in the sample causes a drastic reduction in the lifetime of o-Ps, possibly due to conversion quenching due to the unpaired electrons in molecular oxygen. When the degassing was complete, the sample vial was tilted on its side so the liquid sample in the bottom of the vial flowed to the side arm where the glass source was located. Then the sample vial plus sample was put between the two photomultiplier tubes as shown in Figure 18. To minimize the direct handling of the glass source, the contents of the vial were poured out after each use, and the glass source was left in the side arm and washed with the same solvent used in the solution being measured. A final washing of acetone was used and the vial plus glass source was dried in an oven at 80°C.

A different sample vial was used in the high and low temperature studies. This vial is a two tier vial as shown in Figure 19a. The total length of this vial is 25 cm with an i.d. of 8 mm. One end is



Face of Scintillator →

← Source and Sample

Figure 18. Sample Vial in the Counting Position.

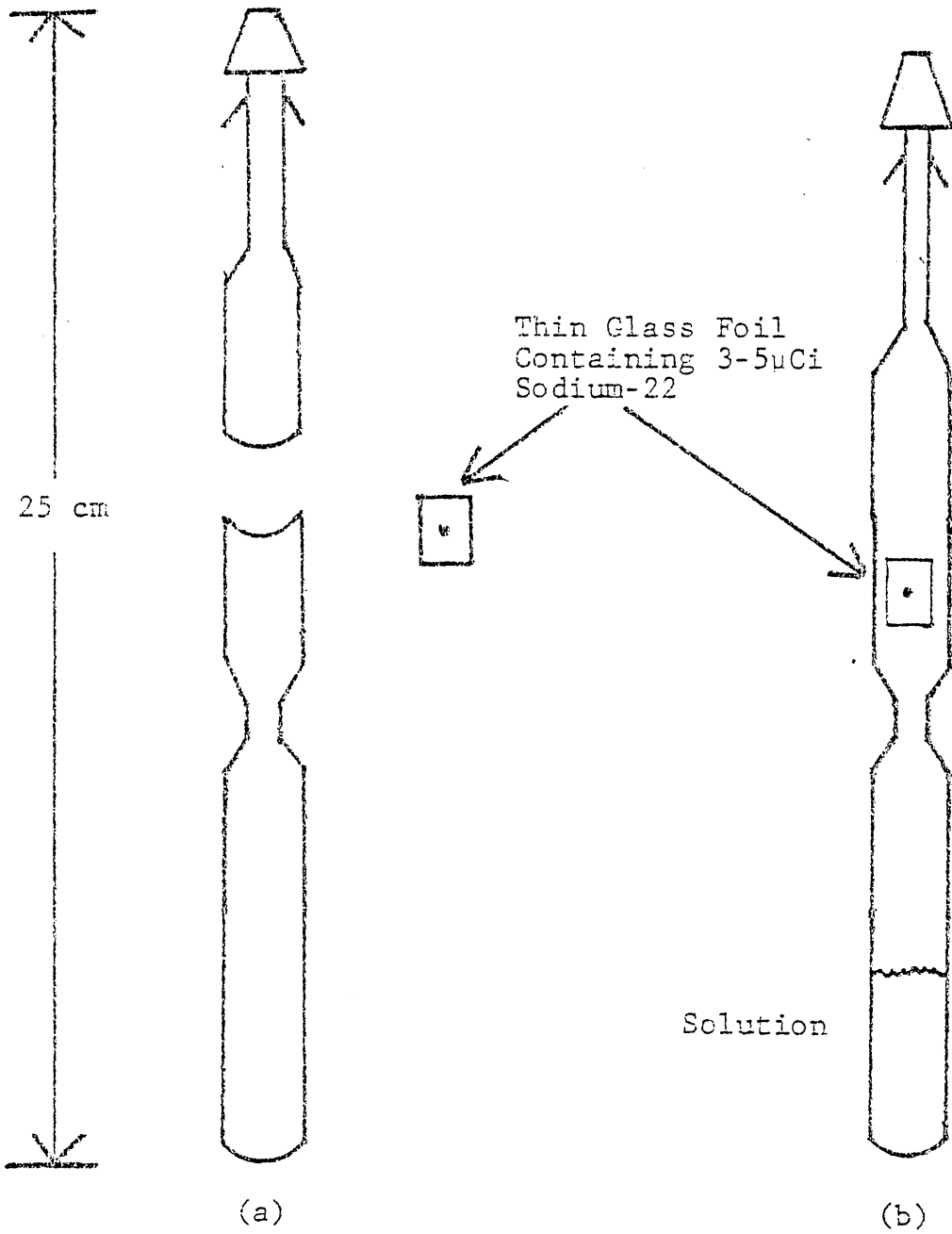


Figure 19. Two-Tier Sample Vial and Source Used for High Temperature Measurements: (a) Disassembled Vial and Source and (b) Assembled Vial and Source.

a 10/40 male ground glass joint which fits into a glass bulb. The glass source is put into the top tier of the vial as shown in Figure 19b. The sample is introduced through the top of the vial by means of a glass capillary syringe. When the bottom tier of the vial is placed in liquid nitrogen, the sample is pulled to the bottom tier. The sample vial is then connected to the female 10/20 joint of the degassing bulb as shown in Figure 20. The male joint of the sample vial extended beyond the female joint by about 10 mm, to prevent the solution from returning to the sample vial in case any sample happened to splash out of the vial during degassing causing contamination with stopcock grease. The degassing bulb was 75 mm in diameter and contained a teflon stopcock to expose the contents of the sample vial to a vacuum and was fitted with a male 10/40 ground glass joint for attaching this system to the vacuum manifold. After the degassing was complete, the glass sample vial was sealed with an oxygen-propane torch while the vial was immersed in liquid nitrogen. The sample vial was then removed from the liquid nitrogen and the contents of the vial were allowed to thaw out at room temperature. The sample vial was then inverted so that the sample in the bottom tier was allowed to flow to the top tier where the glass source was placed. After this, the sample vial was attached to a glass rod by means of heavy duty thread. This assembly was then placed in a specially designed thermostated dewar filled with Dow Corning 704 diffusion pump fluid as shown in Figure 21. The temperature of this thermostat was stable within $\pm 1.0^\circ$ and the maximum temperature that could be reached with this apparatus was 200°C .

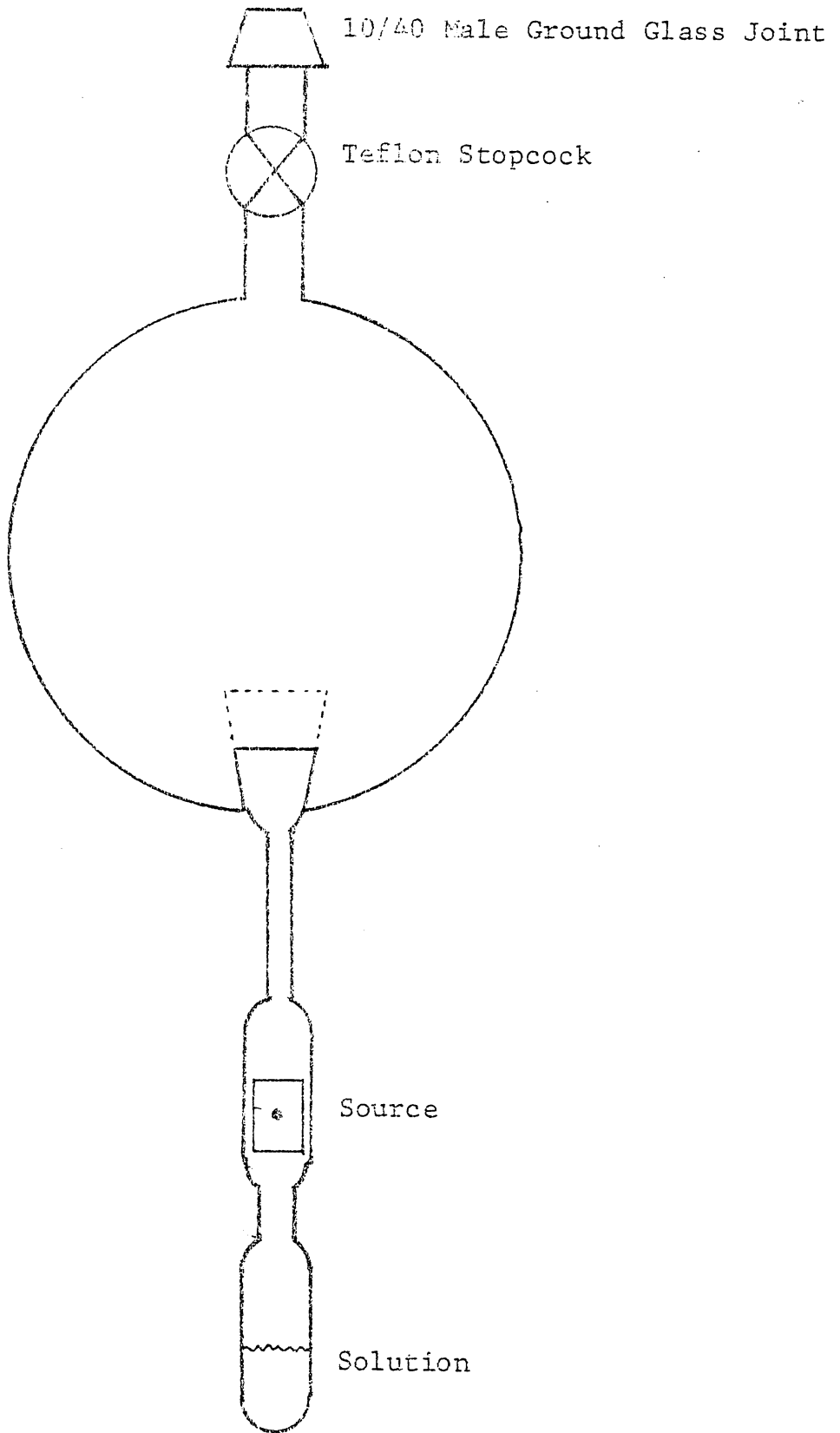


Figure 20. Sample Vial Attached to Degassing Bulb.

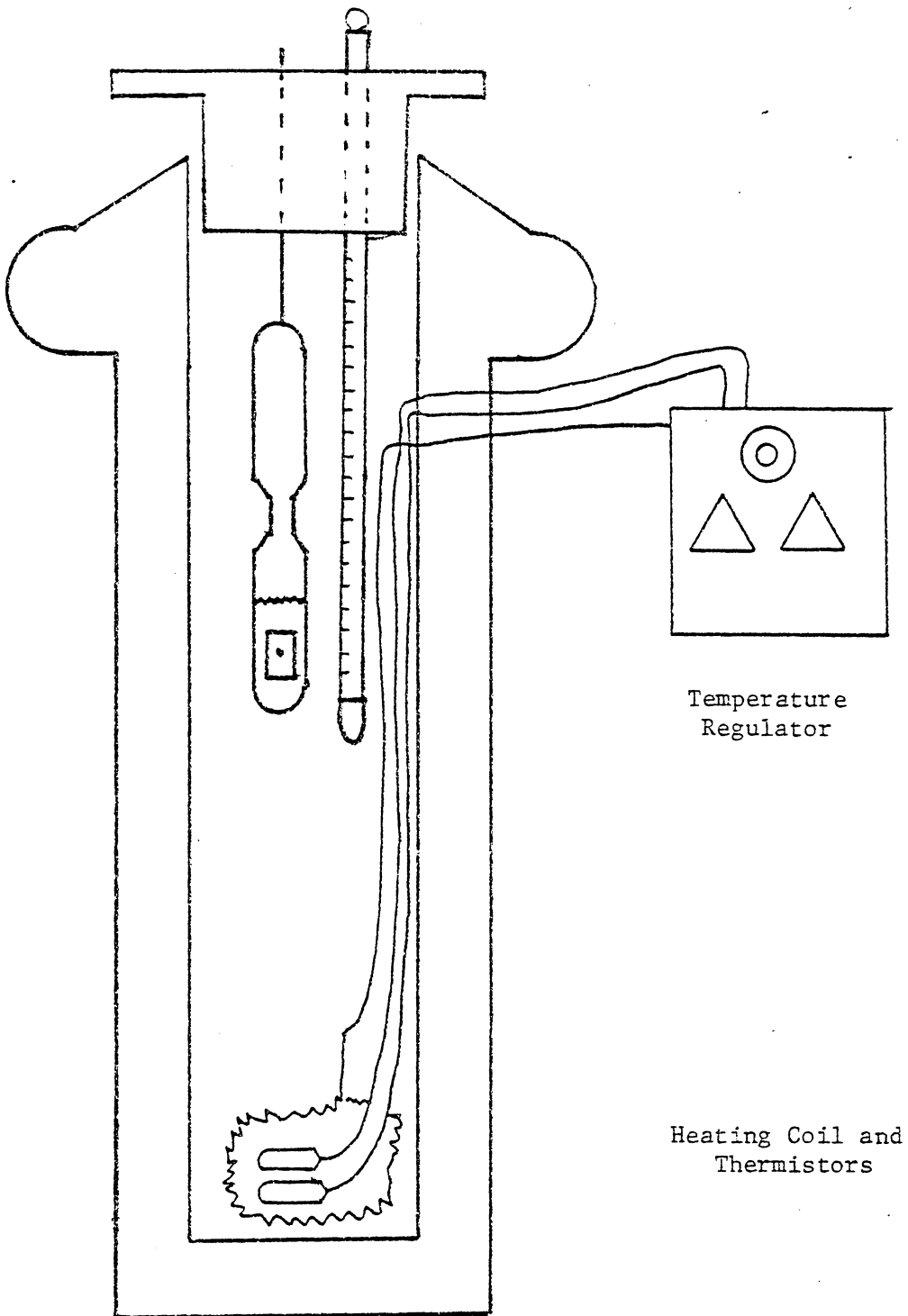


Figure 21. Experimental Arrangement Used for High Temperature Lifetime Measurements.

To recover the glass source for another use, the vial was turned right side up (source in top tier, sample in bottom tier) and immersed in liquid nitrogen. The vial was scratched with a carbide glass cutter and this scratch was touched with a white hot piece of pyrex glass. In this way, the vial could be opened with a clean break preventing any damage to the source. After this, the source was washed in acetone and then dried, thus becoming ready for another use.

For low temperature studies, a specially designed dewar flask with a cold finger was constructed as shown in Figure 22. The sample vial was attached to a glass rod by means of a heavy duty thread and immersed in the low temperature dewar. A low temperature Fischer thermometer was employed to measure the temperature. Several liquids were used along with liquid nitrogen or dry ice to make different slush baths.³⁹ The dewar was filled with the coolant and the apparatus was placed between the two photomultiplier tubes and the counting procedure started. The counting time was usually six hours during which time approximately 20,000 counts (coincidences) were accumulated in the zero channel.

G. Solutes and Solvents

The water used in this study was doubly distilled, deionized water. All solvents were of the highest purity, i.e., spectro grade. Prior to use, these solvents were dried over molecular sieves for 24 hours. The copper chloride was obtained from Fisher Company. For the studies with the inclusion compounds, the pH of the solution was adjusted to 3.5 by titrating an aqueous solution of spectro grade

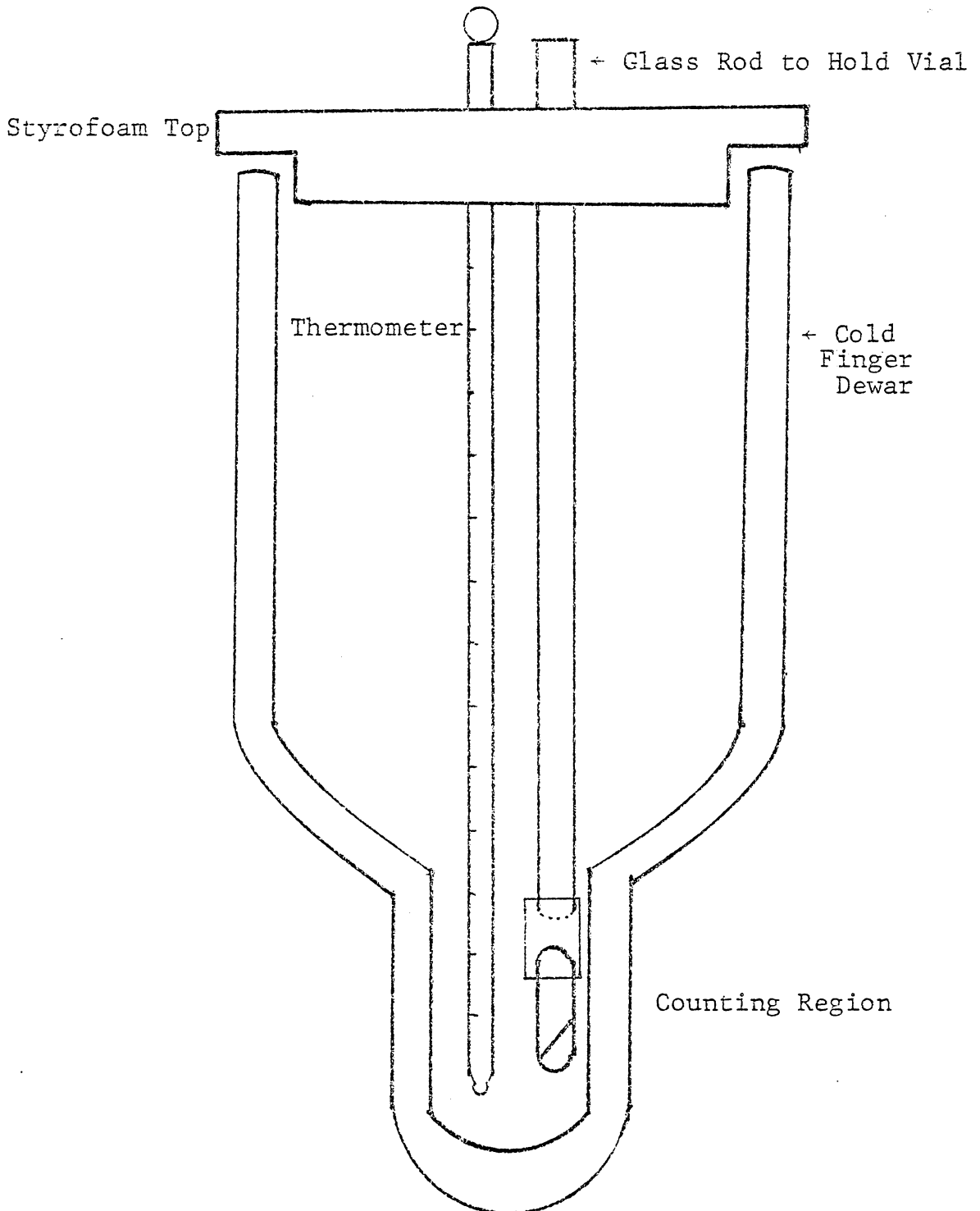


Figure 22. Experimental Setup for Low Temperature Lifetime Measurements.

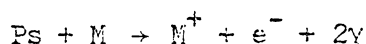
phosphoric acid with a solution of 0.5M NaOH. The final solution had an ionic strength of 0.5. The α -cyclodextrin was obtained from Aldrich Chemical Company in the form of tetrahydrate. The nitroaromatics were obtained from Aldrich in the highest purity obtainable.

REACTIONS OF THERMALIZED o-Ps

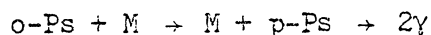
A. Introduction

When thermalized ($KE \approx .025$ eV) o-Ps atoms react, there will be a decrease in its lifetime which can be observed by measuring the slope of the positron lifetime spectrum. As mentioned in Chapter 1, thermal ortho-positronium can undergo the following reactions with matter:

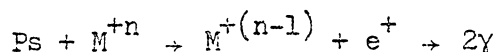
(1) Pickoff



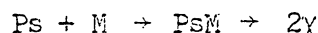
(2) Spin-conversion



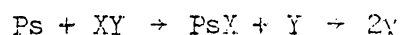
(3) Oxidation



(4) Compound Formation



(5) Double Decomposition

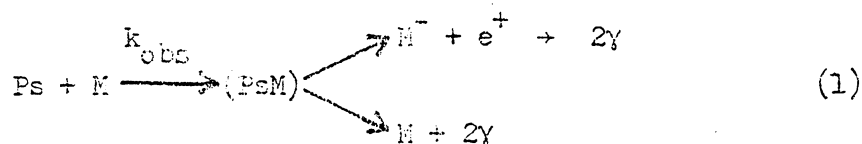


All the work reported in this thesis was mainly concerned with Ps complex formation and oxidation of ortho-positronium in solution.

B. Reactions of Positronium with Diamagnetic Organic Molecules

There are a certain number of organic molecules which can react with positronium. These organic molecules are and include particularly the class of substituted nitroaromatics. Goldanskii^{40,41} was the first to observe this reaction of the nitroaromatics with Ps when he performed lifetime measurements on dilute solutions of nitrobenzene in benzene.

He⁴⁰ proposed the following mechanism to account for the reaction between ortho-positronium and nitro-benzene along with other strongly



reacting compounds where k_{obs} is defined as the observed second order rate constant for the disappearance of positronium or the formation of 2γ . (See Equation 2.)

$$\frac{-d[\text{Ps}]}{dt} = k_{\text{obs}}[\text{Ps}][\text{M}] \quad (2)$$

The experimental determination of k_{obs} will be presented in Section D of this Chapter.

Goldanskii also suggested that positronium may form a complex between a donor molecule, M, and this donor acceptor mechanism represents and electron transfer from positronium to the molecule M, (upper pathway) and the lower pathway represents the positron rapidly annihilating while in the complex. These diamagnetic compounds⁴² are electron acceptors react with solvated electrons but, it must be pointed out that not all electron acceptors react with positronium. For example, benzaldehyde, anthracene, naphthalene and benzonitrile undergo charge transfer with alkali metals in a polar solvent but these compounds are inert towards ortho-positronium. For the reaction to take place in Equation (1), Goldanskii suggested that the molecule, M, must have low lying vacant molecular orbitals. The existence of these orbits was confirmed by Ache,⁴³ et al, when they accounted for the reactivity of diamagnetic compounds by the presence of a trivalent positively charge carbon atom ($:\text{C}^+$), the carbonium ion, in the structure of certain diamagnetic molecules. Madia⁴⁴ et al, showed by using molecular orbital calculations,

that a definite relationship exist between the LUMO, (lowest unoccupied molecular orbital) of these compounds and k_{obs} . This again confirms the existence of low lying vacant molecular orbitals on the reacting molecule. For charge transfer to be energetically possible the following inequality must be satisfied:⁴⁰

$$-I + A + Q + S > 0 \quad (3)$$

where I is the ionization potential, A the electron affinity, Q the coulombic interaction energy between ions, and S is the solvation energy of the ions. The ionization potential in Equation (3) is that of the positronium and is constant. Compounds with large electron affinities (p-benzoquinone = 1.34 eV, tetracyanoethylene = 2.88 eV) should react to some degree with positronium. So one can rule out the upper path mechanism for electron transfer on the grounds that most organic compounds have electron affinities less than 2 eV and the ionization potential for Ps is 6.8 eV.

C. Positronium Complex Formation

At this time it would be appropriate to characterize two groups of compounds which interact with positronium, strong and weak interactions. See Table 1. The first group encompasses those compounds which undergo weak interactions with Ps and their rate constants (k_{obs}) are less than $10^8 \text{ M}^{-1} \text{ s}^{-1}$. The compounds in this group are hydrocarbons, halogenated hydrocarbons, aliphatic nitro compounds and diamagnetic ions that have standard redox potentials in aqueous solution that are more negative than -0.9 eV. When positronium forms a collision type complex with the compounds in this group, it is only

TABLE I
 Examples of Chemical Compounds Showing Strong/Weak
 Interactions With Thermal Ps Atoms

Strong Interaction	Weak Interaction
$k_{\text{obs}} > 10^8 \text{ M}^{-1} \text{ s}^{-1}$	$k_{\text{obs}} < 10^8 \text{ M}^{-1} \text{ s}^{-1}$
Nitroaromatics,	Simple aliphatic or aromatic hydrocarbons:
Quinones,	Alkanes, benzene, anthracene, etc.
Maleic anhydride,	Aniline, phenol, haloalkanes,
Tetracyanoethylene,	Halobenzenes, aliphatic nitro comp.,
Halogens,	Phthalic anhydride, benzonitrile,
Inorganic ions in solution ($E_0 > -0.9\text{eV}$),	(Diamagnetic) inorganic ions in solution ($E_0 < -0.9\text{eV}$)
Organic ions in solution	

From Ref. 50.

held together by weak forces, i.e., van der Waals forces. Direct correlations have been made between k_{obs} and the polarizability of the simple hydrocarbons in the homologous series as shown in Figure 23. Other researchers⁴⁵ have also established a correlation between the annihilation rate, λ_2 , and the surface tension of the liquid which is also related to the polarizability.

The second group encompasses those compounds that display a strong reactivity towards Ps such that $k_{\text{obs}} > 10^8 \text{ M}^{-1} \text{ s}^{-1}$. Compounds in this group are the nitroaromatics, quinones, halogens, conjugated anhydrides, organic ions and inorganic ions in aqueous solution with a standard redox potential larger than -0.9 eV. The strong reactivity of the nitroaromatics in this group are due to the fact that these compounds are highly conjugated and contain strong electronegative atoms such as nitrogen and oxygen.

Madia,⁴⁶ et al., showed that the observed reactions towards Ps vary with the positions of substituents in the nitroaromatic systems. They attributed this behavior to substituent effects which can cause a redistribution of electron density in the nitroaromatic system. On the basis of these and other results, these authors interpreted their results in terms of a reaction mechanism whose basic feature is the formation of a Ps-molecule complex.

Experiments have shown that the observed bimolecular chemical reaction rate constants at room temperature for the reactions of thermalized ortho-positronium with matter range from $10^{10} \text{ M}^{-1} \text{ sec}^{-1}$ down to $10^7 \text{ M}^{-1} \text{ sec}^{-1}$, which is the lower detection limit for the instrumentation used. These values were based on the following general mechanism:

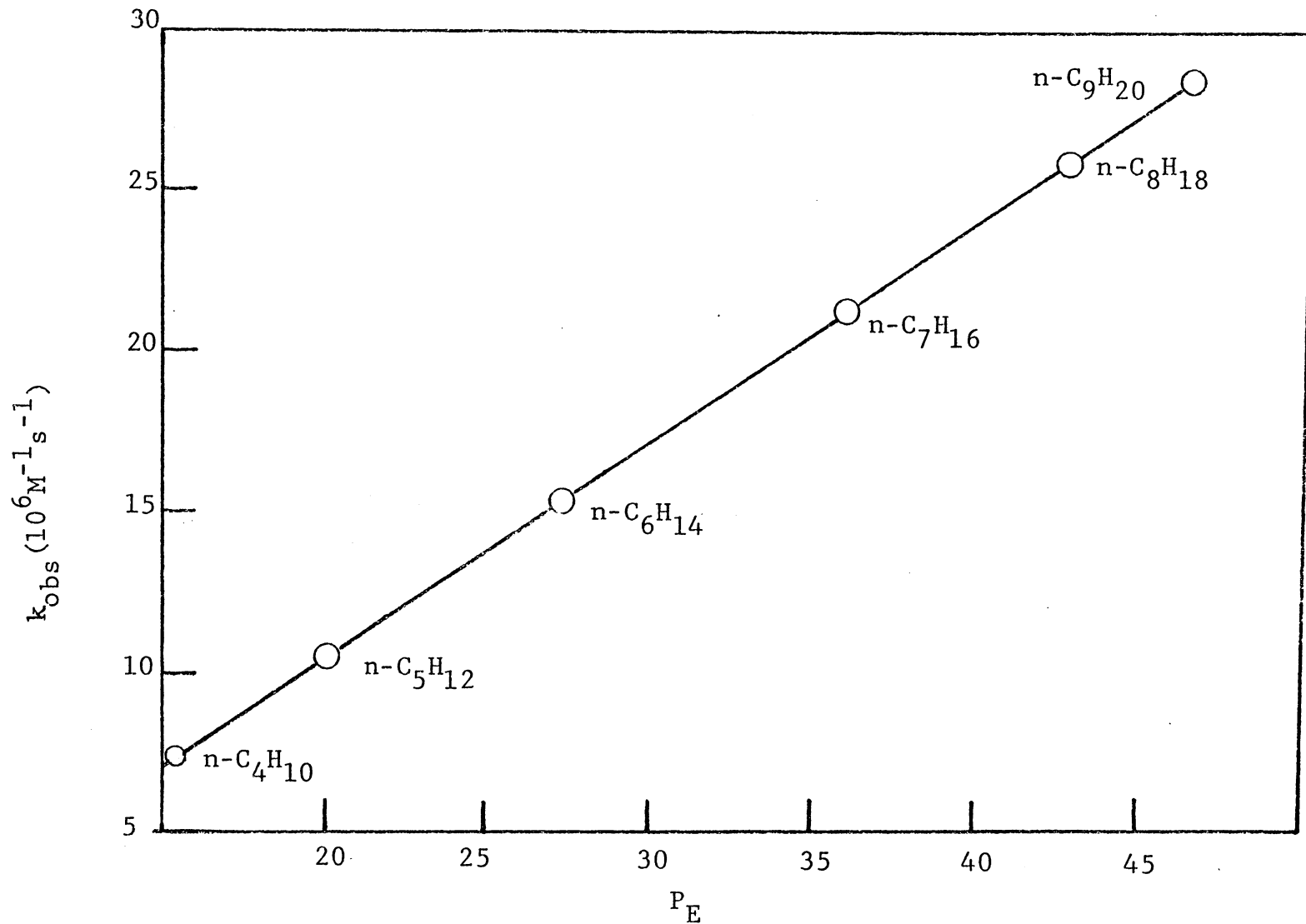
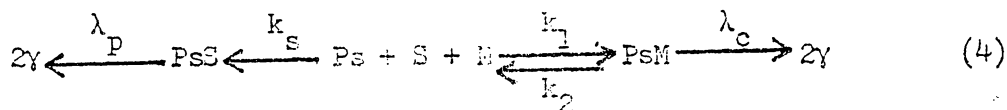


Figure 23. Electronic Polarizabilities, P_E , of Simple Hydrocarbons Plotted Against Rate Constants k_{obs} for Reactions with Ps.



Ortho-Positronium can either react with the solvent S, or the solute M, by forming a collision-type complex. The formation of this complex is the rate determining step. This is shown schematically in Figure 24. In a collision between o-Ps and another molecule, a collision complex with a varying lifetime will be formed. In this complex, the electron density at the position of the positron in o-Ps will be drastically increased hence reducing the lifetime of o-Ps. The average time that o-Ps spends in this complex will depend on how stable this complex is. If only weak forces are operative such as van der Waals forces, o-Ps will spend a very short time in this complex and its mean lifetime will be slightly shorter than the intrinsic lifetime of o-Ps. If strong forces are operative in stabilizing this collision complex, i.e., bond formation, then the positron will find itself for a prolonged period of time in an environment of high electron density which will reduce its lifetime substantially. There is a possibility that this collision complex may be just a transition state leading to electron transfer from Ps to substrate, i.e., oxidation of Ps. Parts of this thesis deals with the one electron transfer reactions between o-Ps and CuCl_2 and will be discussed in detail later on in Chapter 5. In this process a free positron will be formed and it will be quickly annihilated together with an electron whose spin is antiparallel relative to that of the positron. The lifetime of the positron in condensed matter will be 0.1 - 0.5 nsec shorter than o-Ps.

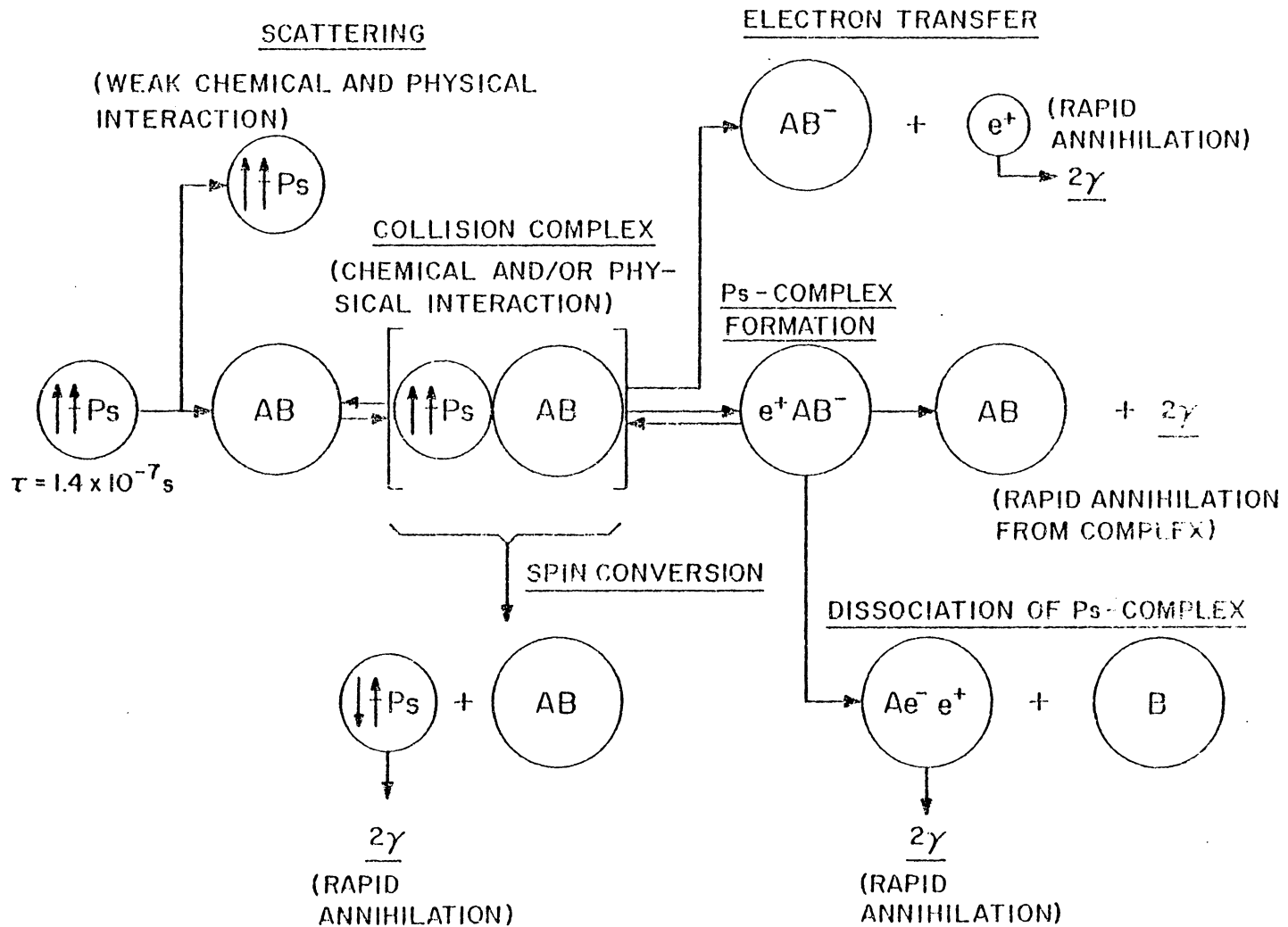


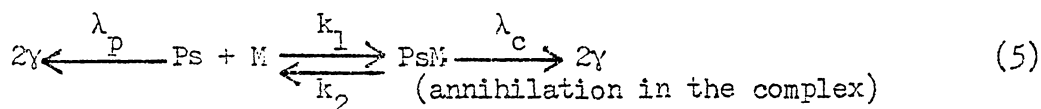
Figure 24. Gas-Kinetic Model of *o*-Ps Interactions with Matter.

D. Analysis of Positronium Lifetime Spectrum

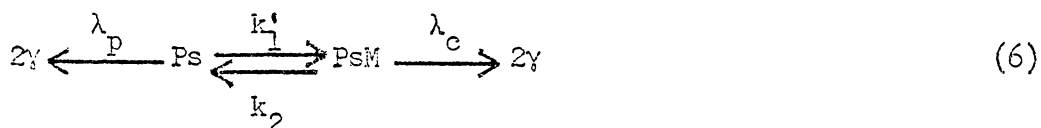
Development of kinetic equations will be based on the fact that only relatively unreactive solvents will be used. Solutes of high reactivity were chosen so that one could see a large change in the lifetime of positronium when these solutes were dissolved in solvents whose reactivity towards positronium is small.

As mentioned above, a more detailed investigation in this laboratory⁴⁷⁻⁵⁰ has shown that positronium reactions can generally be discussed in terms of Ps complex formation with certain molecules. Those of interest here are the substituted nitroaromatics.

As discussed elsewhere in detail,⁴⁷ the mechanism for reversible Ps complex formation in solution can be represented as the following:



where k_1 is the rate constant for the Ps complex formation with molecule M, k_2 is the rate constant for the decomposition of the Ps complex, λ_c is the annihilation constant for positrons in the Ps complex, and λ_p is the annihilation constant for the Ps annihilating in the bulk solvent. Since the concentration of M remains practically constant throughout the experiment, the mechanism can be simplified to



$$k_1' = k_1 [\text{M}]$$

$$\frac{d[\text{Ps}]}{dt} = -(k_1' + \lambda_p) [\text{Ps}] + k_2 [\text{PsM}] \quad (7)$$

$$\frac{d [\text{PsM}]}{dt} = k_1' [\text{Ps}] - (k_2 + \lambda_c) [\text{PsM}] \quad (8)$$

$$\frac{d [2\gamma]}{dt} = \lambda_c [\text{PsM}] \quad (9)$$

These differential equations can be solved exactly according to Pyun⁵¹ for the time dependence of the concentration of Ps, PsM and 2 γ . These solutions are of the form

$$\begin{aligned} [\text{Ps}] &= [\text{Ps}]_0 (S_2 - S_1)^{-1} [(S_2 - k_1') \exp(-S_1 t) - (S_1 - k_1') \exp(-S_2 t)] \\ [\text{PsM}] &= [\text{Ps}]_0 k_1' (S_2 - S_1)^{-1} [\exp(-S_1 t) - \exp(-S_2 t)] \end{aligned} \quad (10)$$

$$[2\gamma] = [\text{Ps}]_0 [1 - S_2 (S_2 - S_1)^{-1} \exp(-S_1 t) + S_1 (S_2 - S_1)^{-1} \exp(-S_2 t)]$$

where

$$S_1 = (p - q)/2 \quad S_2 = (p + q)/2 \quad (11)$$

$$p = k_1' + k_2 + \lambda_c + \lambda_p \quad q = (p^2 - 4k_1' \lambda_c)/2 \quad (12)$$

If $S_1 \ll S_2$, there will be a simple time dependence of $[\text{Ps}]$, $[\text{PsM}]$ and $[2\gamma]$ which will involve only $\exp(-S_1 t)$ after a brief induction period. This condition can be met if $(k_2 + \lambda_c) \gg k_1'$ which is equivalent to invoking steady state conditions for the PsM complex. Then

$$\frac{d[\text{PsM}]}{dt} = 0 \quad \text{and}$$

$$S_1 = \frac{k_1' \lambda_c}{k_2 + \lambda_c} = (k_1' \lambda_c / k_2 + \lambda_c) \quad [\text{M}] \quad (13)$$

and also $S_2 = k_1' + \lambda_c$.

If the steady state assumption is true, then k_{obs} for the disappearance of Ps is

$$\frac{k_1 \lambda_c}{k_2 + \lambda_c} \quad (14)$$

To obtain quantitative information of k_{obs} , the time-dependent two-photon annihilation rate $R_{2\gamma}$ can be used to determine this quantity.

Since

$$R_{2\gamma} = A \exp(-\lambda_1 t) + B \exp(-\lambda_2 t) \quad (15)$$

where A and B are scaling factors which are related to the number of positrons annihilating with rates λ_1 and λ_2 , respectively. Conditions in these studies were such that the concentration of the substrate, M, is in the millimolar range and then the following inequality can be assumed: $(k_2 + \lambda_c) \gg k_1 [M]$ and λ_2 from Equation (9) is then given by the following equation:

$$\lambda_2 = \lambda_p + \frac{k_1 \lambda_c}{k_2 + \lambda_c} [M] \quad (16)$$

or since $k_{obs} = k_1 \lambda_c / (k_2 + \lambda_c)$

$$\lambda_2 = \lambda_p + k_{obs} [M] \quad (17)$$

where λ_2 comes from the measured positron lifetime spectra. The observed rate constant, k_{obs} , can be experimentally determined by plotting λ_2 versus changes in the concentration [M] and the slope of the resulting line can be calculated from linear least squares analysis on the data points (usually 8-10) taken which is $\Delta(\lambda_2 - \lambda_p) / \Delta [M]$ and thus equal to the rate constant k_{obs} . Such a plot is shown in Figure 25 for a solution of nitrobenzene in 0.30 mole fraction Benzene/Hexane. The rate constant is $0.462 \times 10^{10} \text{ M}^{-1} \text{ sec}^{-1}$.

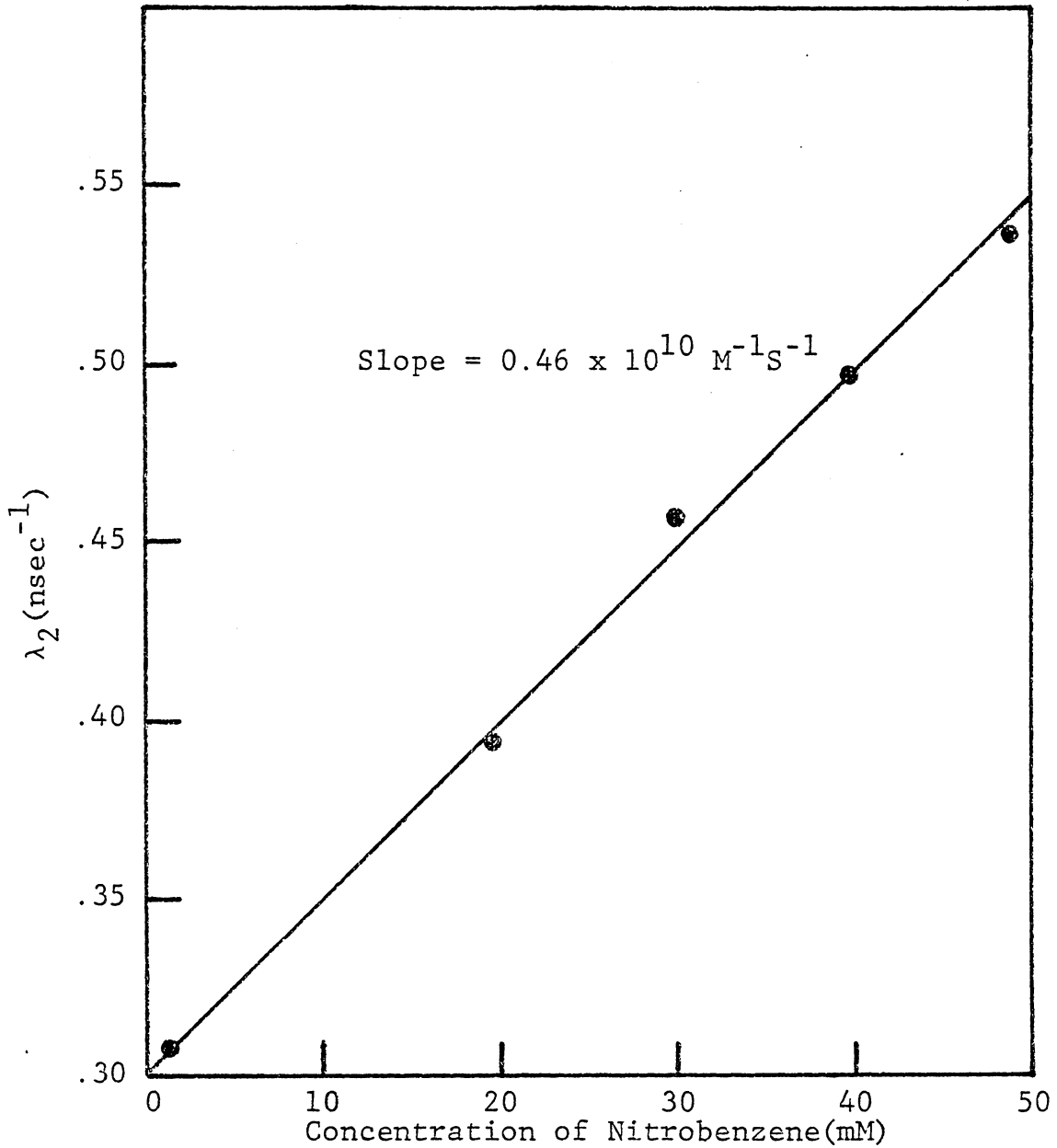


Figure 25. Experimental Determination of k_{obs} for Ps Reacting with Nitrobenzene in .3 MF Benzene/Hexane at 21°C.

The temperature dependence of k_{obs} for a large number of nitro-aromatics reacting with Ps were measured in several solvents by Madia,⁵⁰ et al. They showed that these reactions underwent a temperature inversion giving a non-Arrhenius section as shown in Figure 26.

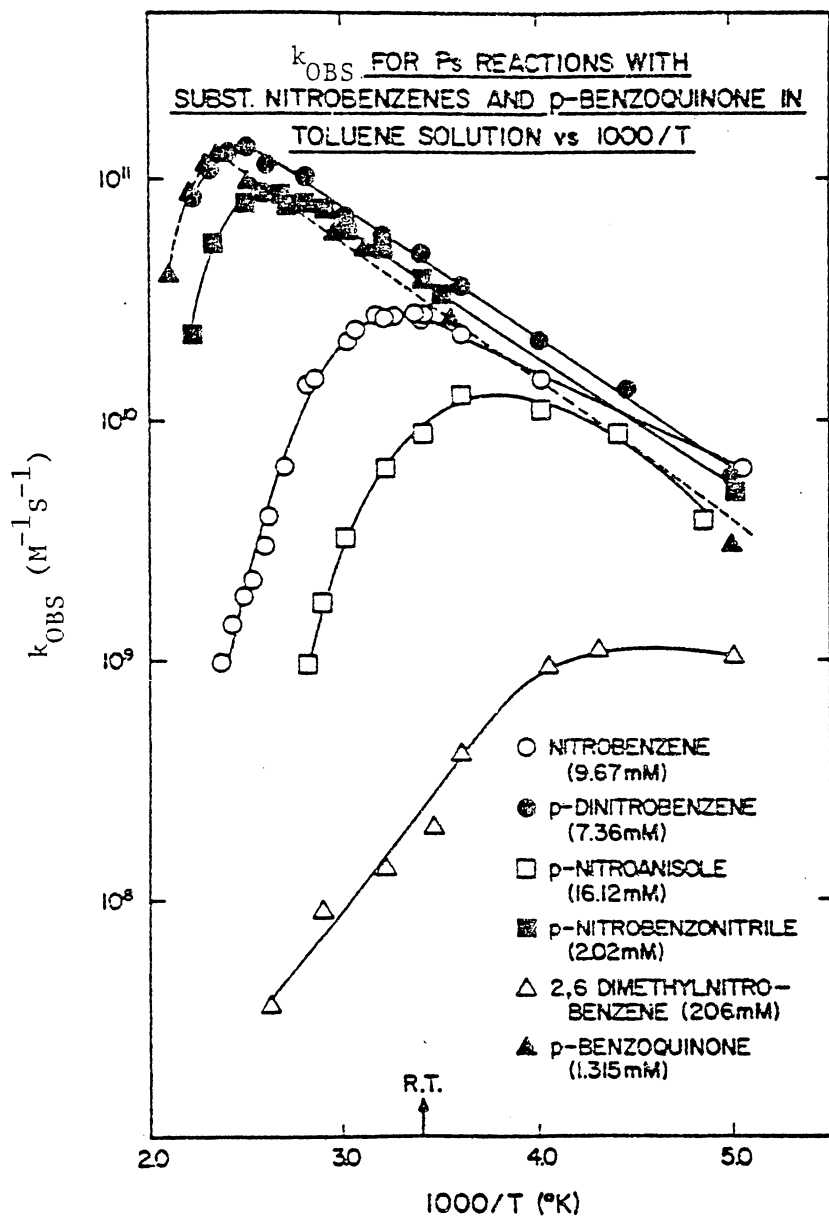


Figure 26. Arrhenius and Non-Arrhenius Behavior of Ps Reacting in Different Systems. (From Ref. 50)

SOLVENT EFFECTS ON THE STABILITY OF POSITRONIUM
COMPLEXES IN SOLUTION

A. Introduction

Recent studies in this laboratory⁴⁷⁻⁵⁰ have shown that different reactions between Ps and various nitroaromatics in different solvents proceed at different rates while the activation energies for these reactions remain fairly constant. Various Ps reactions in this thesis also show the same trend as evidenced by the Arrhenius part of the graph shown in Figure 27. Thus it seemed interesting to investigate what effect the solvent plays in stabilizing the complex formed between Ps and various nitroaromatics in solution. In order to accomplish these studies, the temperature dependence of k_{obs} for the reaction of Ps with nitrobenzene, and o-nitrotoluene was measured in various solvents, such as toluene, n-heptane and n-pentanol.

The experiments were performed in such a way that λ_2 was first measured in the pure solvent under the same conditions, temperature, etc., and subsequently with the solute present. This assures one that the observed rate constant (k_{obs}) is not significantly effected by changes in the viscosity or by changes in the diffusion rate of the Ps atom. To show that the temperature inversion was not caused by decomposition of the solute, the experiments were performed first by a stepwise increase of the temperature and then while decreasing the temperature back to the starting point. All data points were reproducible within experimental error and confirm that decomposition did not occur.

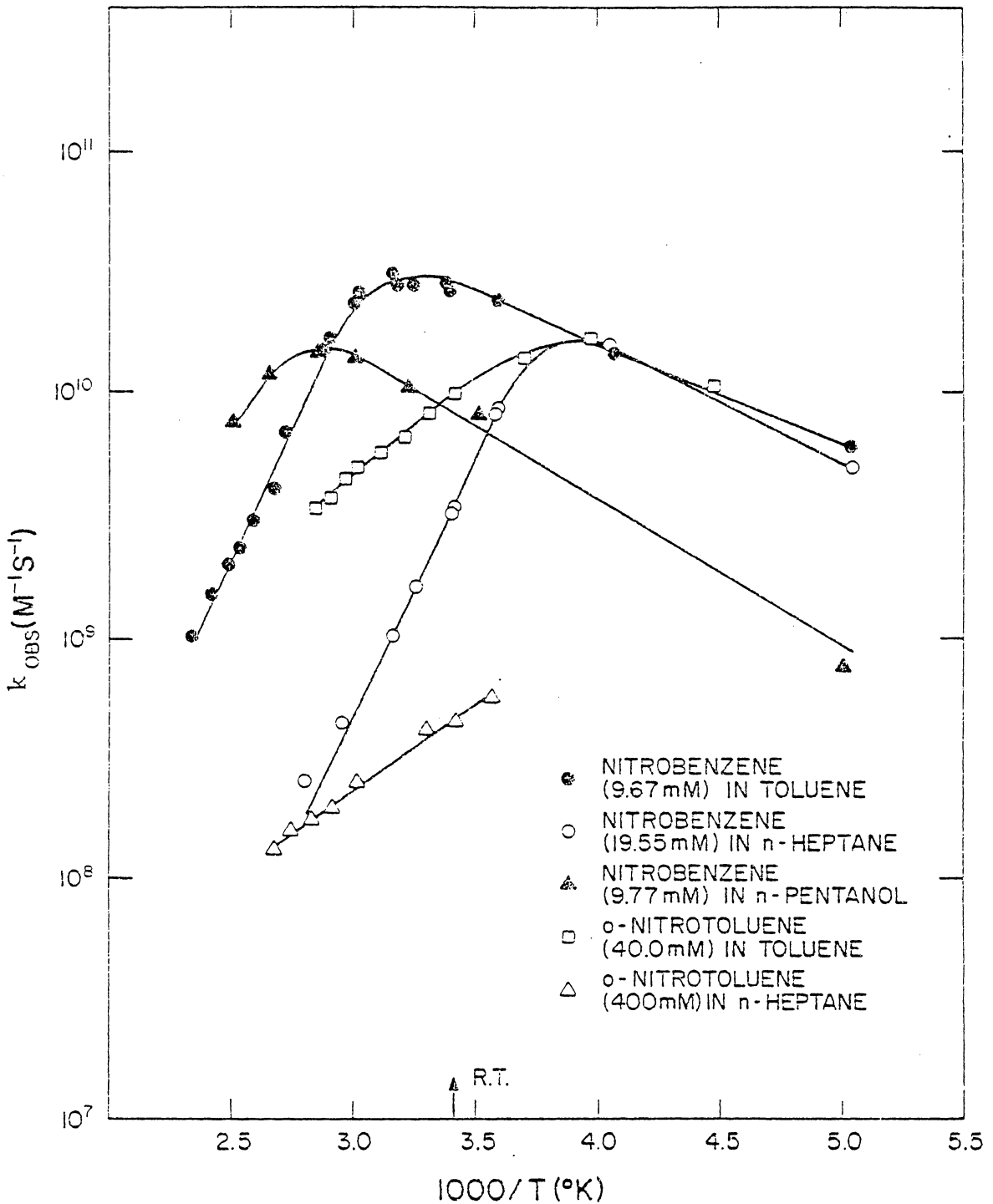
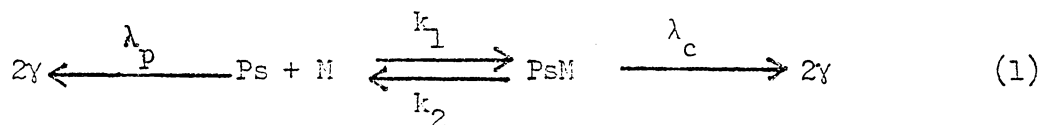


Figure 27. k_{OBS} for Ps Reactions with o-Nitrotoluene and Nitrobenzene in Different Solvents VS $1000/T$.

B. Evaluation of Solvent Effect

A general scheme for a typical Arrhenius plot for the reaction between ortho-positronium and the nitroaromatics is shown in Figure 28. This type of behavior is expected for the equilibrium reaction expressed below in Equation (1).



In Figure 28, the left side of the curves are due to the fact that at higher temperatures $k_2 \gg \lambda_c$, i.e., $k_{\text{obs}} = k_1 \lambda_c / k_2$, whereas at lower temperatures, the right side of the curves, $\lambda_c \gg k_2$, i.e., $k_{\text{obs}} = k_1$. The inversion point in the curves are determined by the relative magnitude of k_1 , k_2 and λ_c in the term $k_{\text{obs}} = k_1 \lambda_c / k_2 + \lambda_c$. λ_c is of the order of $3 - 4 \text{ nsec}^{-1}$ and was found not to differ significantly from one compound to another or from one solvent to another and is considered to be a constant.

According to absolute rate theory, k_1 and k_2 are given by:

$$k_1 = \kappa kT/h \exp(\Delta S_1^\ddagger/R) \exp(-E_{a_1}/RT) \quad (2)$$

$$k_2 = \kappa kT/h \exp(\Delta S_2^\ddagger/R) \exp(-E_{a_2}/RT) \quad (3)$$

where $E_a(1)$ is the Arrhenius activation energy for the complex forming step. (See Figure 29.)

The actual measured Arrhenius plots for several nitroaromatics are shown in Figure 27 and E_a has been determined from the Arrhenius part of the graph and is practically constant in all the systems under investigation (Table 2). Differences in k_1 and k_2 , and thus in the inversion points should therefore be the result of changes in the

TABLE II

Thermodynamic Data for the Reactions of o-Ps in
Toluene, n-Heptane and n-Pentanol Solutions.

Compound	Solvent	E_{A1} Kcal/Mole	ΔH_{EQ} Kcal/Mole
nitrobenzene	toluene	0.8 ± 0.1	-4.5 ± 0.3
	n-heptane	1.3 ± 0.2	-4.4 ± 0.4
	n-pentanol	1.3 ± 0.2	-3.5 ± 0.6
o-nitrotoluene	toluene	1.3 ± 0.2	-3.7 ± 0.3
	n-heptane	---	-3.8 ± 0.3

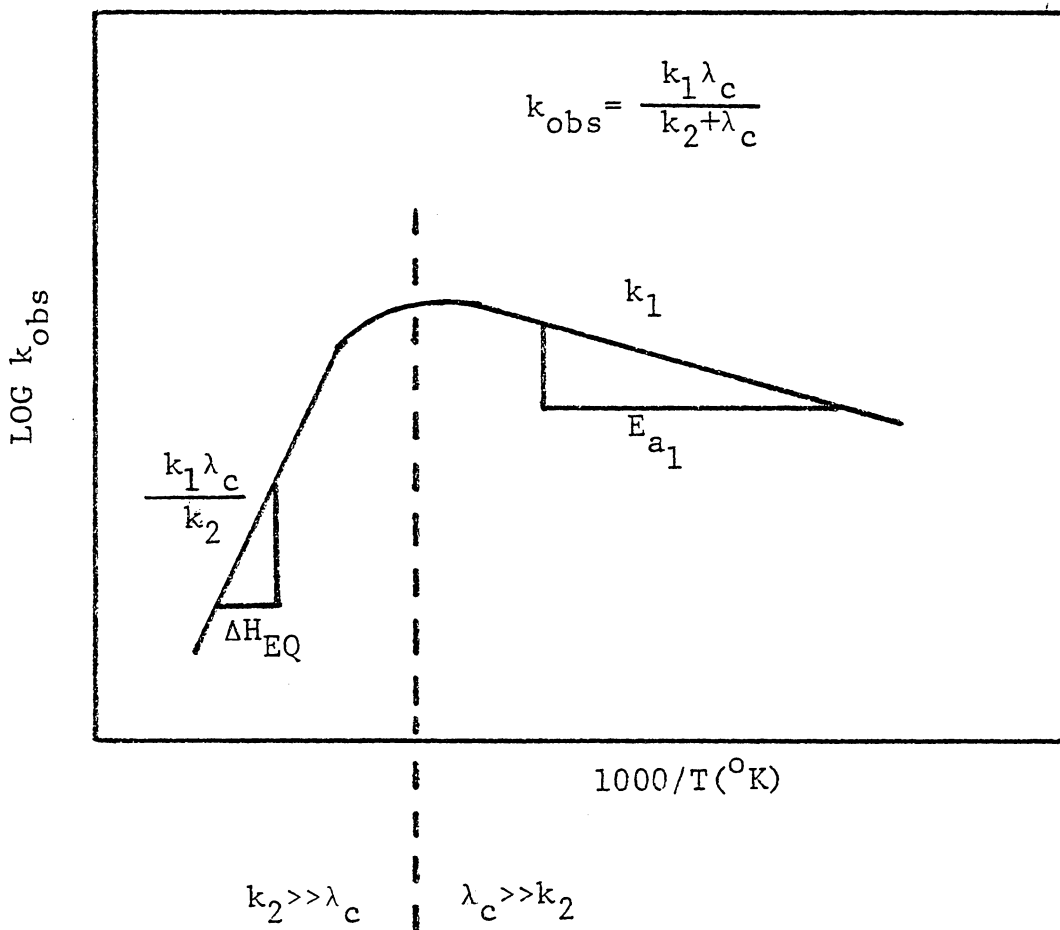


Figure 28. Typical Arrhenius Behavior for Ps Reacting with Nitroaromatics Showing the Thermodynamic Parameters.

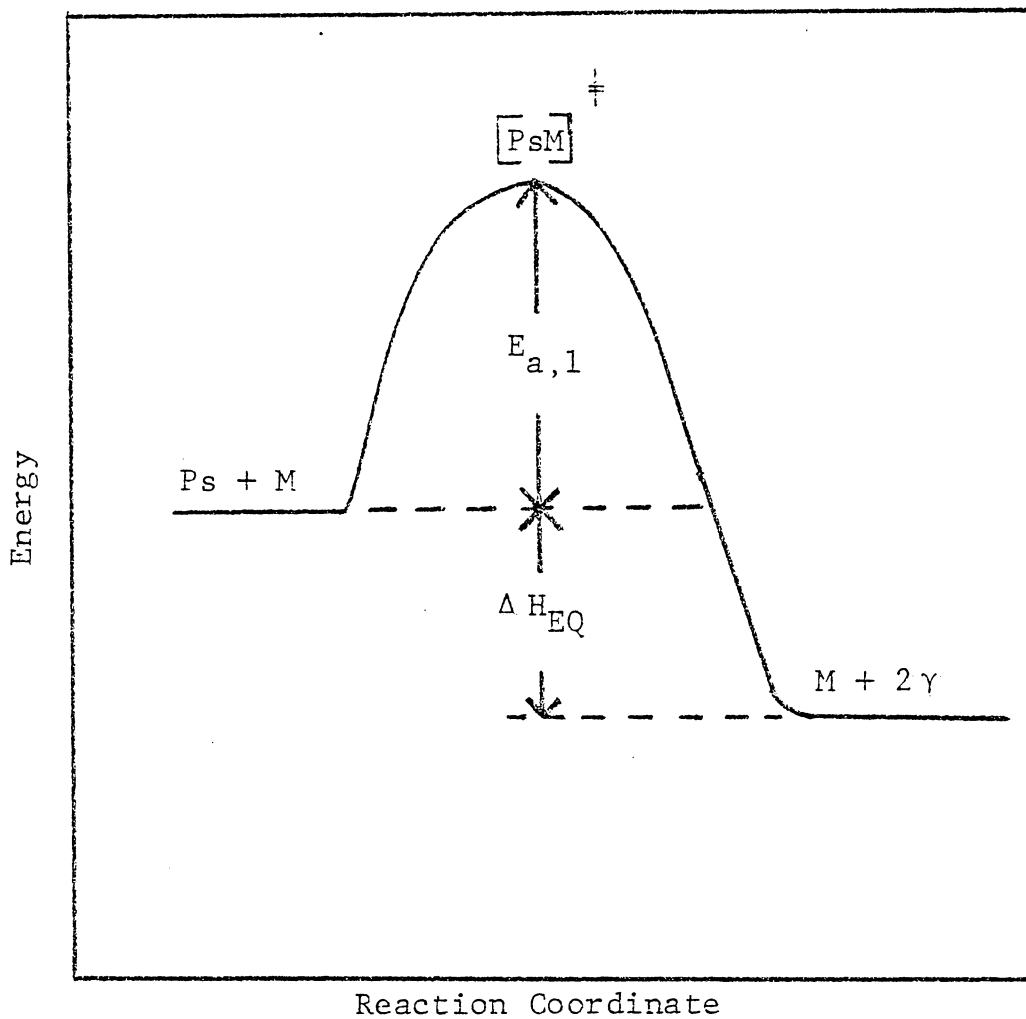


Figure 29. Potential Energy Surface for Ortho-Positronium Reacting with a Molecule VIA Complex Formation.

pre-Arrhenius factor, i.e., due to changes in the transmission factor or more likely due to changes in the entropies $\Delta S_1^\ddagger, \Delta S_2^\ddagger$ which are involved in the formation of the transition state.

In the case of n-heptane and toluene solvent systems where k_1 remains fairly constant, the results suggest that the stability of the complex here is mainly determined by k_2 , through entropy changes involved in the decomposition step.

If k_2 is mainly responsible for the temperature dependence of k_{obs} it seemed interesting to study the effect of solvent composition on k_2 . These studies were done to show the importance of entropy and other thermodynamical factors in Ps complex formation.

In order to evaluate these effects of solvents, a series of experiments were performed in which k_{obs} was measured for Ps reacting with nitrobenzene and o-nitrotoluene in benzene-hexane mixtures of various mole fractions at room temperature. In Figure 30 $1/k_{obs}$ observed for Ps reacting with nitrobenzene is plotted as a function of the molefraction of n-hexane in benzene. No linear or other simple correlation seems to exist in this case between $1/k_{obs}$ and the composition of the solvent. This is not unexpected since the curves in Figure 27 clearly indicate that for the interaction between Ps and nitrobenzene at room temperature, k_{obs} in toluene⁵² is mainly determined by k_1 whereas k_{obs} in n-heptane⁵² is a function of $k_1 \lambda_c / k_2$.

Thus in a second series of experiments the solvent dependence of k_{obs} was studied by using o-nitrotoluene in mixtures of benzene-n-hexane at room temperature. It can be seen from Figure 27 that k_{obs} is given by $k_1 \lambda_c / k_2$ (high temperature limit) in both solvents. To do these experiments, λ_p was first determined in the various pure benzene-

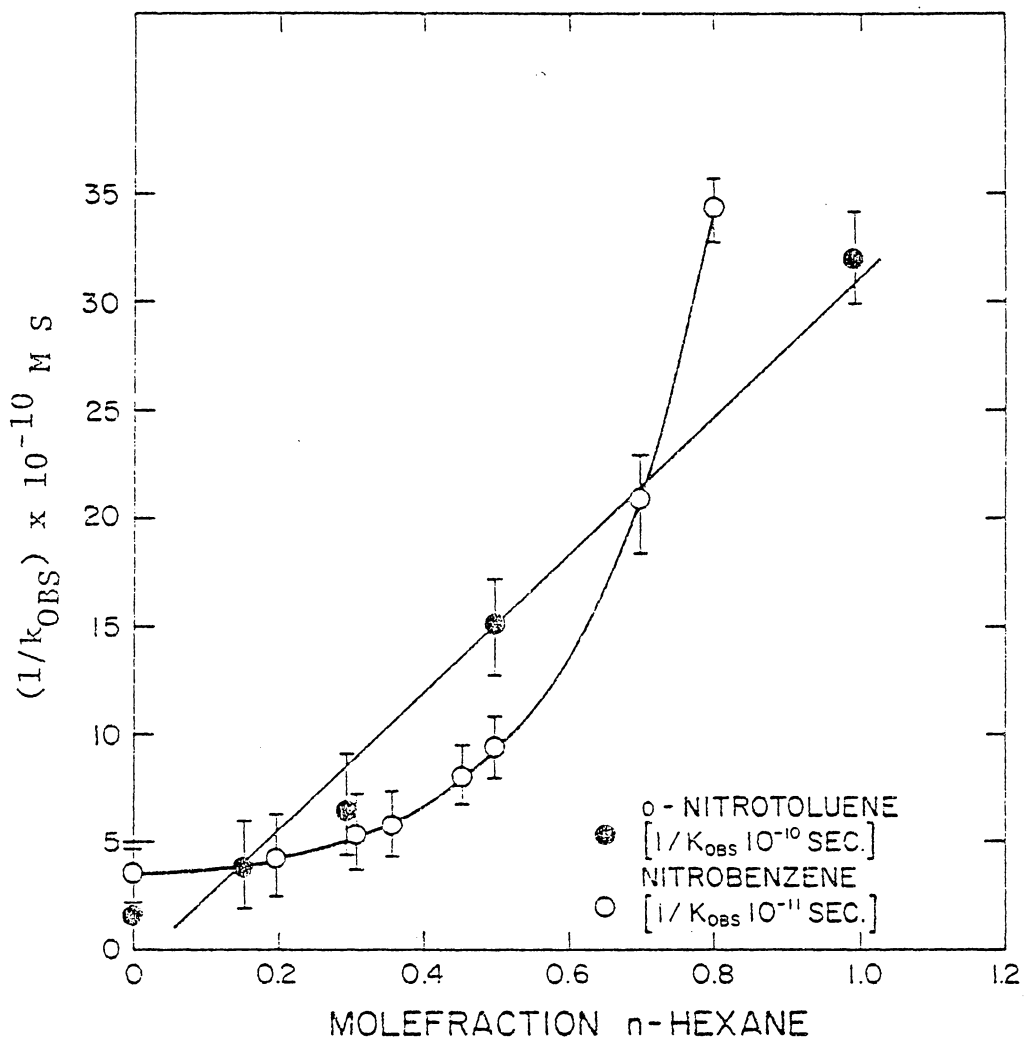


Figure 30. $1/k_{OBS}$ VS Molefraction of N-Hexane in
 N-Hexane - Benzene Solutions of Nitroben-
 zene and o-Nitrotoluene.

n-hexane solvents at room temperature. By varying the concentration of o-nitrotoluene while keeping the mole fraction of benzene in n-hexane constant, k_{obs} was calculated by plotting λ_2 as a function of the concentration of nitrotoluene. This was repeated for about six different mole fractions of benzene in n-hexane thus obtaining values of k_{obs} corresponding to the different mole fractions. From Figure 30 where $1/k_{\text{obs}}$ is plotted as a function of the molefraction of n-hexane, it can be seen that $1/k_{\text{obs}}$ varies linearly with the molefraction of n-hexane.

In analogy to the nitrobenzene system where E_a , and k_1 were found to be identical in n-hexane and toluene at room temperature, $E_a(1)$, the Arrhenius activation energy, and k_1 for the complex forming step, $\text{Ps} + \text{o-nitrotoluene} \xrightarrow{k_1} \text{Ps-o-nitrotoluene}$, have also been assumed to be the same for o-nitrotoluene in these two solvents at room temperature.

Since λ_c remains fairly constant, k_{obs} should be proportional to the reciprocal of k_2 :

$$k_{\text{obs}} = \text{constant}/k_2$$

The straight line in Figure 30, where $1/k_{\text{obs}}$ is plotted as a function of the molefraction of hexane, would thus indicate that the equilibrium entropy changes linearly with the composition of the solvent, which in turn rules out any preferential association of either solvent with the Ps-complex, i.e., there is no indication for cluster formation.

The ability of these two solvents to assist the complex in stabilizing itself is therefore determined by the weighted sum of the

equilibrium entropies involved. It is also consistent with the expectation that the polar or more polarizable solvent n-pentanol or toluene is better able to neutralize the charge separation which occurs if neutral species combine to form polar complexes than a less polarizable solvent, such as n-heptane.

POSITRONIUM REACTIONS:
KINETIC OR DIFFUSION CONTROLLED?

A. Introduction

Goldanskii and Shantarovich⁵³ have attempted to explain some reactions of thermal ortho-positronium with paramagnetic and diamagnetic organic and inorganic compounds in terms of a reversible complex formation based on the "bubble" or free volume model. Whereas, on the other hand, the results presented in this thesis were discussed in terms of a model which is based on the gas kinetic model as mentioned in Chapter 3. The solvent effect was in this case considered to be controlled mainly by entropy differences in the complex formation in the various complexes.

In the past,, several authors have assumed that Ps reactions proceed mainly through a diffusion controlled mechanism because in a few cases the rate constants for these reactions displayed a dependence on solvent viscosity and the observed activation energies in aqueous systems were close to the activation energy of viscosity, E_{η} . On the other hand, the rate constants for the reactions of Ps atoms with simple inorganic ions varied over a large range. (See Table 3). A similar wide range of rate constants was also found for Ps atoms reacting with nitroaromatics in various solvents. (See Table 4). Thus it seemed interesting to evaluate what effect the solvent viscosity plays in these reactions and to assess whether the "bubble model" is valid in predicting rate constants for Ps reactions in various systems studied in this thesis. To accomplish this, positronium complex formation with diamagnetic and inorganic compounds were studied as a function of the solvent viscosity.

TABLE III

Observed Rate Constants, k_{obs} , Entropies of Activation, Energies of Activation and Viscosity for Ps-CuCl₂ Reactions in Various Solutions.

SYSTEMS	^a k_{OBS} ($\times 10^9 \text{ M}^{-1} \text{ sec}^{-1}$)	^{a, b} k_{D}	^c VISCOSITY (cp)	E_{A} (Kcal/Mole)	E_{VISC}	^d ΔS^\ddagger (e.u. at 21°C)
Aq. KMnO ₄	18.0	6.5	1.0	3.3	2.0	---
Aq. Cd(ClO ₄)	> 0.1	6.5	1.0	---	2.0	---
CuCl ₂ in						
Water	3.6 ± 0.5	6.5	1.0	2.8 ± 0.8	2.0	-7.57
Ethanol	7.9 ± 0.5	5.4	1.2	2.6 ± 0.5	3.2	-6.01
Propanol-1	6.8 ± 0.5	2.8	1.5	2.8 ± 0.5	4.9	-6.31
Propanol-2	8.1 ± 0.5	2.8	2.3	2.7 ± 0.5	5.3	-5.96
Hexanol-1	7.0 ± 0.5	1.3	5.4	2.6 ± 0.5	5.1	-6.25
Ethyleneglycol	0.2 ± 0.2	0.3	19.9	7.0 ± 1.0	15.4	1.29

a) Rate constants at 20°C.

b) Derived from Stokes-Einstein-Debye Equation (equation 3)

c) at 20°C.

d) From equation 2.

TABLE IV

Observed Rate Constants, k_{obs} , Energies for Activation and Viscosity for
Ps-Nitrobenzene or p-Dinitrobenzene in Various Solutions.

SYSTEMS	$^a k_{\text{OBS}}$ ($\times 10^9 \text{ M}^{-1} \text{ sec}^{-1}$)	$^b \text{VISCOSITY}$ (cp)	$^c E_A$ (Kcal/Mole)	E_{VISC}
<u>Nitrobenzene in</u>				
H ₂ O	10.1 ± 0.3	1.0	---	2.0
Methanol	5.2 ± 0.8	0.58	---	---
Propanol-1	10.0 ± 0.3	1.5	0.5 ± 0.3	4.9
Pentanol-1	8.6 ± 0.3	0.38	1.3 ± 0.2	5.1
Cyclohexane	13.0 ± 2.0	1.02	---	---
n-Heptane	3.3 ± 0.3	0.41	1.3 ± 0.2	2.1
Benzene	27.0 ± 2.0	0.65	---	---
Toluene	27.9 ± 0.8	0.59	0.8 ± 0.1	2.0
Acetone	4.0 ± 0.5	0.32	---	---
n-Pentane	0.7 ± 0.1	0.24	---	---
<u>p-Dinitrobenzene in</u>				
Toluene	51.3 ± 1.3	0.59	1.1 ± 0.1	2.0
n-Heptane	77.6 ± 3.0	0.41	1.0 ± 0.1	2.1
Pentanol-1	17.8 ± 1.0	0.38	1.8 ± 0.3	5.1

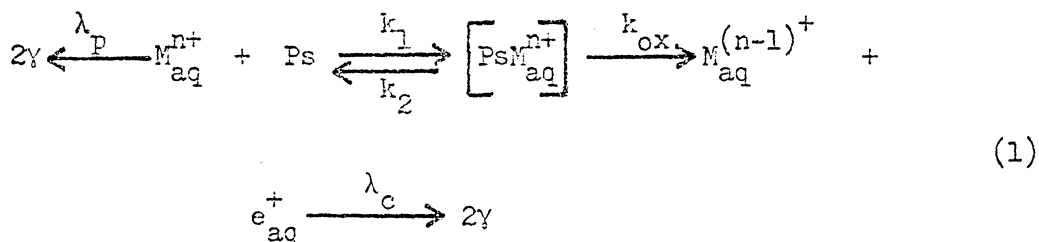
a) Rate constants at 20°C.

b) At 20°C.

c) Calculated from Arrhenius part of plot $\log K_{\text{obs}}$ vs $1/T$.

B. Studies of Positronium Reactions in Various Solutions of CuCl_2

Reactions of positronium with different inorganic salts have been extensively studied by various researchers.⁵⁴⁻⁶⁰ It was assumed that these reactions occur via oxidation of Ps according to the following mechanism:



The positronium (positronide) complex $\text{Ps}M^{n+}$ is considered to be just a transition state leading to electron transfer from Ps to substrate, i.e., oxidation of Ps.

The reaction studied in this thesis was $\text{Ps} + \text{Cu}^{+2} \longrightarrow \text{Cu}^{+1} + e^+$
 $e^- \longrightarrow 2\gamma$ (Rapid annihilation). The standard redox potential for $\text{Cu}^{+2} + e^- \longrightarrow \text{Cu}^+$ is +0.17 V, and it should react effectively with Ps.

It seemed interesting to study the solvent effect on the reactions between CuCl_2 and Ps in different solvents and to determine the activation energies for the reaction of Ps with CuCl_2 in different solvents at different temperatures. By plotting $\log k_{\text{obs}}$ as a function of $1/T$, the Arrhenius activation energy, E_a , could be determined from the slope of the resulting straight line. These plots are shown in Figures 31 and 32. It is clearly evident that the slopes are all equal (with the exception of ethyleneglycol as the solvent) which in turn shows that the activation energy, E_a , is the same and is solvent independent.

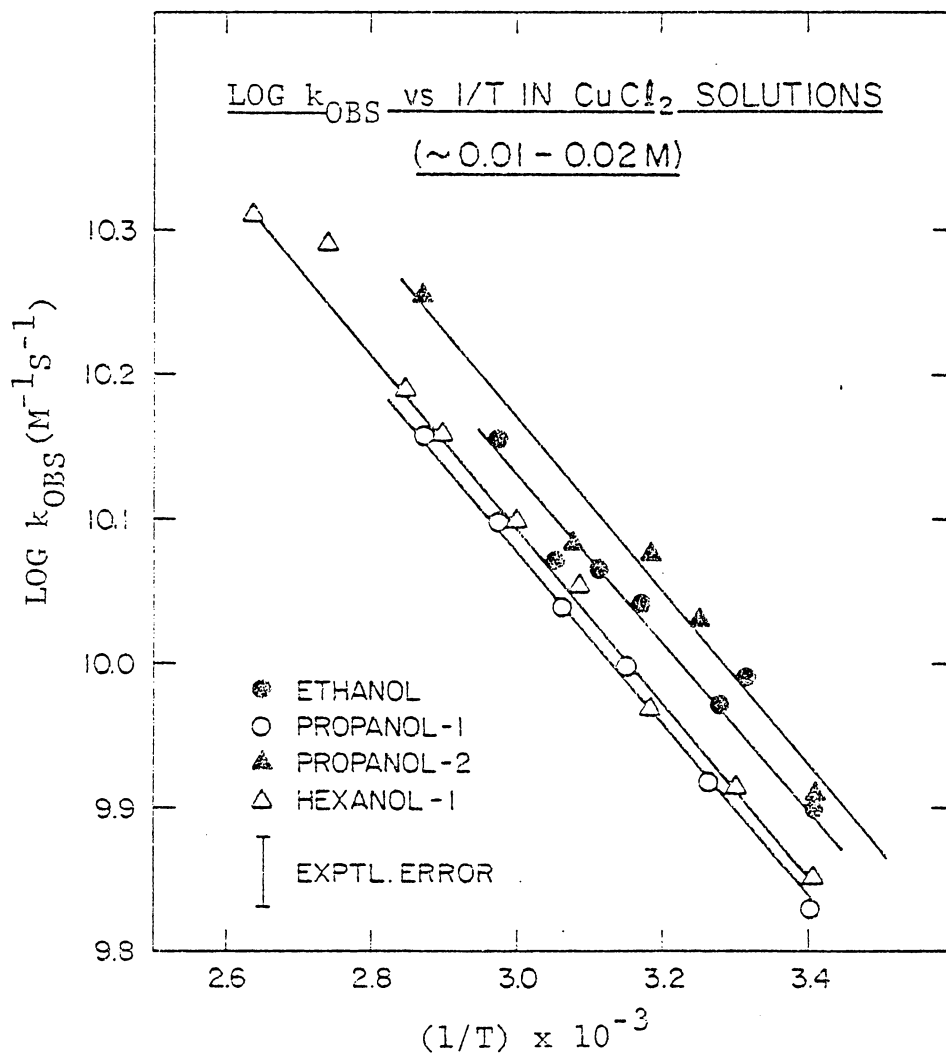


Figure 31. Arrhenius Plots for Ps Reacting with $CuCl_2$ in Different Solvents.

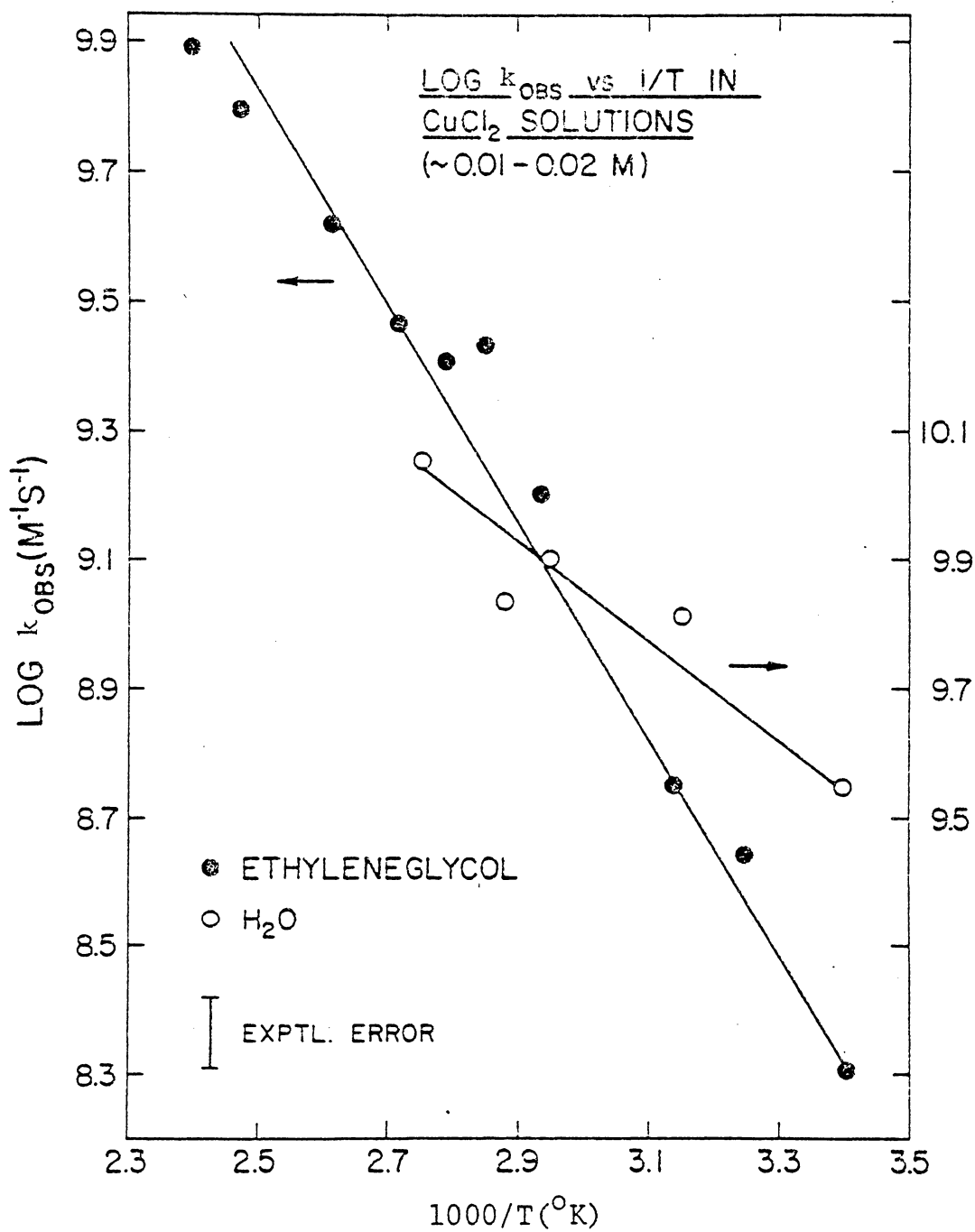


Figure 32. Arrhenius Plots for Ps Reacting with CuCl₂ in H₂O and Ethyleneglycol.

Similar trends were observed for Ps atoms reacting with various nitroaromatics in different solvents as shown in Figure 33. E_{η} , the activation energy of viscosity, can be determined for the different solvents by plotting the log of viscosity vs $1/T$ as shown for n-hexane in Figure 34. It can be seen that in all the cases that E_a is less than E_{η} , (except for water as the solvent, see Table 3), which could indicate that these reactions are not diffusion controlled.

The experiments were performed such that λ_2 was first measured in the pure solvent under the same conditions, temperature, etc., and subsequently, with the solute present. There was no inversion of k_{obs} observed at higher temperatures thus providing no evidence for any Ps complex decomposition over the temperature range studied. This may indicate that electron transfer is occurring extremely rapid in the initially formed Ps-CuCl₂ complex. ($k_{ox} \gg k_2$).

One can, therefore, conclude that the activation energies which remain fairly constant for all systems studied, except for ethyleneglycol, cannot represent solely the activation energy of viscosity, E_{η} , and one could safely argue that changes in the forward rate constant k_1 , which should be equal to k_{obs} since $k_2 \ll \lambda_c$, are due to a substantial degree to changes in the pre-exponential factor, A, of the Arrhenius equation, i.e., by differences in ΔS^{\ddagger} , the entropy of activation. The entropy of activation was determined at room temperature for these systems by using equation 2.

$$\frac{\Delta S^{\ddagger}}{4.576} = \log k_{obs} - 10.753 - \log T + E_a/4.576T \quad (2)$$

The results revealed that water has the lowest value whereas ethyleneglycol has the highest. (See Table 3). The positive

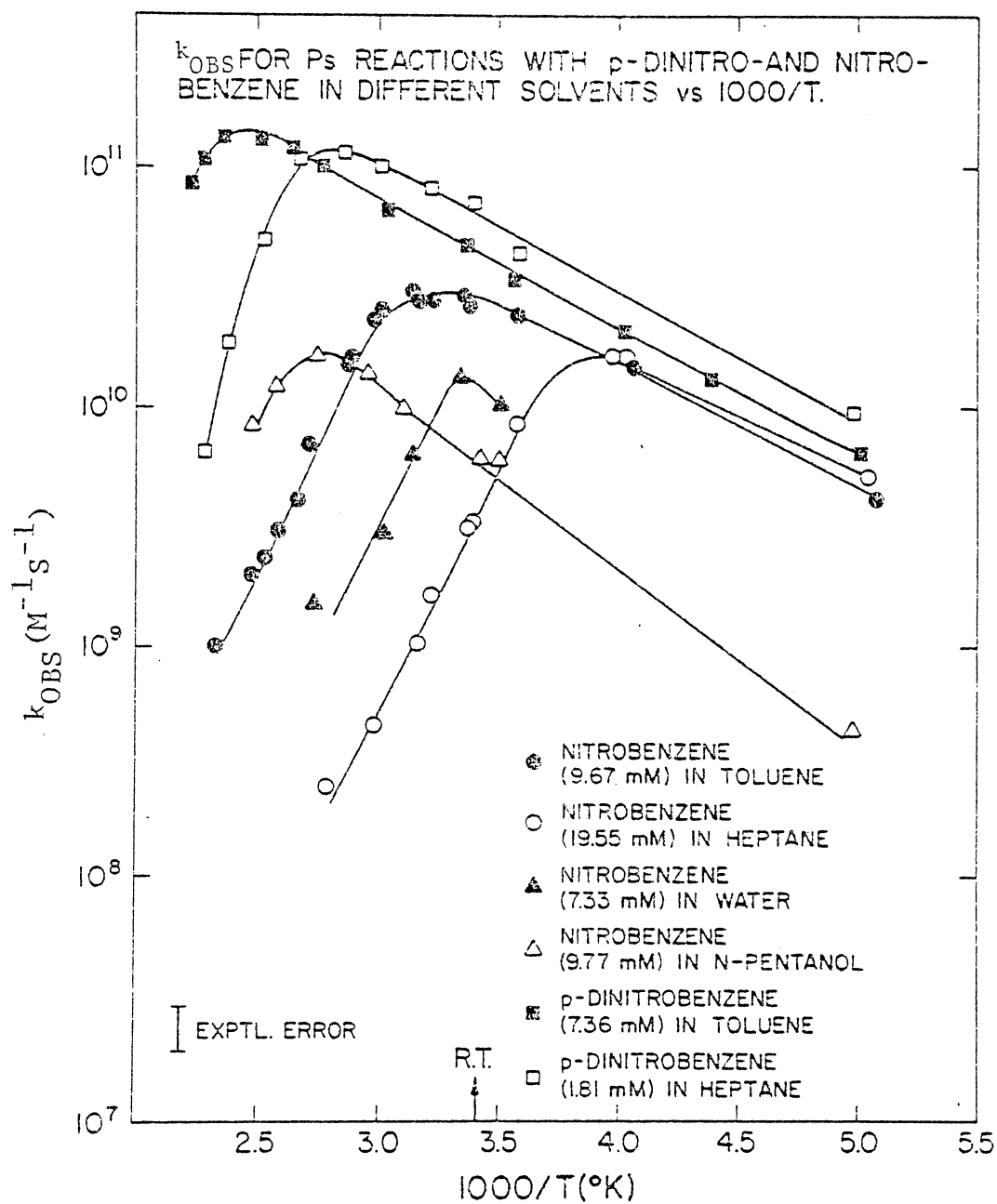


Figure 33. Arrhenius Plots for Ps Reacting with Various Nitroaromatics in Different Solvents.

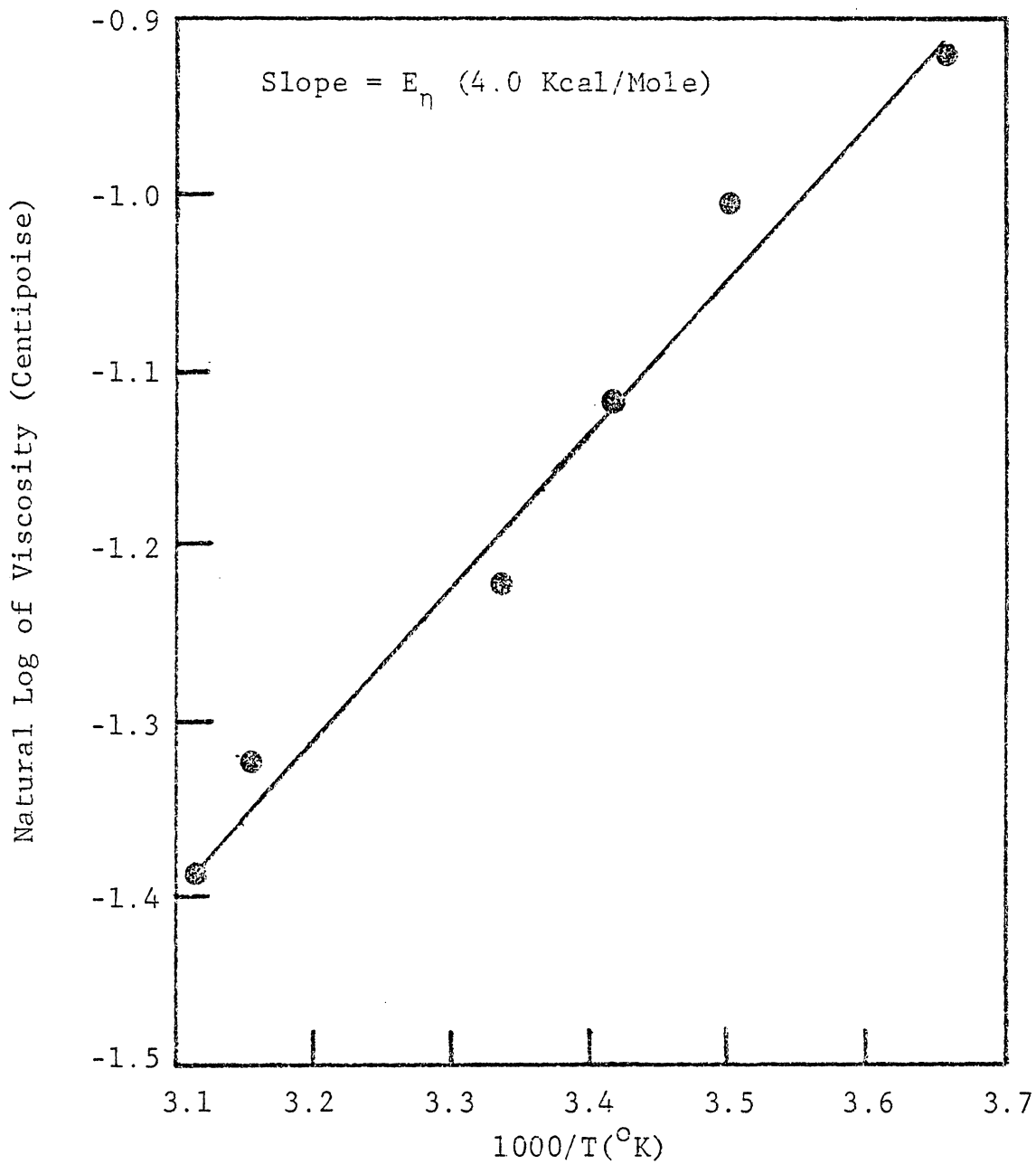


Figure 34. $\ln \eta$ VS $1000/T$ for N-Hexane to Obtain Activation Energy of Viscosity, E_η .

entropy of activation for reactions of Ps with CuCl_2 in ethyleneglycol would imply that the structure of the activated complex has less order than the structure of the separated reactants whereas a negative entropy of activation for the reaction of Ps with CuCl_2 in the other solvents (water, hexanol, etc., see Table 3) would imply that the structure of the activated complex has more order than the structure of the separated reactants. Therefore, this suggests that the (PsCuCl_2) complex in water is better stabilized en route to the transition state than in the other solvents studied in this thesis.

In these systems, the contribution to the solvent effect could be attributed to two different causes. The first could be attributed to the degree of dissociation of CuCl_2 into ions in the various solvents. While in the aqueous solution, an almost total dissociation into ions can be assumed under the experimental conditions employed whereas on the other hand complete dissociation is not the case in the organic solvents. Morgensen, Eldrup and Shantarovich⁶¹ have shown that Ps reacts faster with CuCl_2 ($k_{\text{obs}} = 12 \times 10^9 \text{ M}^{-1} \text{ sec}^{-1}$) than with CuCl^+ ($k_{\text{obs}} = 5 \times 10^9 \text{ M}^{-1} \text{ sec}^{-1}$) than with Cu^{+2} ($k_{\text{obs}} = 2.7 \times 10^9 \text{ M}^{-1} \text{ sec}^{-1}$). Thus, the rate constant for Ps reacting with CuCl_2 in various solvents could depend on a certain degree on the dissociation of CuCl_2 in those solvents. Secondly, CuCl_2 or the other Cu species might be solvated in these solvents and these solvated species may react differently with Ps. An increase in temperature could also cause an increase in dissociation and this should cause the Ps rate constants to decrease but an opposite effect was observed. This possibly could be due to the fact that a complex is being formed between Ps and CuCl_2 and Ps complex formation is the rate determining step.

C. Bubble Model and Diffusion Controlled Mechanism

According to Goldanskii and Shantarovich,⁵³ positronium is believed to occupy a cavity (bubble) in a large majority of liquids. The dependence on temperature and on the nature of the solvent is actually accounted for by formation of a "bubble" around the positronium in these liquids. Therefore, at the moment of complexation, the "bubble" shrinks rapidly depending on the properties of the liquid such as surface tension and viscosity. The molecule can penetrate into this bubble and can induce the formation of an excited complex which is quickly stabilized.

The authors assumed that these types of reactions would be diffusion controlled. In accordance with the Stokes-Einstein-Debye theory, the diffusion rate constant, k_D , can be expressed as

$$k_D = \frac{8RT}{3000\eta} \quad (\text{M}^{-1}\text{sec}^{-1}) \quad (3)$$

and if a reaction is diffusion controlled then

$$\frac{k_{\text{obs}}(T) \eta(T)}{T} = \text{constant (T)} \quad (4)$$

Goldanskii⁷⁵ has shown that this is indeed the case for several compounds reacting with Ps in different solvents. To evaluate if the reactions studied in this thesis research were diffusion controlled or not, similar calculations were performed according to Equation (4) and the results are presented in Figure 35 for the CuCl_2 systems and in Figure 36 for the nitroaromatic systems. If the reactions are diffusion controlled then the plots in these Figures should all be parallel with the temperature axis. Both Figures seem to indicate

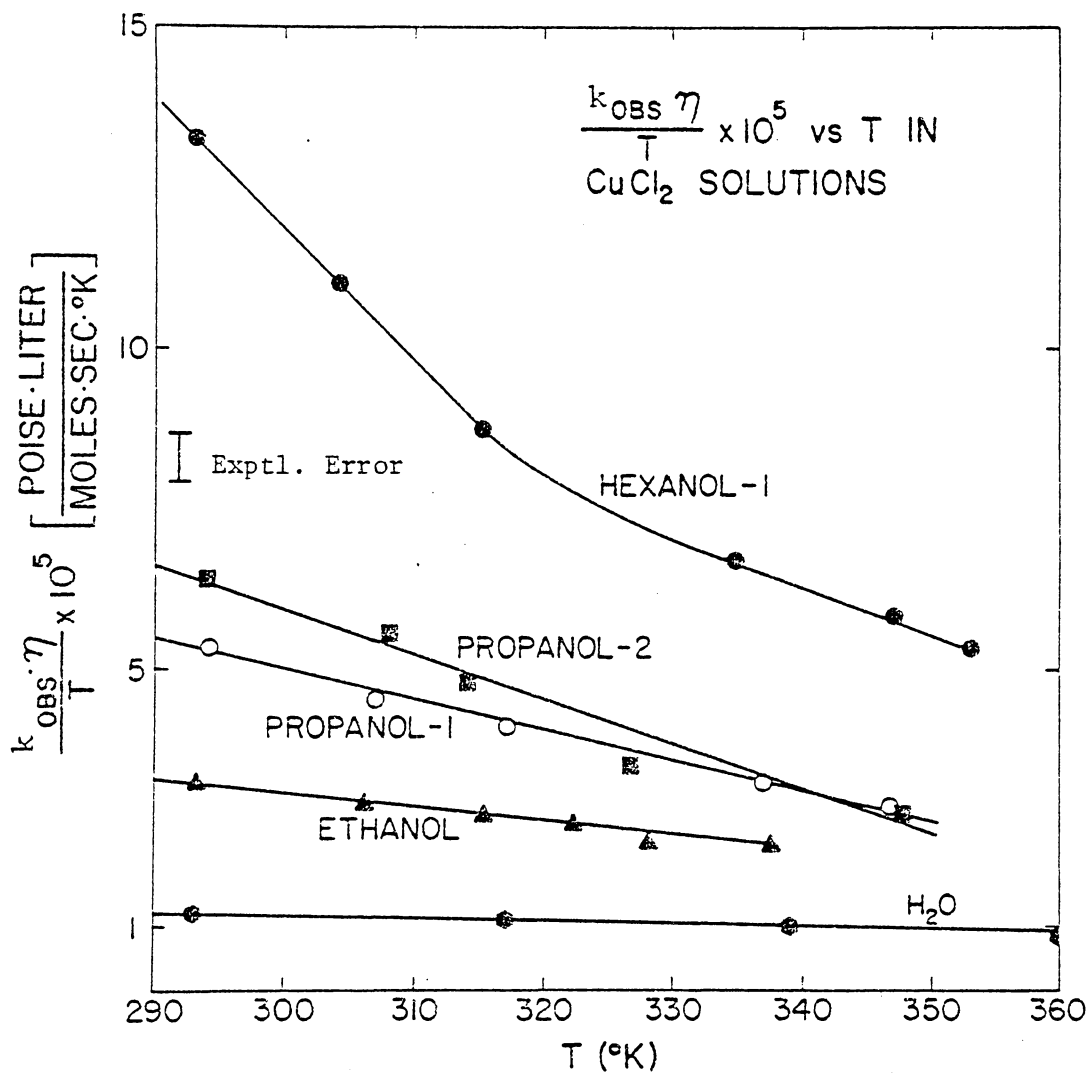


Figure 35. $(k_{OBS} \cdot \eta)/T$ VS T for Ps Reactions with CuCl₂ in Different Solvents.

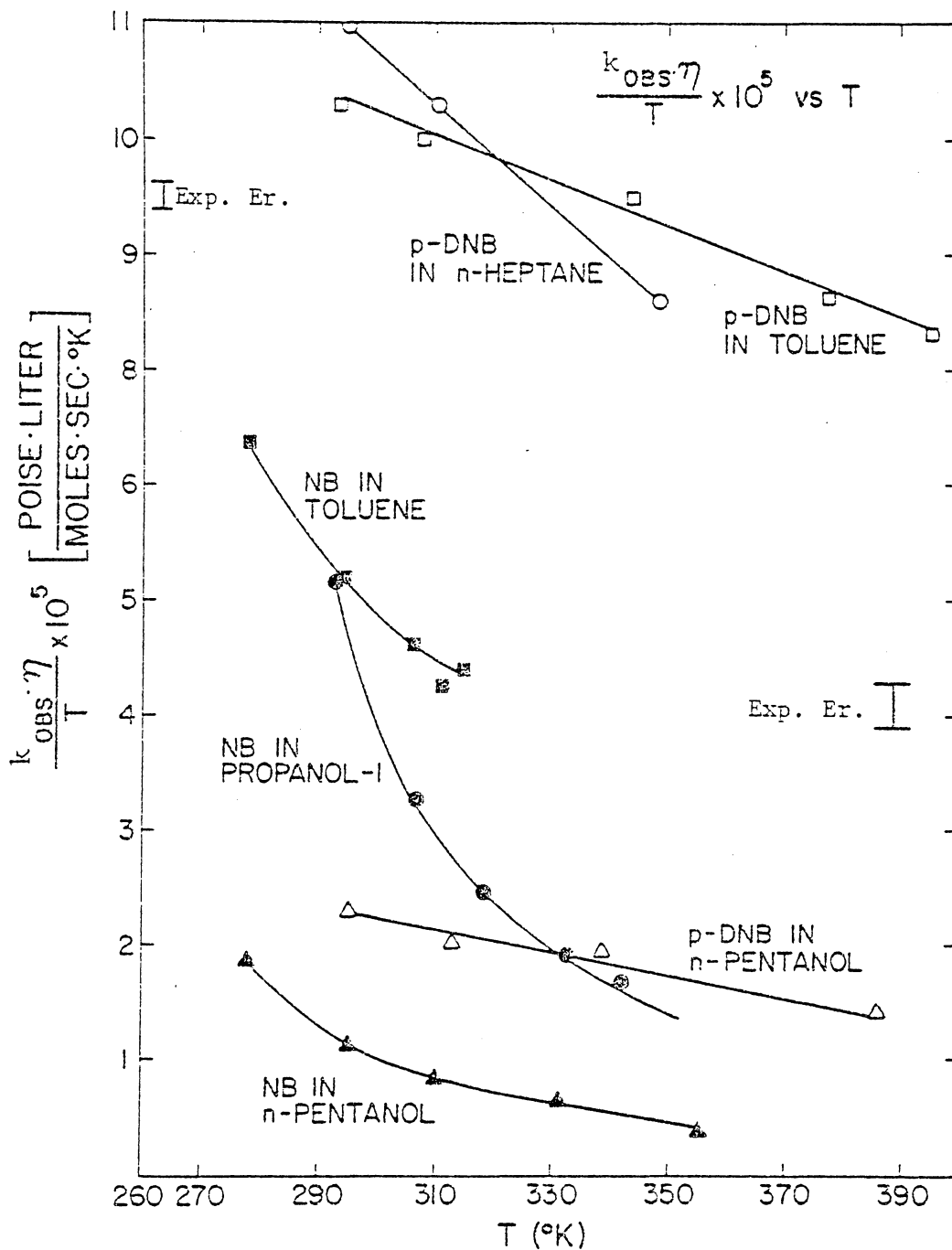


Figure 36. $(k_{OBS} \cdot \eta)/T$ VS T for Ps Reactions with Various Nitroaromatics in Different Solvents.

that these reactions are not diffusion controlled and do not obey Equation (3).

To further investigate the matter of whether Ps reactions are diffusion controlled, the "bubble model" was also applied to the experimental results for CuCl_2 and various nitroaromatics in different solvents. According to Goldanskii and Shantarovich,⁵³ the observed rate constant for positronium reacting with different compounds in solution can be expressed as (for a stable complex)

$$k_{\text{obs}} = \frac{BT}{\eta} \left[1 + q \frac{\sqrt{T}}{\eta} \exp(E_a/RT) \right]^{-1} \quad (5)$$

where E_a is the activation energy, and B and q are constants and as (for an unstable complex)

$$k_{\text{obs}} = \frac{BT}{\eta} \left[1 + q_1 \frac{\sqrt{T}}{\eta} \left(1 + \frac{\lambda_a}{\lambda_c} \right) + q \exp(-E_b/RT) \right]^{-1} \quad (6)$$

where λ_c and λ_a are the annihilation rate in the complex and bubble collapse velocity, respectively. $E_b = E_d - E_a$ where E_a is the activation energy for the formation of the (Ps-M) complex, and E_d is the activation energy for the reverse process. Rearrangement of Equation 5 yields

$$k_{\text{obs}}(i) \left[\eta(i) + q \sqrt{T(i)} \exp(E_a/RT(i)) \right] = BT(i) \quad (7)$$

where the i's correspond to measurements performed at different temperatures. For $i=3$, there are three equations and three unknowns which can be solved by Newton's approximation. The experimental k_{obs} 's were fitted to Equation 7 and the three unknowns, q, B and E_a were

determined. These values were then substituted back into Equation 7. If k_{obs} experimental is a function of η (viscosity) of the solvent, then k_{obs} experimental should be approximately equal to the calculated k_{obs} over the entire temperature range in which the experiment was performed. If k_{obs} experimental cannot be fitted to Equation 7, then k_{obs} experimental is independent of viscosity and k_{obs} experimental will not be equal to k_{obs} calculated. This approach was taken to see how well the experimental activation energy, E_a , agree with the activation energy calculated from Equation 5. The results are listed in Table 5.

There only seems to be a close agreement between the calculated activation energy and the experimental one for the two systems, $CuCl_2$ in ethyleneglycol and in n-hexanol obtained from the Arrhenius plots in Figures 31 and 32. It must be pointed out that the calculated observed rate constant, k_{obs} , agrees well with the experimental results over the entire temperature range studied only in these systems whereas in all other systems listed in Table 5 it does not agree. (See Figure 37).

Thus it seems that the bubble model is only valid above a certain critical value of the viscosity of the solvent used in the reactions between Ps and solute. If the bubble model is used below this value, it would predict a negative activation energy which renders it inapplicable.

The authors of this model have previously observed similar values in other systems and they have not been able to explain these inconsistencies with their model. The fact that a lower limit of viscosity exists for this model to be applicable is substantiated by two experimental facts. First, it seems that a better agreement between

TABLE V

Experimental and Calculated Observed Rate Constants, k_{obs} , and Calculated and Experimental Energies of Activation for Ps-Nitrobenzene and Ps-CuCl₂ Reactions in Various Solvents.

	^a k_{obs} (exp.) ($\times 10^9 \text{ M}^{-1} \text{ sec}^{-1}$)	^b k_{obs} (calc.)	^{b,f} q	^{b,g} B	η (cp)	^c E_a (Kcal/Mole)	^b E_a
Nitrobenzene in Benzene	^d 10.0	---	1.3×10^7	5.6×10^7	0.65		-10.8
Nitrobenzene in Benzene	^e 27.0	---	---	---	0.65	1.0	---
Nitrobenzene in Toluene	^e 23.9	23.9	0.25	6.8×10^8	0.74	0.3	0.8
Nitrobenzene in n-Pentanol	8.6	25.7	2.6×10^{24}	4.5×10^7	0.38	1.3	-36.3
Nitrobenzene in 1-Propanol	10.8	10.8	1.1	2.0×10^8	0.93	1.3	- .87
CuCl ₂ in Ethanol	7.92	8.34	4.3×10^{23}	3.4×10^7	1.2	2.6	-36.4
CuCl ₂ in N-Hexanol	7.5	7.5	-4.8×10^{-3}	-2.8×10^8	5.4	2.6	3.1
CuCl ₂ in Ethyleneglycol	0.5	0.5	4.9×10^{-5}	9.0×10^7	19.9	7.0	6.1

TABLE V (continued)

SYSTEMS	^a k _{obs} (exp.) x10 ⁹ M ⁻¹ sec ⁻¹	^b k _{obs} (calc.)	b,f _q	b,g _B	η (cp)	^c E _a Kcal/Mole	^b E _a
CuCl ₂ in Water	3.6	2.6	-2.8 x 10 ²³	8.8 x 10 ⁶	1.0	2.8	-38.9
CuCl ₂ in 1-Propanol	6.8	7.6	2.0 x 10 ²⁴	6.0 x 10 ⁷	1.5	2.8	-36.8
CuCl ₂ in 2-Propanol	8.1	8.1	1.6 x 10 ⁶	6.9 x 10 ⁷	2.3	2.7	-11.1

- a) From experiment at 21°C.
b) From bubble model. (Equation 5)
c) From Arrhenius plots.
d) From Ref. 53.
e) From Ref. 50.
f) In units of (T^{-1/2} η) where η = viscosity in centipoise.
g) In units of (ηM⁻¹sec⁻¹T⁻¹).

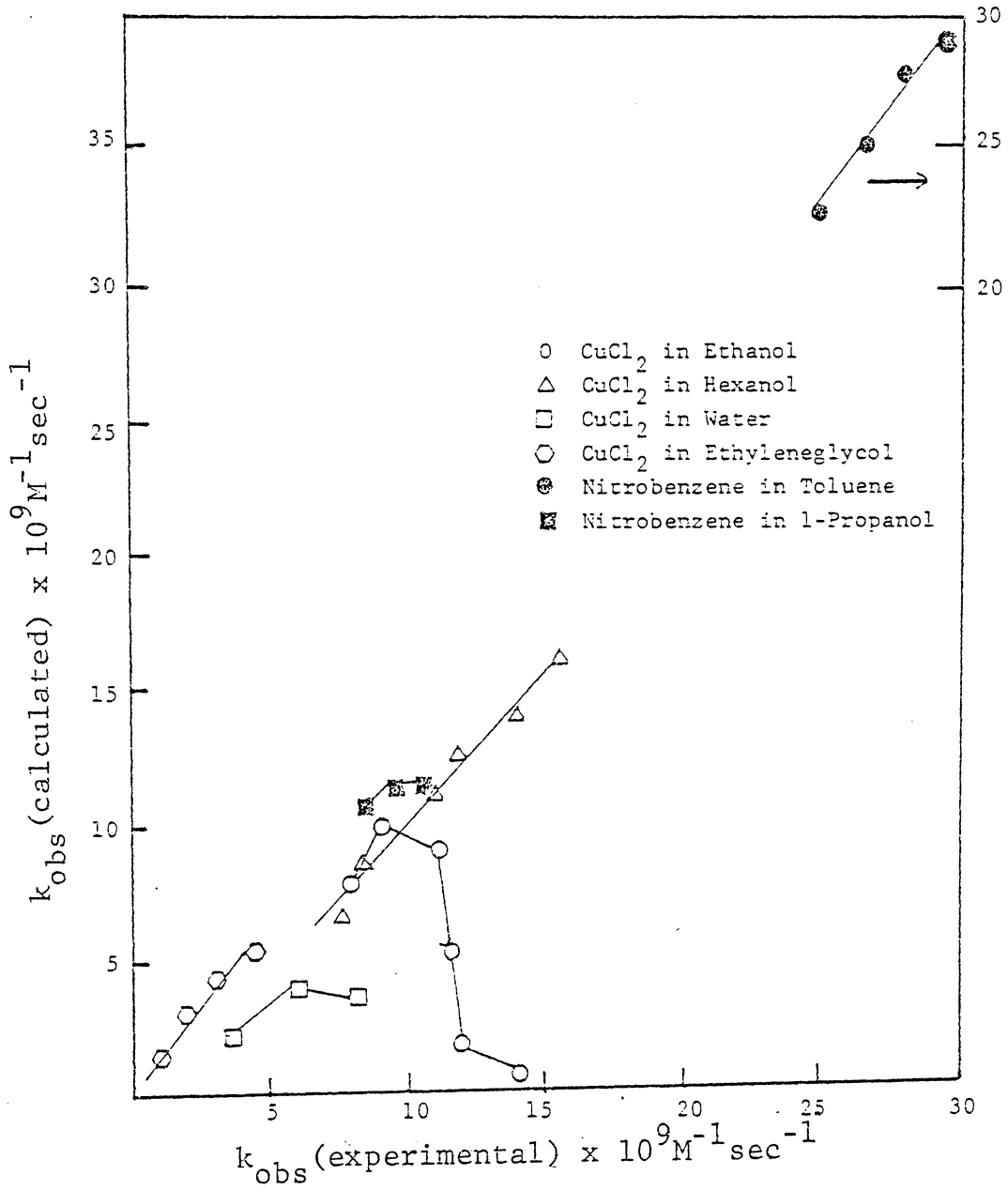


Figure 37. k_{obs} calculated VS k_{obs} experimental for Ps Reactions in Different Systems.

E_a experimental and E_a calculated can be obtained when the viscosity of the solvent is greater than 2.3 cp. For example, in Table 5, the difference between E_a calculated and E_a experimental for Ps reacting with CuCl_2 in 1-propanol ($\eta = 1.5$ cp) is 39.6 kcal/mole, whereas the difference for Ps reacting with CuCl_2 in 2-propanol ($\eta = 2.3$ cp) is considerably less, 13.8 kcal/mole. The second fact is that there is a change in slope for a plot of (k_{obs}/T) vs T for Ps reacting with CuCl_2 in n-hexanol solution. (See Figure 35). This change seems to occur at 320° K which corresponds to a viscosity of approximately 2.4 cp.

To check whether these two arguments are valid, a series of experiments were performed with Ps reacting with CuCl_2 in mixed solvents of ethanol ($\eta = 1.2$ cp) and ethyleneglycol ($\eta = 19.9$ cp) at room temperature. By varying the ratio of these two solvents the viscosity of the mixture was changed. It is interesting to note that in Figure 38 where k_{obs} is plotted as a function of viscosity for Ps reacting in these systems can be observed as a linear behavior of the resulting plot from 19.9 cp to approximately 4.0 cp. The deviation from linearity at 4.0 cp could possibly suggest that at a viscosity below 4.0 cp Ps reactions with CuCl_2 in various solutions are not diffusion controlled and that the bubble model cannot be applied below this viscosity, i.e., in the kinetically controlled region.

Perhaps this argument could be extended to other Ps-solute reactions in solution. However, the Ps-molecule complex formation model in which the correlation of $\log k_{\text{obs}}$ vs $1/T$ results in reasonably straight lines from which the Arrhenius activation energies can be obtained seems to

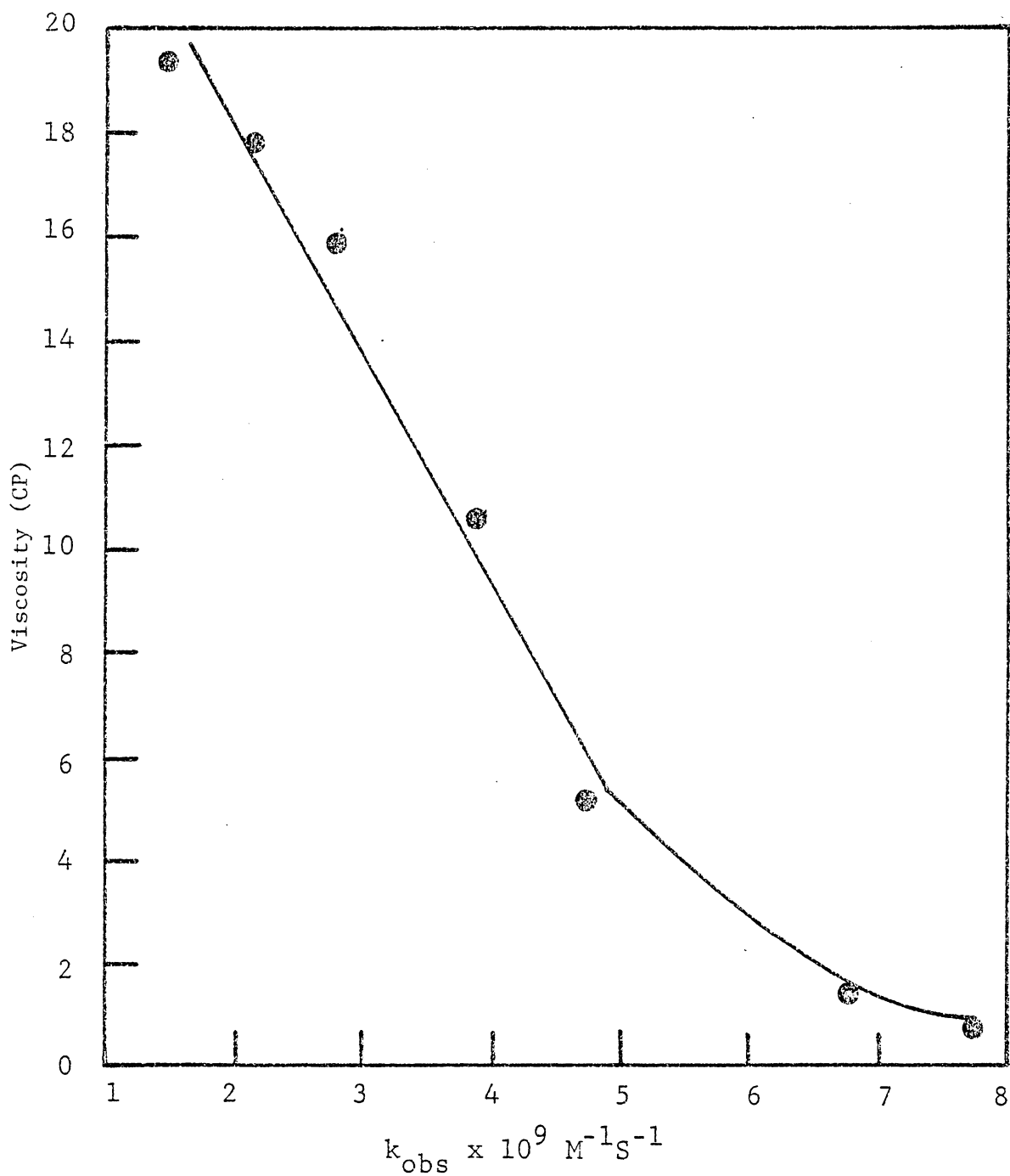


Figure 38. k_{obs} as a Function of Viscosity for Ps Reactions with CuCl_2 in Various Mixtures of Ethyleneglycol/Ethanol Solutions.

be a valid approach over a wide range of temperatures and corresponding viscosities.

In summary, there seems to be no simple correlation between the various macroscopic solvent parameters such as viscosity and the observed rate constants for Ps atoms reacting with different solutes in different solvents. As was shown in the previous Chapter, the differences in the observed rate constants for Ps reacting with CuCl_2 in different solvents may be attributed to the entropy of activation in the absolute rate theory equation. Preliminary results seem to indicate that the alternative, i.e., the bubble model is not applicable below a certain critical viscosity of the solvent and restricted to diffusion controlled reactions.

STUDY OF INCLUSION COMPLEX FORMATION

A. Introduction

A practical application of the positronium complex formation can be found in the experimental determination of K_c (the molecular association constant). In this determination, the Ps atom acts as a probe by sampling the molecular environment. By using certain highly reactive molecules to form a complex with a substrate molecule, one can use Ps to determine how strongly these molecules complex.

Inclusion compounds are formed when the cyclic oligosaccharides accommodate a guest molecule in its cavity.⁶² The cyclic oligosaccharide studied here was cyclohexaamylose (α -cyclodextrin). The molecular dimensions of this compound are shown together with those of other cyclodextrins in Table 6. The structures of these compounds are toroid shape with a hydrophobic (water hating) cavity and surface along with hydrophilic (water loving) faces. (See Figure 39). Due to the lack of free rotation about the glycosidic bond which connects the glucose units, the cycloamyloses are not perfectly cylindrical molecules but are somewhat coned shaped. According to x-ray studies,^{63,64} the six-hydroxyl face is somewhat narrower than the 2,3-hydroxyl face. Also x-ray studies together with nmr studies have shown that the glucose rings are in the 4C_1 (D) chair conformation and that the 3-hydroxyl hydrogen is hydrogen bonded to the 2-hydroxyl oxygen of an adjacent ring. These studies have also confirmed that hydrogen bonding still persists in solution along with the 4C_1 (D) chair conformation. This means that intramolecular bonding is responsible for the cone shape.

TABLE VI
Molecular Dimensions of Cycloamyloses

Cycloamylose	Number of glucose residues	Cavity dimensions (Å) Diameter	Depth
Cyclohexaamylose	6	4.5	6.7
Cycloheptaamylose	7	7.0	7.0
Cyclooctaamylose	8	8.5	7.0

From Ref. 62.

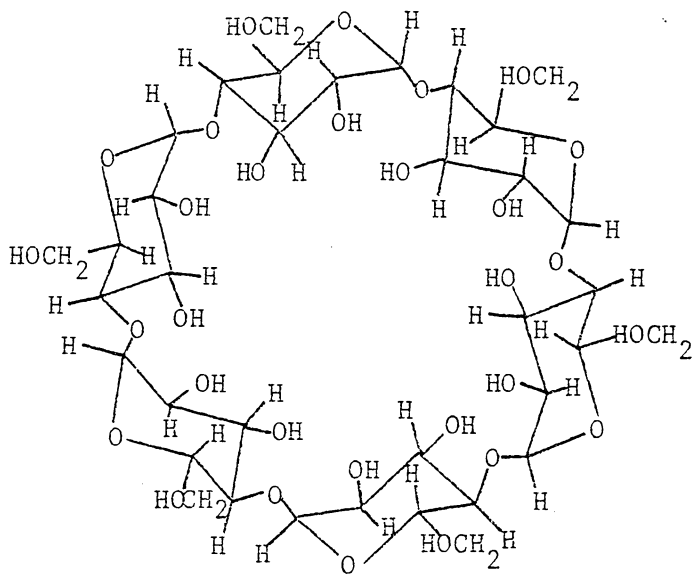


Figure 39. Cyclohexaamylose

The ability of the cycloamyloses to bind molecules in its cavity is due to hydrogen bonding, van der Waals forces, and hydrophobic interactions.^{65,66} X-ray analysis has confirmed that the guest molecule is bound inside the cavity forming a 1:1 complex. These guest molecules can range in size from noble gases up to large molecules such as azo dyes. Experiments have also indicated that the cycloamyloses can bind small inorganic ions⁶⁷ such as ClO_4^- , SCN^- , I^- , Br^- and NO_3^- . The stability of these inclusion compounds will depend on the size of the guest molecule. Thus, if a substrate is too large it will simply not fit into the cavity and, therefore, not bind to the cycloamylose. On the other hand, if a substrate is too small it will pass in and out of the cavity with little binding. The general equilibrium mechanism for this process is



where (D) is the host molecule (cyclohexaamylose), (Q) is the guest molecule (nitrobenzene derivatives) and $K_c (\text{M}^{-1})$ is known as the formation constant, or in some of the literature as the association constant. A list of different guest molecules binding in cyclohexaamylose along with their respective K_c values are shown in Table 7.

Up until now, the basic way of determining K_c was by NMR and UV spectroscopy. The Ps atom as a probe now offers a very sensitive method to determine K_c , which has the additional advantage that it does not perturb the system. By studying the changes in the lifetime of positronium, one accurately determines values of K_c which are within

TABLE VII
 Inclusion Complex Formation Constants, K_c for
 Various Guest Molecules Binding in the
 Cavity of Cyclohexaamylose

Guest Compound	$^a K_c, M^{-1}$	Ref.
p-Nitrophenol	341	68
Nitrobenzene	49	68
p-Benzoquinone	7	68
Cl ⁻	N.B.	67
ClO ₄ ⁻	29	67
NO ₃ ⁻	1.4	67
Benzoic Acid	1000	62
Acetic Acid	6310	62
Pyridine	158	62
^b Azo Dye	270	65
2,6-Dimethyl-4-Nitrophenol	568	65

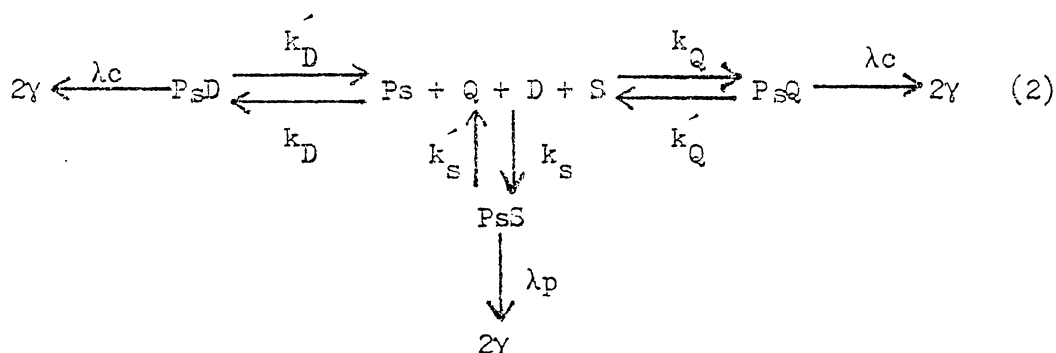
a) Measured at 21°C.

b) 3'-Ethyl-4'-Hydroxyphenylazo-1-Naphthalene-4-Sulfonate.

experimental error of the values quoted in the literature. In fact, Jean and Ache⁶⁸ studied some inclusion compounds and they experimentally determined K_c for p-nitrophenol binding in cyclohexaamylose to be 341 M^{-1} which is in excellent agreement with the value obtained by spectroscopic methods.⁶⁹ The principle of using the o-Ps atom as a probe in these systems is based on the fact that it reacts very rapidly with certain compounds, such as nitroaromatics to form a Ps-molecule complex, but these compounds lose most of their reactivity toward Ps when they are already complexed with another molecule to form a charge transfer complex such as the nitrobenzene-cyclohexaamylose complex. From this, the differences in the reactivity of these compounds in their complexed and uncomplexed forms towards Ps can be used as a new tool to determine molecular association constants (K_c).

B. Kinetic Equations

The general mechanism for a medium consisting of three components, Q, D and S, the various Ps reactions can be set up as the following:



The reactions with Ps to consider are: (1) Reaction of Ps with substrate Q (guest) or D (complex) or with the solvent S which results in the formation of the Ps complexes PsQ, PsD, or PsS with rate constants k'_Q , k'_D ,

or k_S , respectively. (2) Decomposition of PsQ, PsD or PsS with rate constants $k_{Q'}^f$, $k_{D'}^f$ or $k_{S'}^f$, respectively. (3) Positron annihilation in the complex (decay constant λ_c); λ_c is considered to be independent of the type of complex formed (PsQ, PsD, PsS).⁷⁰ Since the concentrations of Q, D, and S remain practically constant in reactions with Ps, then the following kinetic equations can be set up:

$$-d[Ps]/dt = k_Q[Ps][Q] + k_D [Ps][D] + k_S [Ps][S] - \quad (3)$$

$$k_{Q'}^f [PsQ] - k_{D'}^f [PsD] - k_{S'}^f [PsS]$$

$$\frac{-d[PsQ]}{dt} = -k_Q[Ps][Q] + (\lambda_c + k_{Q'}^f) [PsQ] \quad (4)$$

$$\frac{-d[PsD]}{dt} = -k_D[Ps][D] + (\lambda_c + k_{D'}^f) [PsD] \quad (5)$$

$$\frac{-d[PsS]}{dt} = -k_S[Ps][S] + (\lambda_c + k_{S'}^f) [PsS] \quad (6)$$

According to previous calculations performed in our laboratory,⁷⁰ a good approximation for solving these differential equations is by invoking steady state conditions, i.e.,

$$\frac{d[PsQ]}{dt} = \frac{d[PsD]}{dt} = \frac{d[PsS]}{dt} = 0 \quad (7)$$

With this, the number of positrons populating the Ps state can now be derived by solving Equations (4-6) for PsQ, PsD, and PsS, followed by the substitution of these values into Equations (2) and (3) and one obtains the following relation:

$$\frac{d[Ps]}{dt} = - \frac{k_Q \lambda_c}{\lambda_c + k_Q} [Q] + \frac{k_D \lambda_c}{\lambda_c + k_D} [D] + \frac{k_S \lambda_c}{\lambda_c + k_S} [S] \quad (8)$$

The experimental conditions are such that all solutions are dilute (mM range), i.e., the solvent is in large excess and its concentration remains fairly constant throughout the experiment and the third term in Equation (8) can be simplified to

$$(k_s \lambda_c / \lambda_c + k_s) [S] = \lambda_p \quad (9)$$

Integrating Equation (8) gives the time dependent concentration of Ps :

$$[Ps_t] = [P_s^0] \exp - \left\{ \lambda_p + \frac{k_Q \lambda_c}{\lambda_c + k_Q} [Q] + \frac{k_D \lambda_c}{\lambda_c + k_D} [D] \right\} t \quad (10)$$

As mentioned earlier in the previous chapter, the time-dependent two-photon annihilation rate ($R_2\lambda$) can be represented by the following two-exponential equation

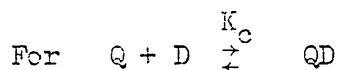
$$R_{2\gamma} = A \exp (-\lambda_1 t) + B (-\lambda_2 t) \quad (11)$$

The annihilation rate for o-Ps, λ_2 , can be related to Equation 10⁷¹ by:

$$\lambda_2 = \lambda_p + \frac{k_Q \lambda_c}{k_Q + \lambda_c} [Q] + \frac{k_D \lambda_c}{k_D + \lambda_c} [D] \quad (12)$$

k_Q (obs) k_D (obs)

Equation (12) predicts a linear relationship with two compounds present. This was found to be valid in separate experiments where various mixtures of m-nitrobenzene and o-nitrotoluene were allowed to react with Ps in benzene solution.⁷¹

C. Calculation of K_c (Molecular Complex Formation Constant)

let QD be the equilibrium concentration of the complex QD , and let Q and D be the initial concentrations of the guest (Q) and host (D) molecules, respectively. The formation constant (K_c) of the complex is given by

$$K_c = \frac{[QD]}{([Q] - [QD])([D] - [QD])} \quad (13)$$

It must be pointed out that this equation is only valid for a 1:1 complex. Under the experimental conditions used in these studies, the host (D) was always in excess relative to that of the host. (92 mM host, 6 mM guest). Then QD can be approximated as:

$$[QD] = [Q][D] K_c / (1 + [D] K_c) \quad (14)$$

Because the amounts of Q , D , or QD reacting with Ps are negligible as compared to the concentrations $[Q]$, $[D]$, or $[QD]$, one can safely say that the complex formation equilibrium is not shifted by the reaction with Ps . The final equation for λ_2 can be written taking into account the equilibrium concentration of the uncomplexed molecules $[Q] - [QD]$ by

$$\lambda_2 = \lambda_p + k_{Q(\text{obs})} [Q] + \frac{[Q][D] K_c}{1 + [D] K_c} (k_{QD(\text{obs})} - k_{Q(\text{obs})}) \quad (15)$$

According to Jean and Ache,⁷² the first two terms in Equation (15) can be obtained by measuring the annihilation rate of the guest in water without any host present:

$$\tilde{\lambda}_2^0 = \lambda_p - \lambda_2^0 + k_{Q(\text{obs})} [Q] \quad (16)$$

Substitution of Equation (16) into (15) gives

$$\frac{1}{\tilde{\lambda}_2 - \tilde{\lambda}_2^0} = \frac{1}{K_c [Q] [D] (k_{QD(\text{obs})} - k_{Q(\text{obs})})} + \frac{1}{[Q] (k_{QD(\text{obs})} - k_{Q(\text{obs})})} \quad (17)$$

where $\tilde{\lambda}_2$ is the difference between the annihilation rate of the host (λ_2 host) and the annihilation rate of the complex (λ_2 host & guest) and $\tilde{\lambda}_2^0$ is the difference between the annihilation rate of the guest in water (λ_2 guest) and the annihilation rate (λ_p) in the buffered solution of pH 3.5.

First, λ_2 was determined in the buffered solution. Then λ_2 was determined for different concentrations of the host, cycloamylose, in the buffered solution without any guest present. Then λ_2 was determined and hence $k_{Q(\text{obs})}$ for a known concentration of guest present without any host. After all this was done, λ_2 was determined by keeping the guest concentration constant while varying the concentration of the host. The results for six different nitroaromatics are shown in Figure 40, where $-1/(\tilde{\lambda}_2 - \tilde{\lambda}_2^0)$ is plotted as a function of $1/[D]$. By extrapolating $1/[D]$ to zero concentration, one can obtain the intercept $1/[Q] (k_{QD(\text{obs})} - k_{Q(\text{obs})})$ by linear least squares analysis. Since $k_{Q(\text{obs})}$ was determined separately without any host present and one knows the concentration of the guest $[Q]$, $k_{QD(\text{obs})}$ can be determined. The slope of the plot is $1/K_c [Q] (k_{QD(\text{obs})} - k_{Q(\text{obs})})$ and the complex formation constant, K_c , can be determined by simply dividing the intercept by the slope. The results of these experiments are summarized in Table 8. As expected the

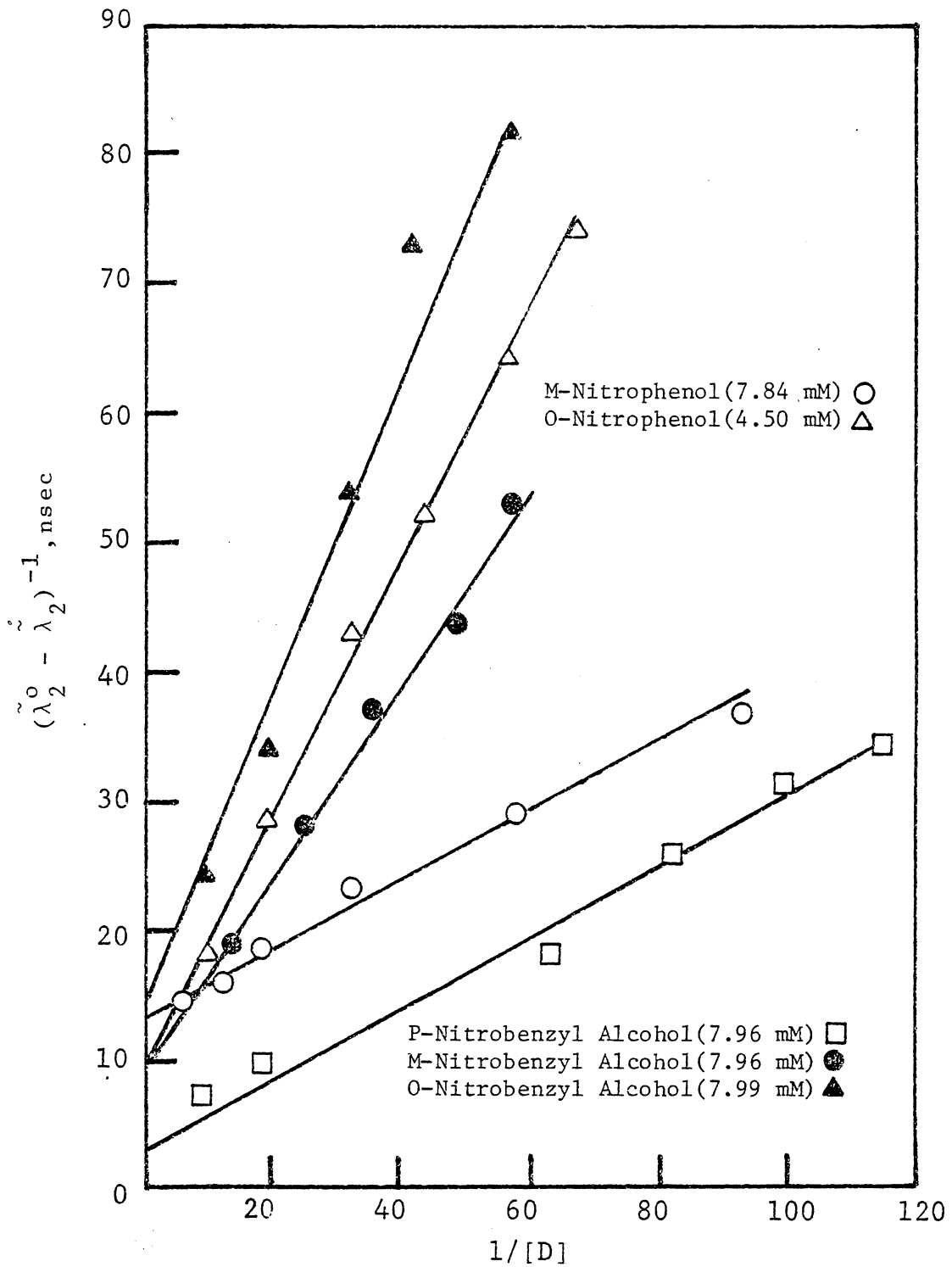


Figure 40. $(\tilde{\lambda}_2^0 - \tilde{\lambda}_2)^{-1}$ VS $1/[\text{Cyclohexaamylose}]$ for the Determination of K_c (Molecular Formation Constant)

TABLE VIII

Inclusion Complex Formation Constants, K_c , and Rate Constants, $k_{\text{QD(OBS)}}$, for the Interaction of the Inclusion Complexes of Various Nitroaromatics with Cyclohexaamylose (CD) at pH 3.5, Ionic Intensity 0.5, in Aqueous Solution at 22°C.

Inclusion Compounds		
Compound	$k_{\text{qd(ops)}}$ $10^{10} \text{ M}^{-1} \text{ s}^{-1}$	$K_c, \text{ M}^{-1}$
p-Nitrophenol	0.88	
p-Nitrophenol-CD	0.11	^a 341
m-Nitrophenol	1.15	
m-Nitrophenol-CD	0.28	91
o-Nitrophenol	0.99	
o-Nitrophenol-CD	b	19
p-Nitrobenzyl Alcohol	1.46	
p-Nitrobenzyl Alcohol-CD	b	43
m-Nitrobenzyl Alcohol	0.99	
m-Nitrobenzyl Alcohol-CD	0.18	28
o-Nitrobenzyl Alcohol	1.14	
o-Nitrobenzyl Alcohol-CD	b	7

a) From Ref. 68.

b) Not detectable. The reactivity of the molecular complex towards Ps is below the detectable limit ($k_{\text{obs}} < 0.05 \times 10^{10} \text{ M}^{-1} \text{ s}^{-1}$) inherent to method of evaluation.

results also show that the reactivity of the guest molecules in their complexed form is reduced by a factor of ten or more.

D. Steric and Geometric Factors

The molecular association constants (K_c) for the compounds in Table 9 can be put in the following order according to the magnitude of K_c : p-nitrophenol > m-nitrophenol > nitrobenzene > p-nitrobenzyl alcohol > o-nitrophenol > p-benzoquinone. But the reactivity of these compounds with Ps shows a reverse trend as listed in Table 9 which is somewhat surprising since one would expect K_c to follow the same order as the reactivity. If one assumes that similar forces are operating for the complexation of nitrobenzene and other nitroaromatics with Ps or with cyclohexaamylose, then these drastic differences in K_c would have to be attributed to steric hinderance and geometric factors. The size of the p-nitrophenol molecule approaches the dimensions of the depth of the cavity in cyclohexaamylose thus providing the best fit of all the compounds studied, thus providing the largest K_c . On the other hand compounds such as nitrobenzene and p-benzoquinone might be too small to undergo efficient binding in the cavity due to their size.

Bergeron and Pillor⁷³ have shown that substituted nitrobenzenes bind nitro end first into the cavity of α -cyclodextrin. As mentioned earlier, the diameter of α -cyclodextrin is 4.5 \AA whereas its depth is 6.7 \AA and the substituted nitrobenzenes should fit into this cavity. The formation constant (K_c) can be used to see how effective the binding of substituted nitrobenzenes in this cavity. A high value ($K_c = 341$) as compared to a low value ($K_c = 7$) can be interpreted as relatively strong binding of the substituted nitrobenzenes into the α -cyclodextrin cavity.

TABLE IX

Comparison of Different Rate Constants (k_{obs}) for Ps Reacting with Various Guest Molecules in Aqueous Solution at pH 3.5, Ionic Intensity 0.5 and Inclusion Complex Formation Constants, K_c , for the Interaction of Various Guest Molecules in the Cyclohexaamylose Cavity.

Guest Molecule	$k_{\text{obs}} \times 10^9 \text{M}^{-1} \text{sec}^{-1}$	${}^b K_c, \text{M}^{-1}$
p-Nitrobenzyl Alcohol	1.46	43
^a Nitrobenzene	1.38	48
^a p-Benzoquinone	1.37	7
m-Nitrophenol	1.15	91
o-Nitrophenol	0.99	19
^a p-Nitrophenol	0.88	341

a) From Ref. 68.

b) at 21°.

Bergeron⁶⁹ has shown that K_c is reduced for the substituted nitrobenzenes depending on where the substitution is on the benzene ring (p,m). Bergeron and Pillor have also shown that several substituted nitrophenols show a drastic decrease in K_c depending on the position of the substituents on the benzene ring. (See Table 10) In several cases the substitution resulted in no complex being formed. Both papers attribute this decrease in binding to steric hinderance of the guest molecules.

The effect can be seen in going from p, m, to o with an accompanying drastic decrease in K_c or weaker binding of the guest molecule into the α -cyclodextrin cavity. The results from this study follow the same trend which confirms the argument of steric hinderance which lowers the effectiveness of the nitro end to bind in the hydrophobic region of the α -cyclodextrin cavity.

Looking at the models in Figure 41, one can see how the effectiveness of the binding of the guest molecules are affected by steric hinderance.

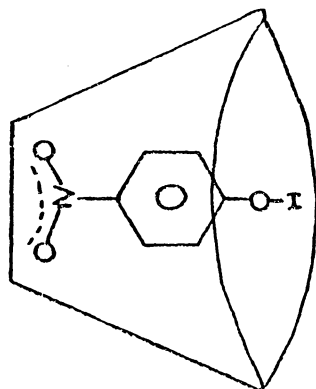
Another reason for a lower K_c can be seen if one looks at the molecular dimensions of the guest molecules. Since nitrobenzene is short as compared to p-nitrophenol and since p-nitrophenol has two ends which it can bind in the cavity, one would expect it to have a higher K_c than nitrobenzene. The length of p-nitrophenol is 6.54 Å and the depth of the cavity is about 6.7 Å and one can see this is almost a perfect fit. Looking at p-nitrobenzyl alcohol one notices its dimensions to be 8.02 Å long which means it does not fit well into the α -cyclodextrin cavity thus lowering its ability to bind,

TABLE X

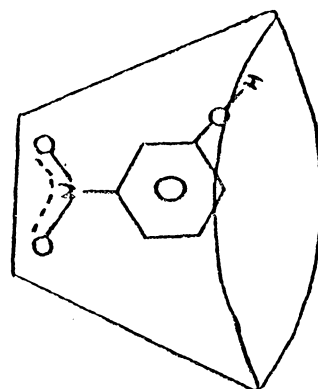
Influence of the Steric Effect in Lowering the Inclusion Formation Constants, K_c , for Various Guest Molecules in the Cavity of Cyclohexaamylose.

Guest Molecule	$^a K_c, M^{-1}$	Ref.
p-Nitrophenyl Acetate	83	69
m-Nitrophenyl Acetate	53	69
2,6-Dimethyl-4-Nitrophenol	568	69
3,5-Dimethyl-4-Nitrophenol	N.B.	69
p-Nitrophenol	341	68
m-Nitrophenol	91	--
p-Nitrobenzyl Alcohol	43	--
m-Nitrobenzyl Alcohol	28	--

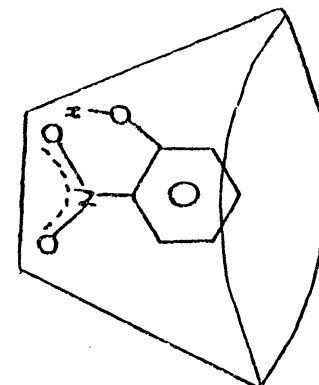
a) Measured at 21°C.



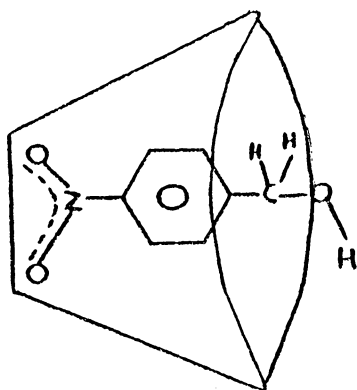
P-NITROPHENOL
 $K_C = 341$



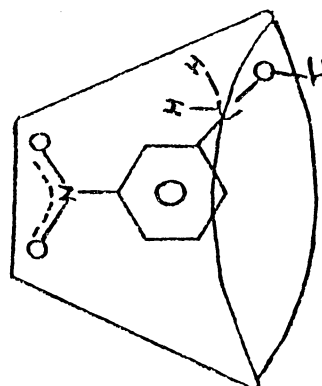
M-NITROPHENOL
 $K_C = 91$



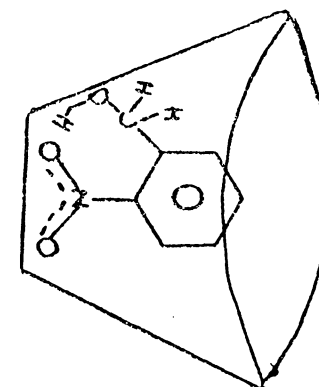
O-NITROPHENOL
 $K_C = 19$



P-NITROBENZYL ALCOHOL
 $K_C = 43$



M-NITROBENZYL ALCOHOL
 $K_C = 28$



O-NITROBENZYL ALCOHOL
 $K_C = 7$

Figure 41. Steric Factors Involved in Lowering of K_C .

thus producing a lower value of K_c which is borne out by the experimental results.

Now considering *o*-nitrophenol and *o*-nitrobenzyl alcohol, one can see that two factors might be responsible for the much lower value of K_c and the weaker binding. One being that the incorporation of these molecules into the cavity are drastically sterically hindered. The second factor being the possibility of intramolecular hydrogen bonding in the guest molecule, which can compete with intermolecular hydrogen bonding between the guest molecule and the hydrophobic cavity inside the host molecule. This competition can reduce the strength of binding and hence give rise to a much lower value of K_c .

It must be pointed out that the water inside the cavity of the host is different from the bulk water. A reaction in which a solvent becomes more disordered will usually proceed with a favorable change in entropy but the disordering of the solvent will be accompanied by the breaking of at least some solvent-solvent bonds which will result in an unfavorable enthalpy change. The driving force for binding in the cavity could also be attributed to the fact that the water removed from the carboxy-group or in the cyclodextrin cavity becomes bulk water and as such is hydrogen bonded. The net result will be a gain in the number of hydrogen bonds and unfavorable entropy changes might result in the greater ordering of the "kicked out" water molecules in the bulk water structure. A large value of K_c can be attributed to a compound that is effective in "kicking out" water molecules from the cavity.

Another theory proposed by Bergeron to account for binding in the cavity, is that the guest molecule relieves the ring strain energy in

the cavity. So the only requirements for a molecule to bind in the cavity are size, displacement of the high-energy cavity water and the lowering of the ring strain energy in the cyclodextrin.

Summarizing then, the mechanism for the formation of an inclusion complex can be divided into several steps: (1) the approaching of the guest molecule to the cyclodextrin molecule; (2) breakdown of the water structure inside the cyclodextrin cavity and subsequent removal of some water molecules out of the cavity; (3) breakdown of the solvated water molecules around the guest molecule, which also includes this process in the cyclodextrin cavity, and subsequent transport of some water molecules into the bulk; (4) interaction of the substituents on the guest molecules with the hydroxyl groups on the rim or on the inside of the cyclodextrin cavity; (5) possible formation of hydrogen bonds between guest and cyclodextrin (hydrogen bond formation has been shown to be very fast and cannot be the rate determining step for inclusion compound formation);⁷⁴ (6) reconstruction of the water molecules around the exposed parts of the guest molecule after the inclusion complex is formed. In steps 1, 4, and 5, steric factors play an important role in the stability or rate of formation of the complex. The results in this thesis showed that this is indeed the case.

These inclusion compounds play an important role in chemistry and biochemistry because of their ability to inhibit or catalyze different reactions. The cyclodextrins seem to bind a large number of substrates and if specificity of substrate binding is a necessary criterion for a workable model for substrate binding to enzymes, then the cyclodextrins fail to satisfy this criterion.

In all the examples studies so far, a trend is seen to develop. From Table 8 and from other studies⁶¹ done on donor-acceptor complexes, it can be seen that complex formation resulted not only in a reduction of reactivity towards Ps, but this reduction in reactivity was more pronounced if a weaker complex (smaller K_c) was formed than when strong complexing occurred. In the first case, most of the complexing capability of the guest molecule is used for binding and very little will be left to interact with Ps, whereas a strong complex can itself complex with Ps, thus forming a strong double complex.

CONCLUSIONS

A. Summary

The thermal reactions of *o*-Ps with certain highly reactive nitroaromatics in various solvents were found to be dependent on the solvent environment whose effect was related to the entropy of activation which in turn is due to the stabilization of the PsM complex by the solvent. This entropy term in the pre-Arrhenius factor was assumed to be mainly responsible for the differences in the rate constants for these reactions since it has been found that all the reactions investigated had the same activation energies. This was also found to be true for Ps reacting with CuCl_2 in various solvents.

It was shown that Ps reacting with various nitroaromatics and inorganic ions in solution are not solely diffusion controlled as was once thought because of the observed extremely fast rate constants for these reactions. The "bubble shrinkage model" was tested using the results obtained in the reactions of Ps with various inorganic and organic molecules in different solvents and it was found that this model is definitely not applicable below a certain critical viscosity of the solvent and appears to be restricted to diffusion controlled reactions. It was also shown that in almost all the cases that the Arrhenius activation energy, E_a , was always less than the activation energy of viscosity, E_η . Furthermore, the rate of reaction between *o*-Ps and various nitroaromatics and CuCl_2 in different solvents does not seem to be related to any properties of the solvent such as surface tension, dielectric constant, and viscosity.

Positronium can be used as a probe to sample the environment and to obtain valuable information about how effectively certain nitro-aromatic guest molecules bind in the cavity of cyclohexaamylose to form an inclusion compound. The strength of binding of these guest molecules in the cavity is strongly dependent on geometric and steric factors. The usefulness of using Ps as a probe to determine K_c (molecular formation constant) comes into play when current existing techniques cannot be applied to the systems.

B. Future Possibilities

Further studies of the reactions between Ps and inorganic or organic molecules in different mixtures of solvents would be necessary to correlate the rate constants for these reactions with the properties of the solution and to find out more about the contributions made by diffusion or kinetically controlled processes to the overall reaction. This can be accomplished by varying the composition of the solvent mixture which allows to change the viscosity of the solution over a large range. Of special interest are those cases where strongly reacting molecules are undergoing reactions in a solution displaying a low viscosity because in these systems, the reaction is completely kinetically controlled. The factors responsible for the reactivity of substrate molecules towards Ps can then be accurately evaluated. This could add to a better understanding about what factors control the reactions of Ps in solutions.

The study of gas phase reactions between Ps and various substrates could also provide a better understanding about the mechanism responsible for Ps complex formation. This study could also be complemented with

angular correlation experiments to provide information about the nature of the electrons which are responsible for the annihilation of the positron.

REFERENCES

1. Dirac, P.M., Camb. Phil. Soc., 26, 361 (1930).
2. Anderson, C.D., Phys. Rev., 41, 405 (1932); Phys. Rev., 43, 491 (1933); Phys. Rev., 44, 405 (1933).
3. Feynman, R.P., Phys. Rev., 76, 749 (1949).
4. Joliot, F. and Curie, I., Nature, 133, 201 (1934).
5. Hamilton, J.H., Langer, L.M. and Smith, W.G., Phys. Rev., 112, 2010 (1958).
6. Fermi, E.Z., Physik, 88, 161 (1934).
7. Lee, T.D. and Yang, C.N., Phys. Rev., 105, 1591 (1957).
8. Tao, S.J. and Green, J.H., J. Chem. Soc., A, 408 (1968).
9. Goldanskii, V.I., Atomic Energy Rev., 6, 3 (1968).
10. Heilner, W., The Quantum Theory of Radiation, Clarendon Press, Oxford, England, 1954.
11. Ore, A. and Powell, J.L., Phys. Rev., 75, 1696 (1949).
12. Mohorovicic, S., Astronn. Nachr., 253, 94 (1934).
13. Deutsch, M., Phys. Rev., 83, 866 (1951).
14. Ruark, A.E., Phys. Rev., 68, 278 (1945).
15. McGervey, J. and De Benedetti, S., Phys. Rev., 114, 495 (1959).
16. Ore, A., Univ. Bergen Arbok Naturvitenskap. Rekke, 9, (1949).
17. Gittleman, B. and Deutch, M., Ann. Prog. Report, Lab. Nucl. Sci., M.I.T., 139 (1958).
18. Morgensen, O.E., J. Chem. Phys., 60, 998 (1974).
19. Wild, R.E., Ph.D. Dissertation, VPI & SU., 1976.
20. Tao, S.J., Appl. Phys., 10, 67 (1976).
21. Cook, C.E., Grey, P.R. and Sturm, C.P., J. Chem. Phys., 48, 1145 (1968).

22. Berko, S., Brandt, W., and Walker, W.W., Phys. Rev., 120, 1289 (1960).
23. Henderson, G.A. and Millett, W.E., Bull. Am. Phys. Soc., 7, 58 (1962).
24. Johnson, P.D., Stump, R. and Wilson, R.K., Phys. Rev., 129, 2091 (1963).
25. Stevens, J.R. and Mao, A.C., J. of Appl. Phys., 41, 4273 (1970).
26. Stewart, A.J., Can. J. Phys., 35, 168 (1957).
27. Ferrell, R.A., Rev. Mod. Phys., 28, 308 (1956).
28. Chuang, S.Y. and Hogg, B.G., Can. J. Phys., 45, 3895 (1967).
29. Ferrell, R.A., Phys. Rev., 110, 1355 (1958).
30. Siegbahn, K., Alpha - Beta - Gamma-Ray Spectroscopy, Vol. 2, North-Holland Publishing Co., Amsterdam, 1968.
31. Bell, R.E. and Green, R.E., Nucl. Instr., 3, 127 (1958).
32. Lederer, C.M., Hollander, J.M. and Perlman, I., Table of Isotopes, 6th. Ed., John Wiley and Sons, Inc., N.Y.C., N.Y., 1967.
33. Dezei, I., Kajcsos, Z. and Molnair, B., Central Research Institute for Physics, H-1525, Budapest, Hungary.
34. Cumming, J.D., ENL Report No. 6470.
35. Tao, S.J., IEEE Trans. Nucl., 175, (1968).
36. Kinkegaand, P. and Eldrup, M., Comp. Phys. Comm., 3, 240 (1972).
37. Celitans, G.J. and Lee, J. Chem. Phys., 44, 2506 (1966).
38. Cooper, A.M., J. Chem. Phys., 46, 2441 (1967).
39. Rondeau, R.E., J. Chem. and Eng. Data, 11, 124 (1966).
40. Goldanskii, V.I., Mogensen, C.E. and Shantarovich, U.P., Phys. Lett., 32, 98 (1970).
41. Goldanskii, V.I., Positron Annihilation Conference, Kinston, Canada, Sept. 1971.
42. Gordon, J., Hart, E.J. and Thomas, J.K., J. Chem. Phys., 68 1272 (1964).

43. Ache, H.J. and Bartal, L.J., *J. Phys. Chem.*, 77, 2060 (1973).
44. Madia, W.J., Nichols, A.L. and Ache, H.J., *Appl. Phys.*, 3, 189 (1974).
45. Tao, S.J., *Appl. Phys.*, 3, 1 (1974).
46. Madia, W.J., Nichols, A.L. and Ache, H.J., *J.A.C.S.*, 97, 5041 (1975).
47. Madia, W.J., Nichols, A.L. and Ache, H.J., *J. Chem. Phys.*, 60, 189 (1974).
48. Jean, Y.-C. and Ache, H.J., *J. Phys. Chem.*, 81, 2093 (1977).
49. Madia, W.J., Ph.D. Dissertation, V.P.I. & S.U., 1975.
50. Madia, W.J., Nichols, A.L. and Ache, H.J., *J. Phys. Chem.*, 78, 1881 (1974).
51. Pyun, C.W., *J. Chem. Ed.*, 48, 194 (1970).
52. Toluene was substituted for benzene and n-heptane was substituted for n-hexane in the temperature studies so as to expand the temperature range. It does not effect the positron lifetime spectra to any significant degree.
53. Goldanskii, V.I. and Shantarovich, V.P., *Appl. Phys.*, 3, 335 (1974).
54. Bartal, L.J., Nicholas, J.B. and Ache, H.J., *J. Phys. Chem.*, 76, 1124 (1972).
55. Bartal, L.J. and Ache, H.J., *Radiochimica Acta*, 17, 205 (1972).
56. Bartal, L.J. and Ache, H.J., *Radiochimica Acta*, 19, 49 (1973).
57. Nicholas, A.L., Wild, R.E., Bartal, L.J. and Ache, H.J., *Appl. Phys.*, 4, 37 (1974).
58. McGervey, J.O., Positron Annihilation, A.T. Stewart, L.O. Roellig, Ed., Academic Press, N.Y.C., N.Y., 1967.
59. Horstman, H., *J. Inorg. Nucl. Chem.*, 27, 1191 (1965).
60. Bartal, L.J. and Ache, H.J., *J. Inorg. Nucl. Chem.*, 36, 922 (1974).
61. Eldrup, M., Shantarovich, V.P. and Mogensen, O.E., *Chem. Phys.*, 11, 129 (1975).

62. For recent reviews on inclusion compounds, see, e.g., (a) Bergeron, R.J., J. Chem. Ed., 54, 204 (1977); (b) Griffiths, D.W. and Bender, M.L., Adv. Catal., 209 (1973).
63. von Dietrich, H. and Cramer, F., Chem. Ber., 87, 806 (1954).
64. Hybl, A., Rundle, R.E. and Williams, D.E., J.A.C.S., 87, 2779 (1965).
65. Cramer, F., Angew. Chem., 73, 49 (1967).
66. Nemethy, G. and Scheraga, H.A., J. Chem. Phys., 36, 3401 (1962).
67. Rohrbach, R.P., Rodriguez, L.J. and Eyring, E.M., J. Phys. Chem., 81, 944 (1977).
68. Jean, Y.-C. and Ache, H.J., J. Phys. Chem., 81, 2093 (1977).
69. Bergeron, R.J., J. Chem. Ed., 54, 204 (1977).
70. Madia, W.J. and Ache, H.J., J. Phys. Chem., 80, 451 (1976).
71. Madia, W.J., Nichols, A.L. and Ache, H.J., J.A.C.S., 97, 5041 (1975).
72. Jean, Y.-C. and Ache, H.J., J. Phys. Chem., 80, 1693 (1976).
73. Bergeron, R.J. and Pillar, D.M., J.A.C.S., 99, 5146 (1977).
74. Schwary, G., J. Mol. Biol., 11, 64 (1965).

APPENDIX

APPENDIX: DATA TABLES

A. Rate Constants for the Reaction of Thermal Ortho-Positronium with Nitrobenzene or o-Nitrotoluene in Various Molefractions of n-Hexane/Benzene Solutions at 21°C.

<u>Solute and Solvent</u> <u>k, (M⁻¹nsec⁻¹)</u>	<u>Concentration, mM</u>	<u>$\lambda_{2,-1}$</u> <u>nsec</u>	<u>I₂'</u> <u>%</u>
Nitrobenzene .2MF 20.8 ± 1.2	0.0	0.357	38.1
	10.0	0.543	36.5
	20.0	0.720	35.5
	30.0	0.957	37.5
	40.0	1.193	42.5
Nitrobenzene .3MF 18.8 ± 1.1	0.0	0.332	40.1
	10.0	0.696	39.5
	20.0	0.863	38.5
	30.0	0.924	37.8
	40.0	1.117	38.7
Nitrobenzene .35MF 17.5 ± 1.0	0.0	0.321	38.8
	10.0	0.520	37.1
	20.0	0.620	36.3
	30.0	0.873	40.5
	40.0	0.897	39.4
Nitrobenzene .4MF 18.9 ± 1.1	0.0	0.302	41.2
	10.0	0.470	37.6
	20.0	0.693	38.5
	30.0	0.890	39.0
	40.0	1.037	38.6
Nitrobenzene .45MF 12.9 ± 0.8	0.0	0.317	40.2
	10.0	0.448	37.4
	20.0	0.663	38.2
	40.0	0.824	41.2
Nitrobenzene .5MF 10.5 ± 0.6	0.0	0.313	41.2
	10.0	0.416	38.1
	20.0	0.500	37.2
	30.0	0.688	38.0
	40.0	0.705	39.5

<u>Solute and Solvent</u> <u>k, (M⁻¹nsec⁻¹)</u>	<u>Concentr-</u> <u>ation, mM</u>	<u>$\lambda_{2,1}$</u> <u>nsec</u>	<u>I₂,</u> <u>%</u>
Nitrobenzene .7MF 4.6 ± 0.3	0.0	0.305	41.2
	20.0	0.388	41.0
	30.0	0.463	39.3
	40.0	0.489	39.0
	50.0	0.531	38.9
Nitrobenzene .8MF 2.9 ± 0.2	0.0	0.306	39.0
	10.0	0.327	41.0
	20.0	0.360	40.8
	30.0	0.430	38.8
	40.0	0.415	39.6
o-Nitrotoluene .3MF 1.6 ± 0.2	0.0	0.332	37.8
	200.0	0.697	30.4
	300.0	0.789	34.6
	400.0	0.990	29.1
	500.0	1.067	29.9
o-Nitrotoluene .5MF .66 ± .03	0.0	0.311	37.4
	100.0	0.375	33.3
	200.0	0.424	29.7
	400.0	0.594	23.2
	500.0	0.626	22.8
o-Nitrotoluene .75MF .27 ± .03	0.0	0.280	33.1
	400.0	0.391	20.3
	500.0	0.415	21.3
	800.0	0.512	23.6
o-Nitrotoluene 1.0MF .20 ± .02	0.0	0.279	34.6
	100.0	0.300	32.7
	200.0	0.325	23.9
	300.0	0.377	19.6
	400.0	0.336	19.1
	500.0	0.426	18.0

B. Temperature Dependence of the Annihilation Rate, λ_2 , for the Reaction of Thermal Ortho-Positronium with Different Solvents.

<u>Solvent</u>	<u>T, °C</u>	<u>λ_2, nsec⁻¹</u>	<u>I₂, %</u>
Ethanol	21	0.331	18.8
	47	0.325	19.2
	51	0.323	19.4
	72	0.319	19.2
	21	0.333	18.9
1-Propanol	21	0.317	21.8
	27	0.314	22.2
	34	0.318	21.6
	44	0.311	22.3
	56	0.316	22.4
	64	0.309	22.5
	75	0.312	22.7
	83	0.306	22.7
	21	0.318	22.3
2-Propanol	20	0.295	22.3
	27	0.298	22.6
	39	0.298	22.8
	47	0.290	22.4
	60	0.295	22.4
	70	0.292	22.7
	20	0.295	22.4
n-Hexanol	20	0.400	20.1
	31	0.400	20.3
	42	0.401	20.2
	52	0.402	20.1
	62	0.404	20.3
	74	0.401	20.0
	80	0.410	20.1
	90	0.415	20.4
	100	0.408	20.5
20	0.401	20.2	
H ₂ O	21	0.586	26.9
	32	0.629	28.4
	43	0.604	28.0
	49	0.619	28.3
	65	0.630	29.7
	94	0.572	27.5
	21	0.580	26.5

<u>Solvent</u>	<u>T, °C</u>	<u>$\lambda_2, \text{nsec}^{-1}$</u>	<u>I₂, %</u>
Ethyleneglycol	20	0.424	19.5
	32	0.460	21.1
	45	0.447	20.7
	55	0.447	21.0
	66	0.449	21.0
	74	0.450	22.0
	94	0.459	23.1
	108	0.449	23.1
	120	0.442	23.3
	138	0.435	24.0
	150	0.433	24.4
	173	0.424	25.1
	192	0.421	25.6
	20	0.430	20.8
0.92 MF Ethanol/ Ethyleneglycol	20	0.303	21.5

C. Temperature Dependence of the Observed Rate Constants for the Reaction of Ortho-Positronium with CuCl_2 or Substituted Nitroaromatics in Different Solvents.

Solvent and Solute	T, °C	$\lambda_2, \text{nsec}^{-1}$	$I_2, \%$	$k, \text{M}^{-1} \text{nsec}^{-1}$
Ethanol	20	0.407	18.2	7.9
	27	0.424	19.7	9.8
	33	0.419	18.8	9.4
$\text{CuCl}_2, 9.6 \text{ mM}$	42	0.432	19.5	11.0
	49	0.435	19.7	11.5
	55	0.437	19.8	11.9
	64	0.405	18.0	14.2
	20	0.405	18.0	7.9
1-Propanol	21	0.432	21.7	6.8
	34	0.460	22.2	8.4
	44	0.491	23.6	10.2
$\text{CuCl}_2, 17.5 \text{ mM}$	54	0.506	22.7	11.0
	64	0.531	24.5	12.5
	74	0.564	25.0	14.3
	21	0.432	21.8	6.8
2-Propanol	21	0.402	19.7	8.1
	35	0.440	20.1	11.0
	41	0.453	20.7	12.0
$\text{CuCl}_2, 13.2 \text{ mM}$	54	0.454	20.3	12.0
	65	0.403	20.4	8.2
	75	0.533	22.2	18.0
	21	0.404	20.0	8.1
n-Hexanol	20	0.467	31.7	3.7
	31	0.488	32.3	5.0
	42	0.509	29.2	6.3
$\text{CuCl}_2, 16.6 \text{ mM}$	52	0.541	28.7	8.2
	62	0.558	28.5	9.2
	74	0.595	28.0	11.5
	80	0.611	29.7	12.4
	90	0.678	32.6	16.5
	100	0.694	32.7	17.4
	20	0.465	32.0	3.7
H_2O	20	0.653	22.6	3.6
	32	0.761	26.2	5.5
	44	0.758	24.7	6.4
$\text{CuCl}_2, 24.0 \text{ mM}$	66	0.825	26.2	8.1
	76	0.843	24.1	9.7
	89	0.930	30.5	14.8
	96	0.926	29.1	14.7
	20	0.660	23.2	3.7

Solvent and Solute	T, °C	λ_2 , nsec ⁻¹	I ₂ , %	k, M ⁻¹ nsec ⁻¹
Ethyleneglycol	20	0.436	20.3	.51
	35	0.457	20.7	.56
	45	0.465	20.3	.84
CuCl ₂ , 17.8 mM	57	0.482	21.4	1.97
	67	0.475	20.6	1.53
	76	0.500	21.7	2.81
	86	0.502	21.5	2.82
	96	0.512	21.3	2.98
	108	0.525	22.1	4.27
	130	0.552	23.1	6.38
	143	0.579	24.7	8.20
	20	0.430	20.7	.50
1-Propanol	20	0.413	18.9	10.0
	34	0.421	19.3	10.8
	45	0.419	19.2	10.6
Nitrobenzene, 10 mM	60	0.422	19.7	10.9
	69	0.427	20.2	11.4
	77	0.416	19.7	10.3
	89	0.387	19.9	7.4
	95	0.380	20.2	6.7
	20	0.410	18.8	10.0
n-Heptane	-20	0.579	25.0	7.1
	0	0.481	19.1	5.2
	21	0.445	22.8	4.5
o-Nitrotoluene, 400 mM	30	0.425	23.4	4.1
	40	0.338	22.6	2.1
	48	0.332	23.1	2.1
	58	0.341	25.6	2.4
	68	0.316	26.5	1.9
	79	0.304	29.2	1.8
	90	0.293	29.8	1.6
	103	0.281	29.7	1.5
	21	0.451	22.7	4.6
0.14 MF Ethanol/ Ethyleneglycol	20	0.420	22.4	-
0.22 MF Ethanol/ Ethyleneglycol	20	0.380	21.5	-
0.49 MF Ethanol/ Ethyleneglycol	20	0.371	22.1	-
0.76 MF Ethanol/ Ethyleneglycol	20	0.343	21.2	-

<u>Solvent and Solute</u>	<u>T, °C</u>	<u>$\lambda_2, \text{nsec}^{-1}$</u>	<u>I₂, %</u>	<u>k, M⁻¹ nsec⁻¹</u>
Toluene	-59	0.904	42.3	13.8
	-20	0.899	40.6	13.8
o-Nitrotoluene, 40 mM	0	0.818	40.8	11.2
	20	0.736	51.8	10.3
	30	0.654	49.9	8.4
	39	0.591	47.9	7.0
	49	0.537	51.8	5.8
	57	0.509	55.3	5.2
	65	0.467	52.7	4.3
	73	0.433	52.6	3.6
	82	0.416	51.5	3.3
	94	0.415	54.8	3.3
	20	0.740	51.3	10.3
Ethyleneglycol CuCl ₂ , 12 mM Viscosity = 20 cp	20	0.431	20.1	0.9
0.14 MF Ethanol/ Ethyleneglycol CuCl ₂ , 13.5 mM Viscosity = 18.1 cp	20	0.400	20.3	1.3
0.22 MF Ethanol/ Ethyleneglycol CuCl ₂ , 14.3 mM Viscosity = 16.2 cp	20	0.391	20.7	1.5
0.49 MF Ethanol/ Ethyleneglycol CuCl ₂ , 11.6 mM Viscosity = 10.6 cp	20	0.375	21.0	2.8
0.76 MF Ethanol/ Ethyleneglycol CuCl ₂ , 15.0 mM Viscosity = 4.9 cp	20	0.373	20.9	3.8
0.92 MF Ethanol/ Ethyleneglycol CuCl ₂ , 15.2 mM Viscosity = 1.6 cp	20	0.388	20.4	5.6

D. Reactions of Thermal Ortho-Positronium with Nitroaromatics, Cyclohexaamylose (CH) or Inclusion Complex (Nitroaromatics + CH) in H₂O at 21°C, pH 3.5 and Ionic Intensity 0.5.

System	Cyclohexaamylose Concentration, mM	$\lambda_2, \text{nsec}^{-1}$	I ₂ , %
Cyclohexaamylose	6.8	0.551	26.4
	8.6	0.548	26.3
	9.2	0.541	26.5
	11.6	0.543	27.0
	12.5	0.545	27.3
	16.7	0.547	26.8
	18.4	0.547	26.7
	25.0	0.533	26.8
	50.0	0.531	26.4
	69.3	0.538	26.5
	75.0	0.533	27.0
92.1	0.534	26.6	
H ₂ O pH 3.5 Ionic Intensity 0.5	-	^a 0.550	27.3
7.84 mM m-Nitrophenol+CH	0.0	^b 0.640	25.8
	6.8	0.625	26.0
	11.6	0.610	26.4
	26.4	0.585	26.0
	49.3	0.576	26.4
	69.3	0.566	25.9
	92.4	0.559	26.3
4.5 mM o-Nitrophenol+CH	0.0	^b 0.593	26.5
	8.3	0.589	26.4
	9.2	0.589	27.0
	12.5	0.595	27.3
	18.4	0.577	26.6
	25.0	0.577	26.7
	50.0	0.541	26.8
	92.0	0.526	26.1

a) Average of ten different runs. ($\pm .002$)

b) Average of five different runs. ($\pm .003$)

<u>System</u>	<u>Cyclohexaamylose Concentration, mM</u>	<u>$\lambda_2, \text{nsec}^{-1}$</u>	<u>$I_2, \%$</u>
p-Nitroben- zyl Alcohol + CH 7.96 mM	0.0	^a 0.666	26.0
	8.6	0.630	25.7
	9.2	0.620	25.8
	12.5	0.622	26.0
	25.0	0.605	25.9
	49.5	0.547	26.1
	92.6	0.534	26.0
8.5 mM m-Nitroben- zyl Alcohol + CH	0.0	^a 0.637	27.0
	8.3	0.638	27.1
	9.2	0.634	26.6
	12.5	0.621	26.4
	18.6	0.605	26.7
	25.0	0.591	26.7
	50.0	0.583	26.8
92.0	0.563	26.9	

a) Average of five different runs. ($\pm .003$)

<u>System</u>	<u>Cyclohexaamylose Concentration, mM</u>	<u>$\lambda_2, \text{nsec}^{-1}$</u>	<u>$\bar{I}_2, \%$</u>
8.0 mM o-Nitroben- zyl Alcohol + CH	0.0	^a 0.641	27.0
	8.6	0.641	27.0
	9.2	0.634	27.4
	12.5	0.630	27.9
	18.4	0.624	26.7
	25.0	0.610	27.6
	50.0	0.591	26.8
	75.0	0.583	27.0
	92.0	0.569	27.1

a) Average of five different runs. (\pm .003)

**The vita has been removed from
the scanned document**

POSITRONIUM COMPLEX FORMATION: MECHANISMS, SOLVENT EFFECTS
AND ITS APPLICATION TO THE STUDY OF MOLECULAR PHENOMENA

by

Eugene Stephen Hall

(ABSTRACT)

One of the most widely studied "exotic atoms" in Chemistry and Physics is positronium. Positronium (Ps) is the bound state of an electron and positron. It is formed in two ground states, para-positronium (p-Ps) and ortho-positronium (o-Ps) whose lifetimes in free space are 0.125 nsec and 140 nsec respectively.

When thermalized o-Ps forms a complex with a molecule, the electron density at the position of the positron will be drastically increased thus shortening its lifetime.

A study was performed to evaluate what role the solvent plays in stabilizing the complexes formed between Ps and nitroaromatics in solution and the various thermodynamic variables associated with these processes. This study also included the evaluation of the effects displayed by several different solvents on complexes formed between Ps and CuCl_2 . The interpretation of the solvent effects of Ps reactions in terms of the "bubble shrinkage model" was tested using the results obtained in the reactions of Ps with various inorganic and organic molecules in different solvents. It was found that this model is definitely not applicable below a certain critical viscosity of the solvent and appears to be restricted to diffusion controlled reactions.

The fact that the reactivity of Ps towards nitroaromatics is drastically reduced when the latter molecules are already complexed with other conventional molecules can be utilized to determine the molecular formation constant, K_c , for inclusion compounds. A study was made using Ps as a probe to provide valuable information about the influence of steric factors on the ability of guest molecules to bind in the cavity of cyclohexaamylose.